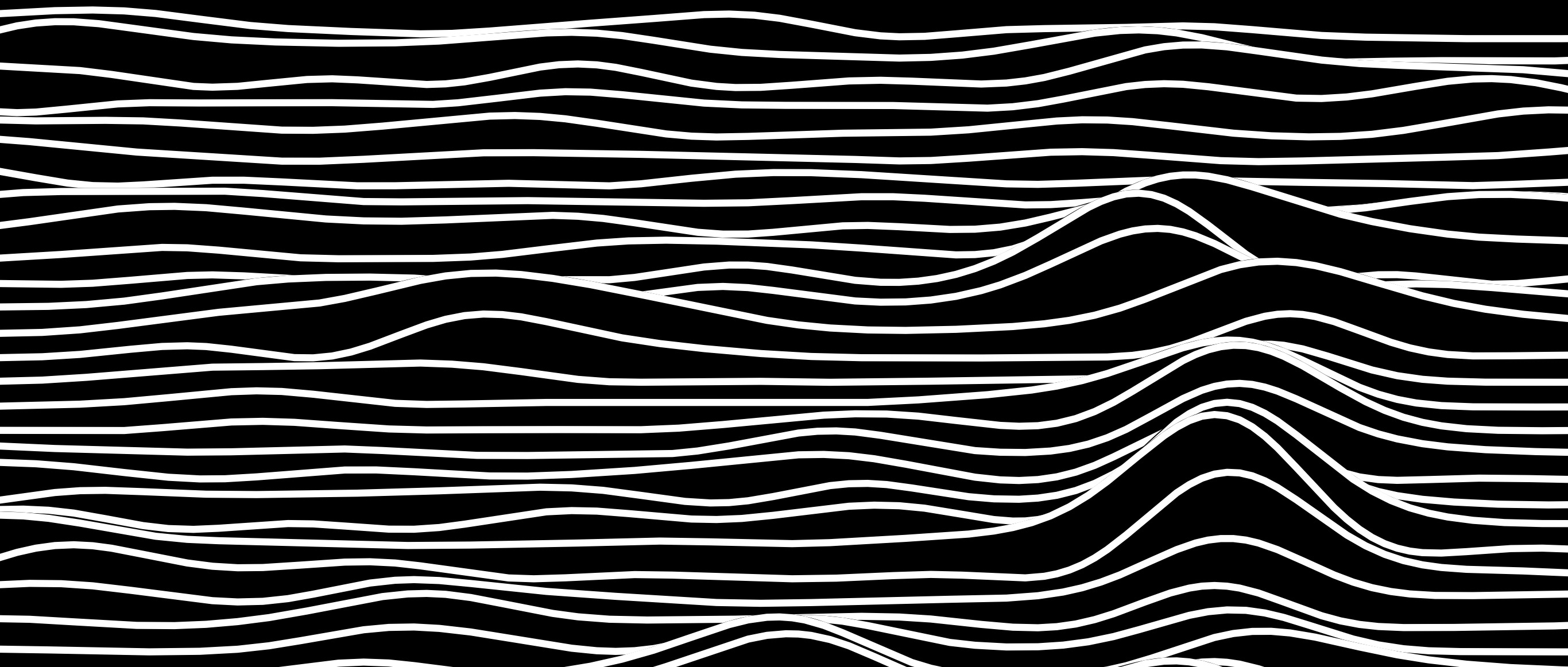


# New Understanding from Binary Black Hole detections

Chris Messenger - University of Glasgow  
SUPA Lectures 2019



# Outline

---

- Gravitational wave brief introduction
- The detections
  - The 1st detection - GW150914
  - The rest of the 1st observing run (O1)
  - The 2nd observing run (O2)
  - The current observing run (O3)
- Additional properties - populations
- Summary

interspersed throughout are tutorial slides including some based on “The basic physics of the binary black hole merger GW150914” LIGO-Virgo Collaboration, arXiv:1608.01940 (2016)

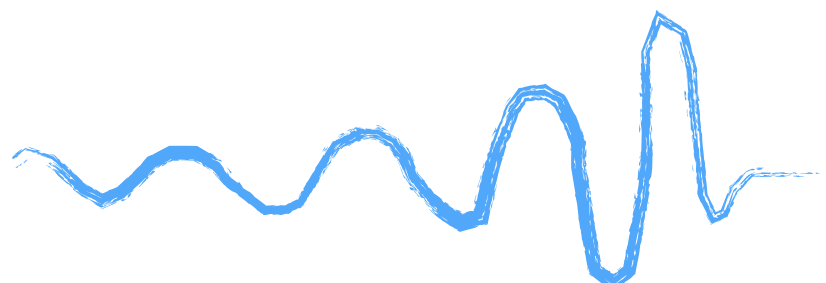
# Gravitational wave basics

---

Just to warm you up

# Astrophysical source types

compact binary  
coalescence



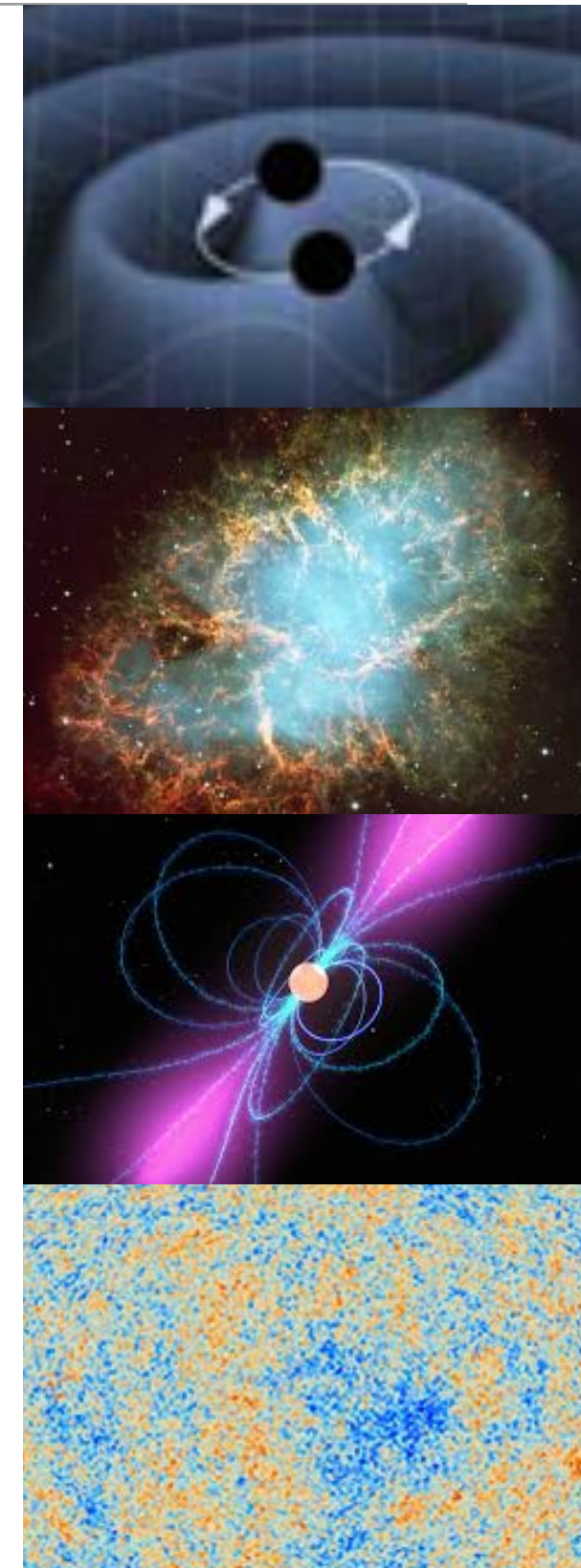
burst



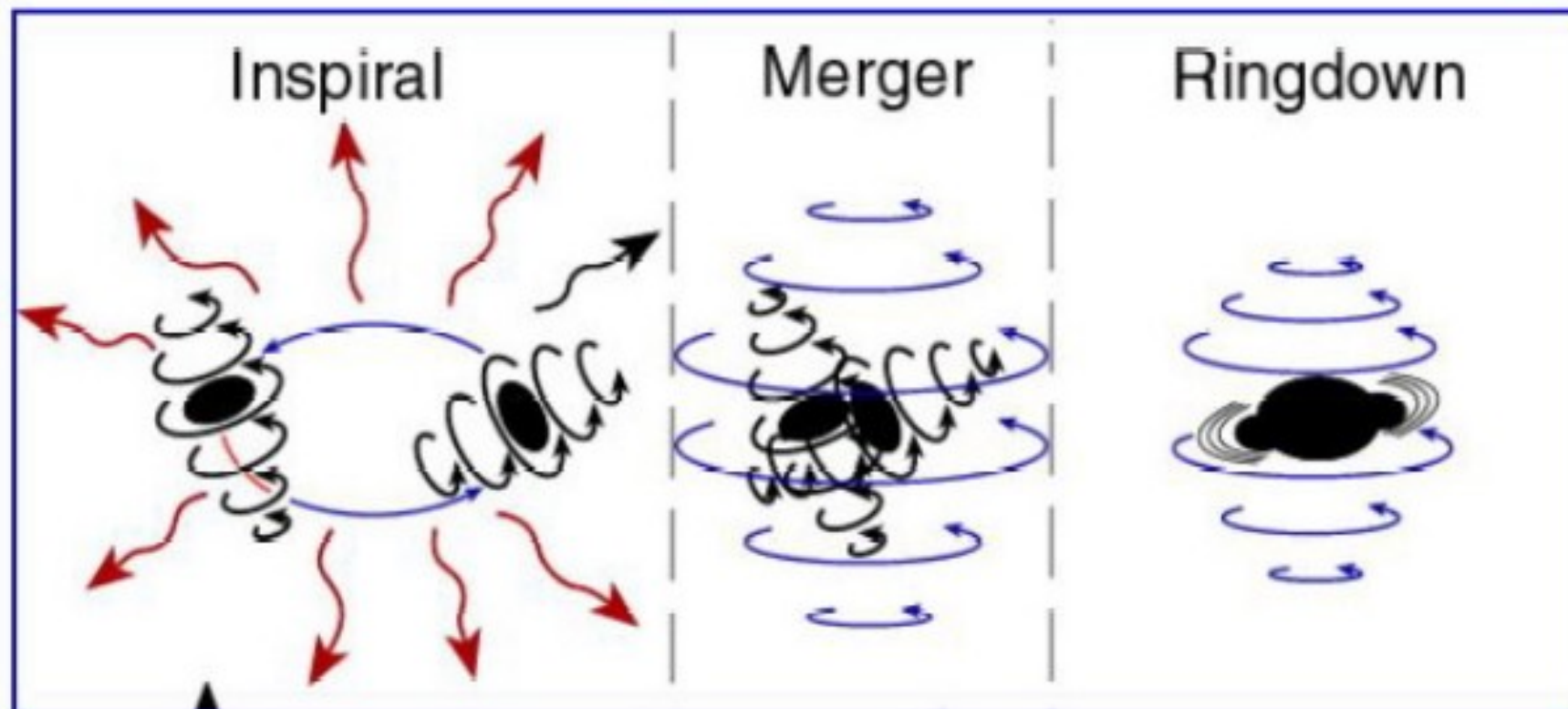
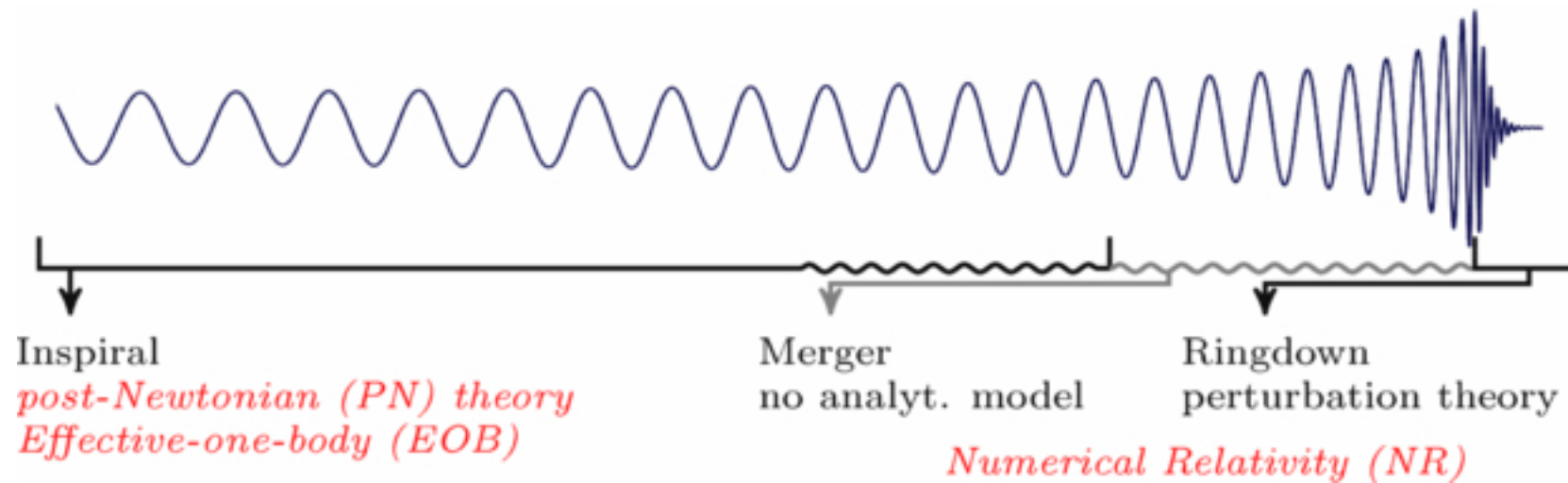
continuous



stochastic



# Compact binary coalescence



# Radiation from a binary

- First we calculate the quadrupole moment

$$Q_{ij} = \int d^3x \rho(\mathbf{x}) \left( x_i x_j - \frac{1}{3} r^2 \delta_{ij} \right) = \sum_{A \in \{1,2\}} m_A \begin{pmatrix} \frac{2}{3} x_A^2 - \frac{1}{3} y_A^2 & x_A y_A & 0 \\ x_A y_A & \frac{2}{3} y_A^2 - \frac{1}{3} x_A^2 & 0 \\ 0 & 0 & -\frac{1}{3} r_A^2 \end{pmatrix},$$

- For a circular orbit where

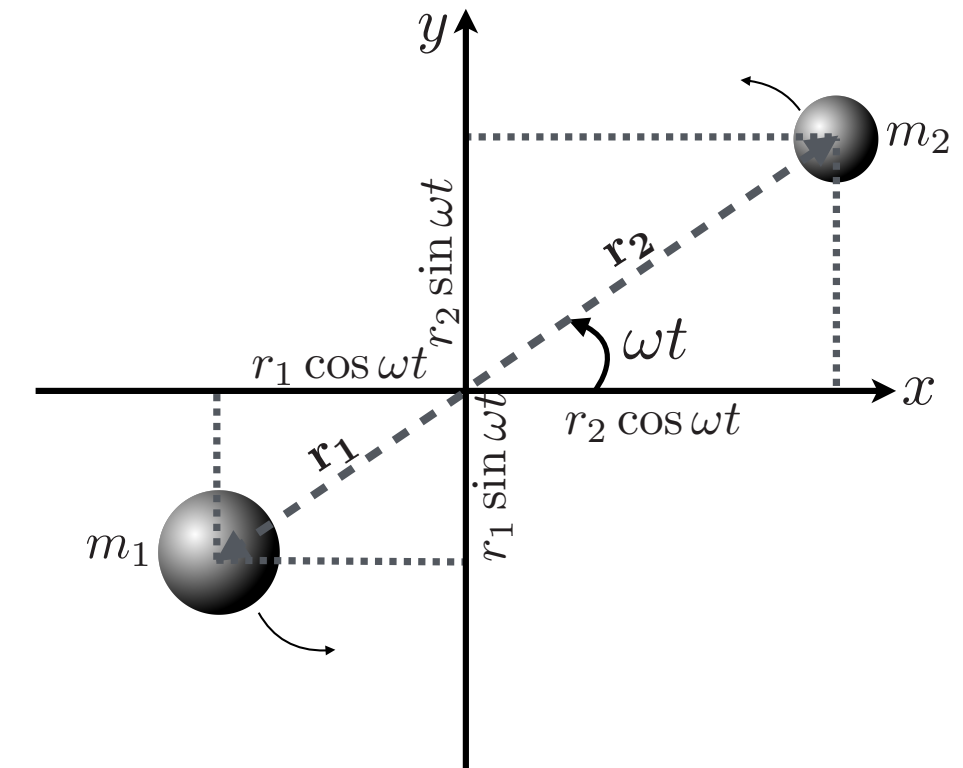
$$I_{xx} = \cos(2\omega t) + \frac{1}{3}, \quad I_{yy} = \frac{1}{3} - \cos(2\omega t), \quad I_{xy} = I_{yx} = \sin(2\omega t) \quad \text{and} \quad I_{zz} = -\frac{2}{3}$$

$$Q_{ij}^A(t) = \frac{m_A r_A^2}{2} I_{ij},$$

- Einstein found that the strain is then

$$h_{ij} = \frac{2G}{c^4 d_L} \frac{d^2 Q_{ij}}{dt^2},$$

- Where the individual masses are replaced by the reduced mass in defining  $Q_{ij}$ .



# Radiation from a binary

- Energy is then radiated according to the quadrupole formula

$$\frac{dE_{\text{GW}}}{dt} = \frac{c^3}{16\pi G} \iint |\dot{h}|^2 dS = \frac{1}{5} \frac{G}{c^5} \sum_{i,j=1}^3 \frac{d^3 Q_{ij}}{dt^3} \frac{d^3 Q_{ij}}{dt^3} = \frac{32}{5} \frac{G}{c^5} \mu^2 r^4 \omega^6$$

where  $|\dot{h}|^2 = \sum_{i,j=1}^3 \frac{dh_{ij}}{dt} \frac{dh_{ij}}{dt}$ ,

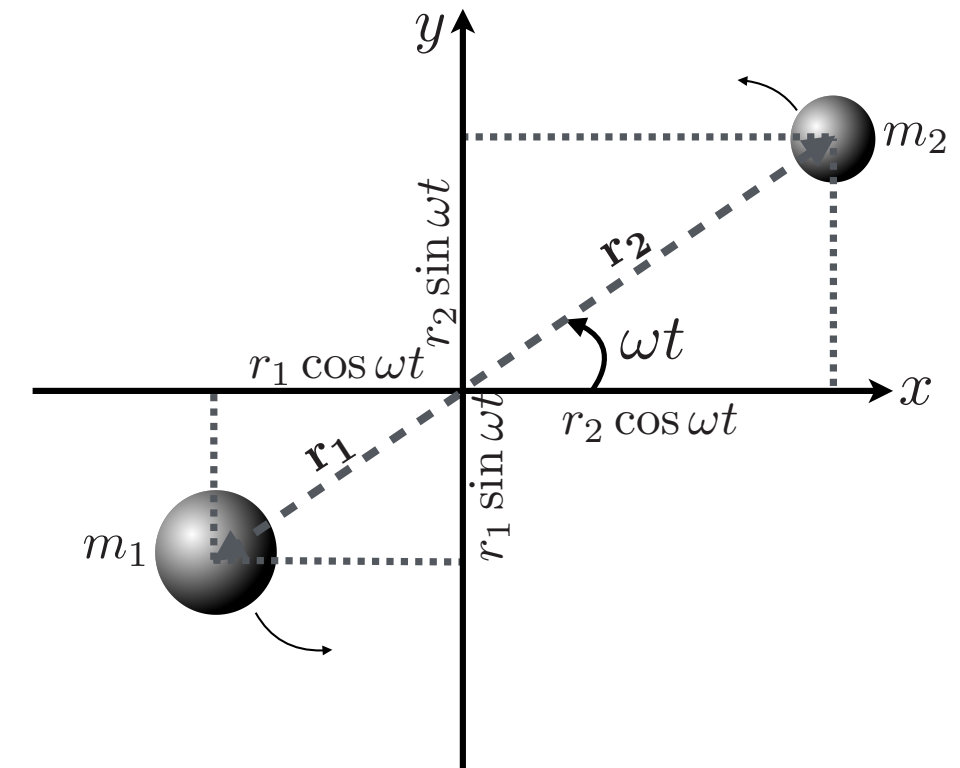
- This drains the orbital energy

$$\frac{d}{dt} E_{\text{Orb}} = \frac{GM\mu}{2r^2} \dot{r} = -\frac{d}{dt} E_{\text{GW}}$$

- Which leads to the evolution of the systems as an inspiral

$$\dot{\omega}^3 = \left(\frac{96}{5}\right)^3 \frac{\omega^{11}}{c^{15}} G^5 \mu^3 M^2 = \left(\frac{96}{5}\right)^3 \frac{\omega^{11}}{c^{15}} (G\mathcal{M})^5$$

- where  $\mathcal{M} = (\mu^3 M^2)^{1/5}$  is the chirp mass



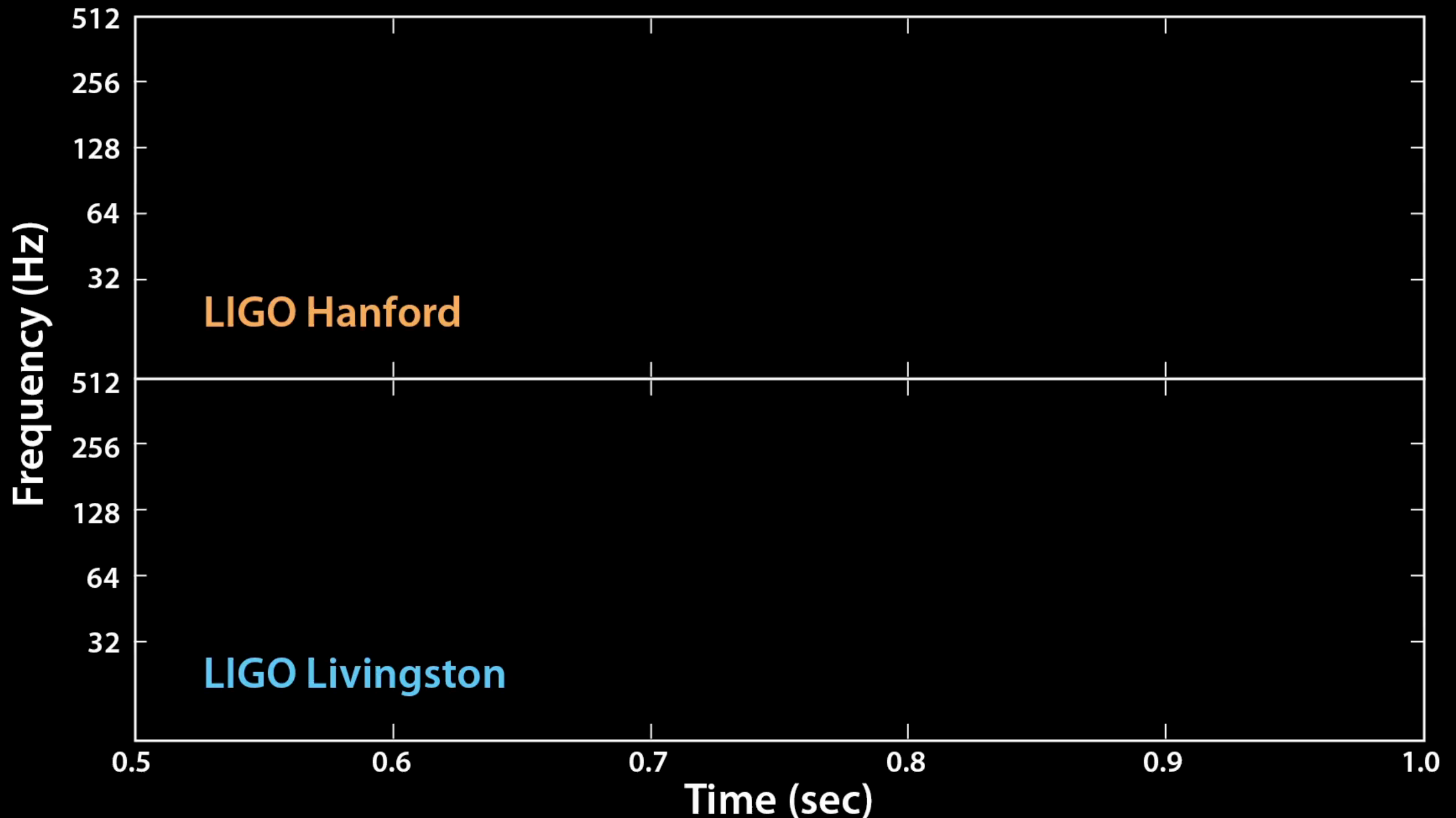


# The 1<sup>st</sup> detection

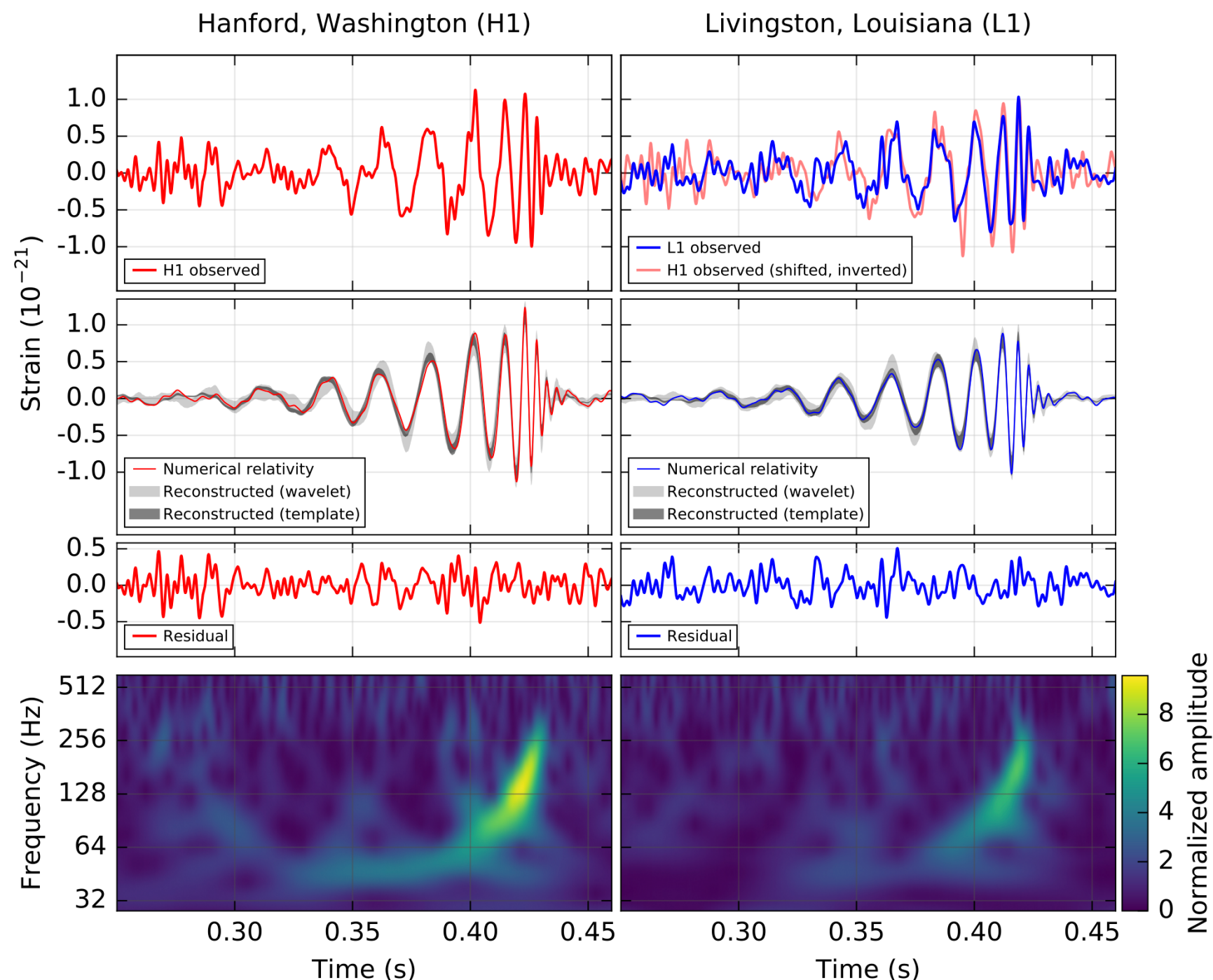
---

GW150914

09:50:45 UTC, 14th September, 2015



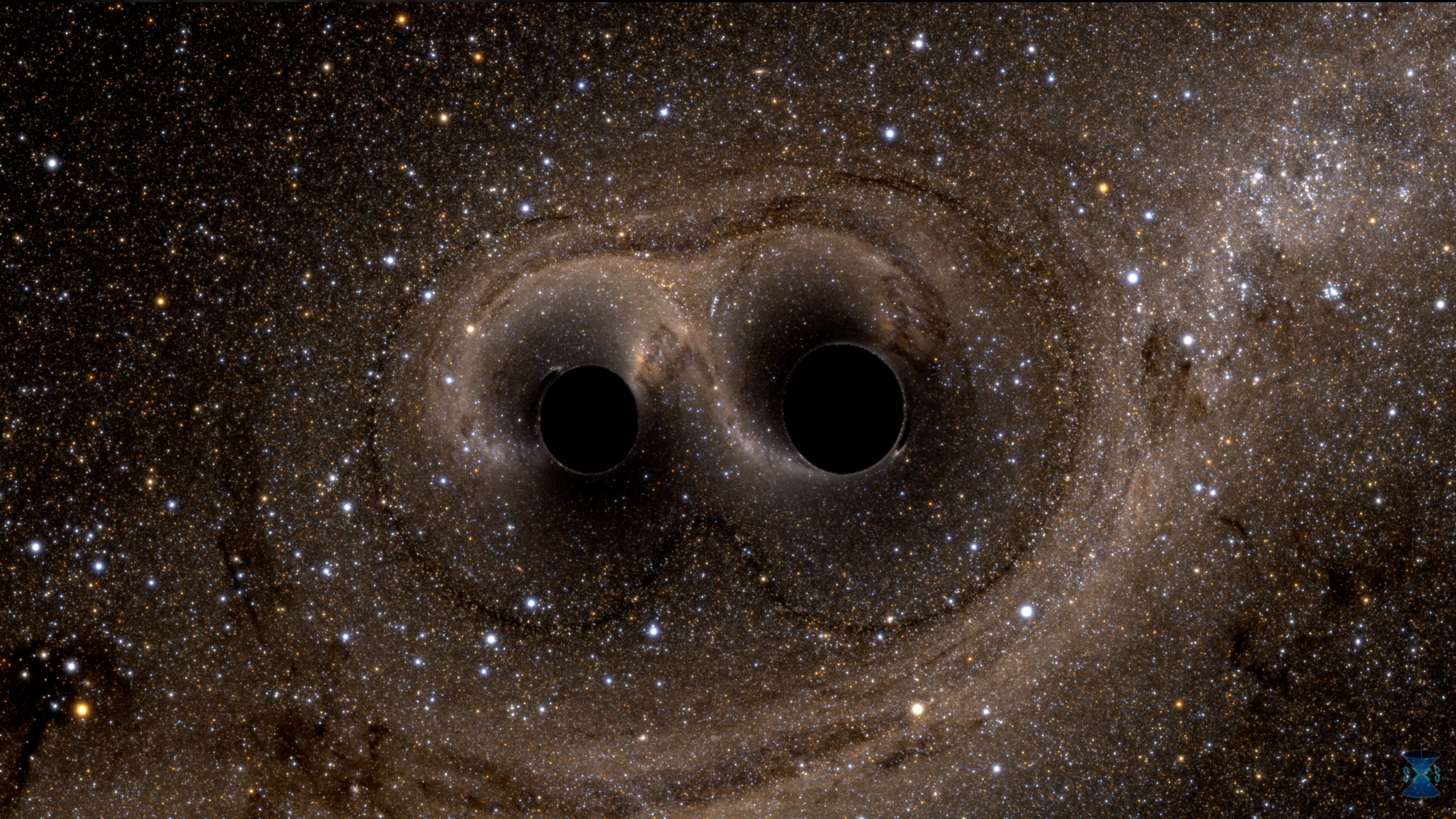
# The data



# The data



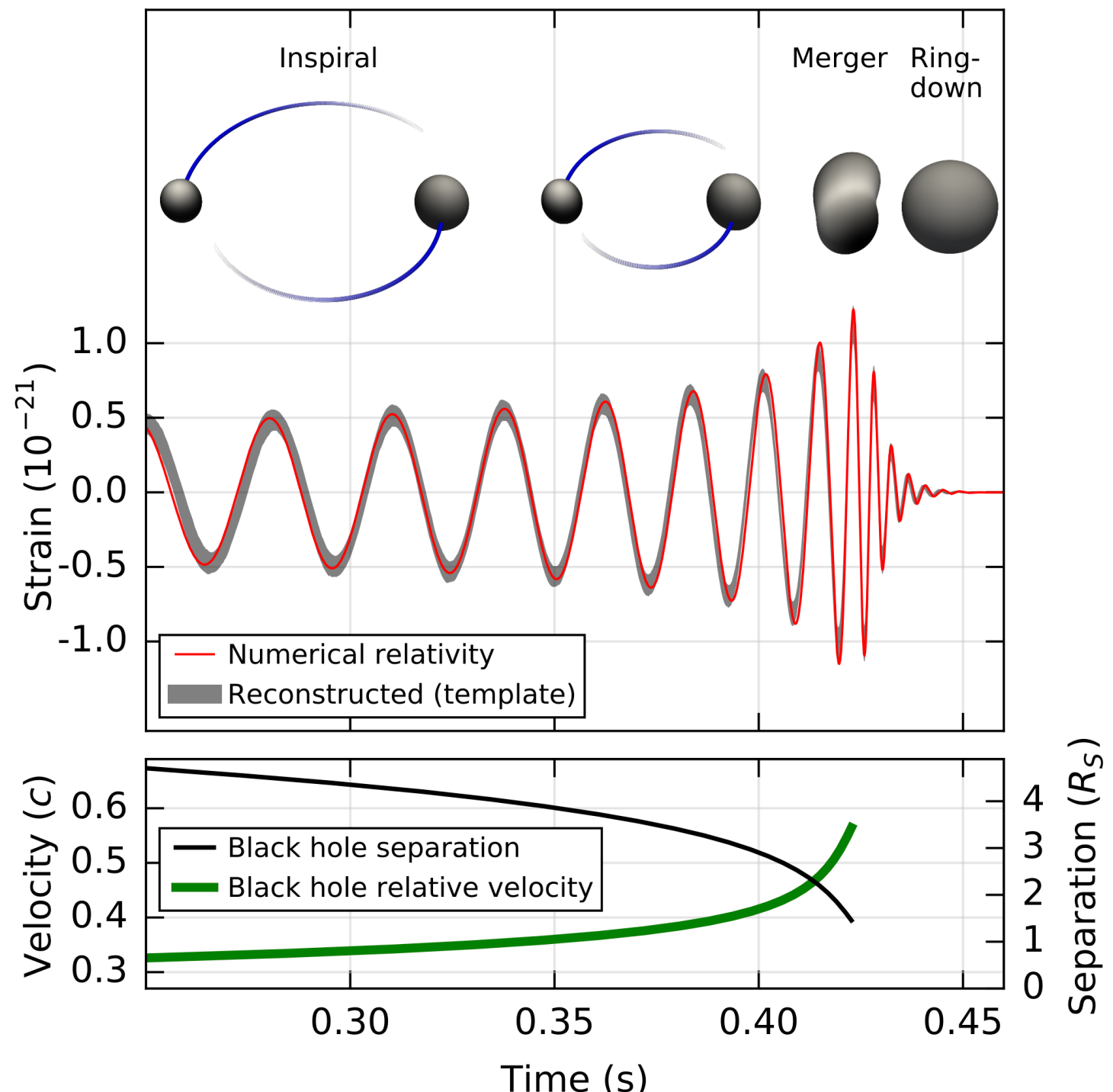
# The binary system



Credit: SXS Collaboration

# A binary black hole?

- The first direct\* detection of gravitational waves.
- The first unambiguous detection of a black hole.
- The first observation of a binary black hole.
- The most luminous event ever detected!
- Still the highest SNR BBH signal observed!



\* the definition of “direct” in this case is subjective

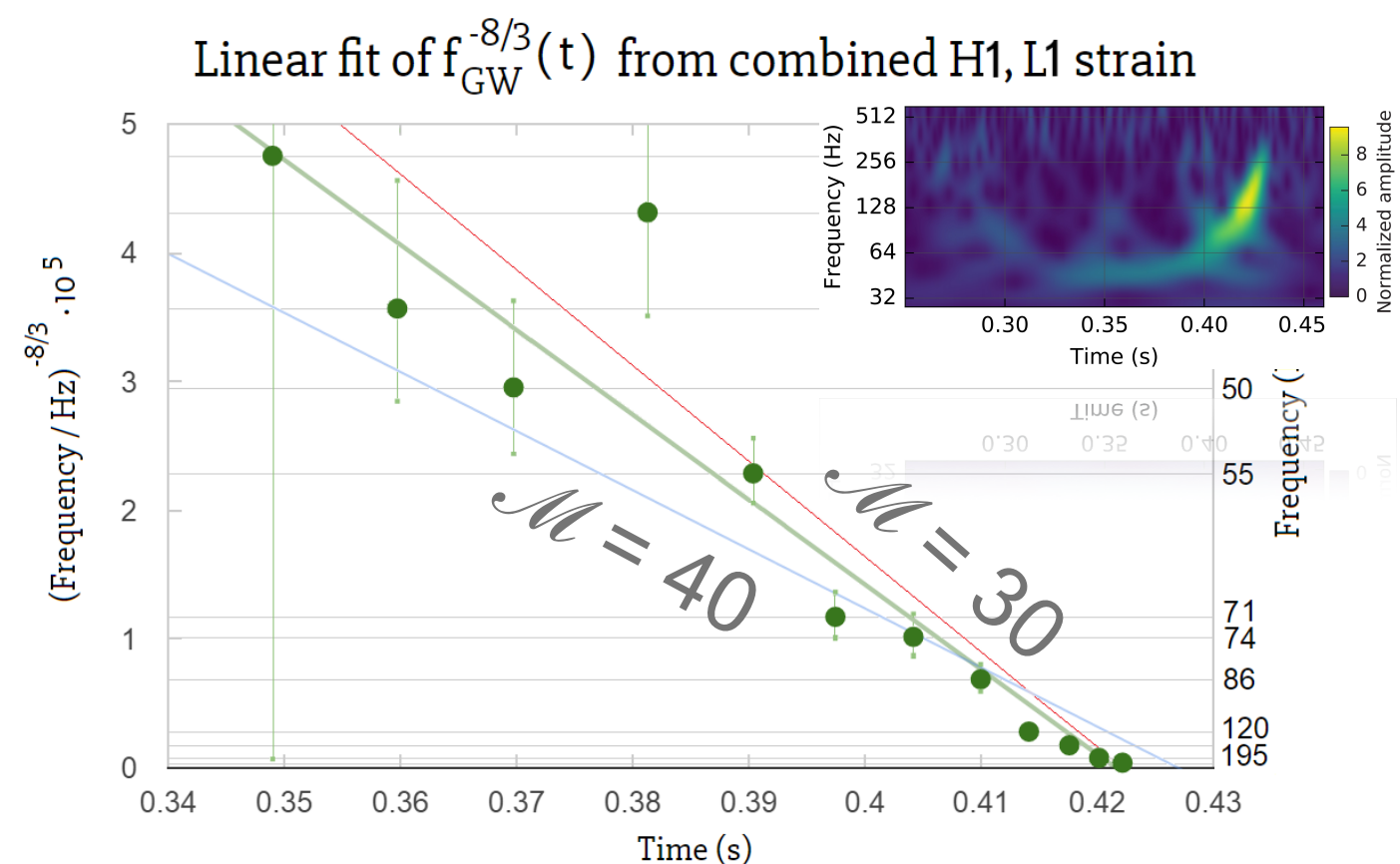
# The mass scale

- We can rearrange the expression for frequency evolution to give

$$\mathcal{M} = \frac{c^3}{G} \left( \left( \frac{5}{96} \right)^3 \pi^{-8} (f_{\text{GW}})^{-11} (\dot{f}_{\text{GW}})^3 \right)^{1/5}$$

- Then integrate to obtain

$$f_{\text{GW}}^{-8/3}(t) = \frac{(8\pi)^{8/3}}{5} \left( \frac{G\mathcal{M}}{c^3} \right)^{5/3} (t_c - t)$$



- We use the value  $\mathcal{M} = 30$  for the remainder of this tutorial.
- We estimate the minimum mass of the lightest component later on.

# Proving compactness

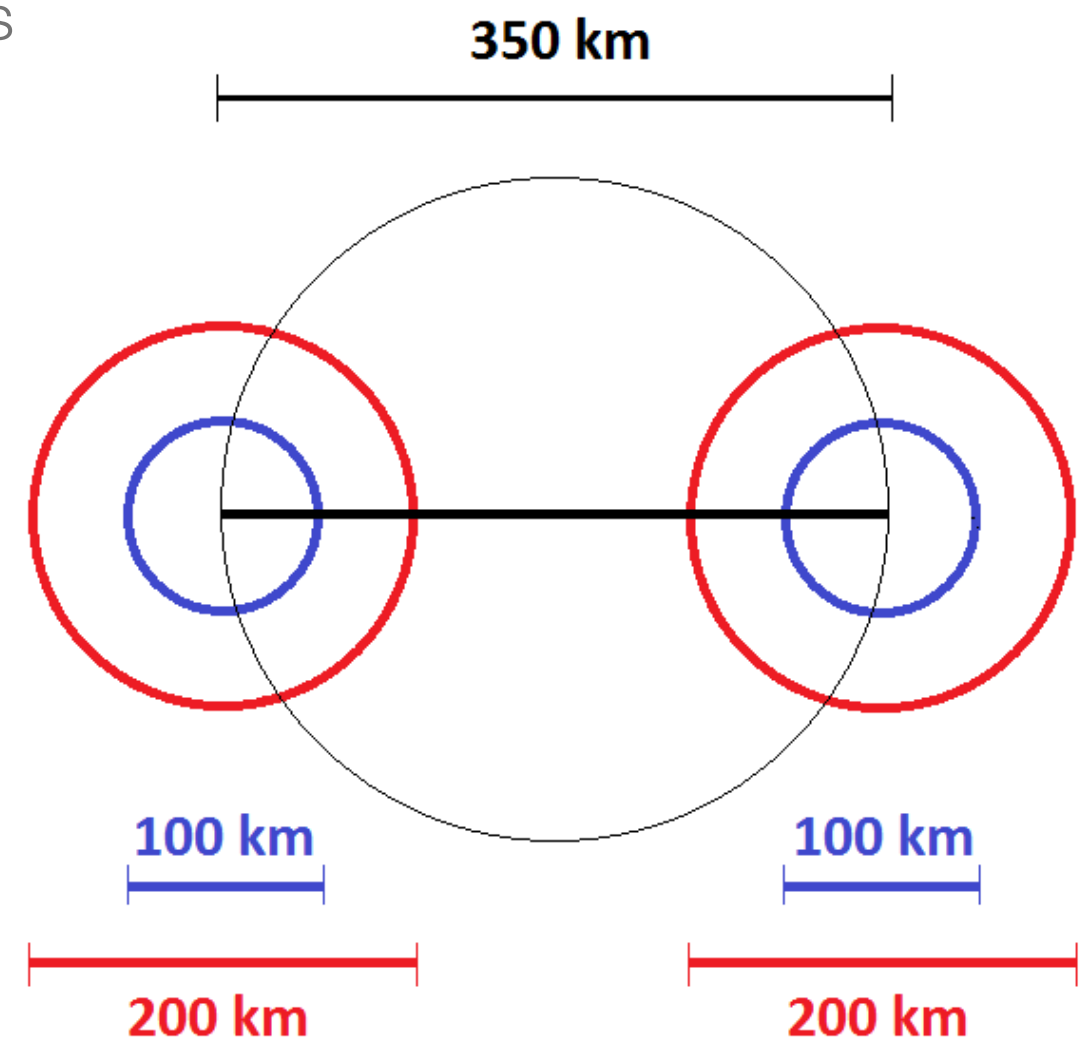
- For an equal mass system the chirp mass implies that  $m_1 = m_2 = 2^{1/5} \mathcal{M} = 35 M_{\odot}$   $M = m_1 + m_2 = 70 M_{\odot}$

- For non-spinning objects with Keplerian orbit at the time of peak GW amplitude the orbital separation is

$$f_{\text{GW}}|_{\text{max}} \sim 150 \text{ Hz}, \quad R = \left( \frac{GM}{\omega_{\text{Kep}}^2|_{\text{max}}} \right)^{1/3} = 350 \text{ km}$$

- Compared to normal stars this is tiny and although NSs could have this compactness NSs could not have this mass.
- The compactness ratio  $\mathcal{R}$  is defined as the orbital separation divided by the sum of the smallest possible radii.
- The Schwarzschild radii of these objects is 103km allowing us to define the compactness ratio

$$\mathcal{R} = 350 \text{ km} / 206 \text{ km} \sim 1.7$$



# Timeline of GW150914

---

- **1.3 billion years ago:** 2 black holes merge and release  $3 M_{\odot}$  of gravitational wave energy into the universe.
- **100,000 years ago:** these waves arrive at the edge of the milky way galaxy.
- **November 25, 1915:** Albert Einstein presents his General Theory of Relativity to the Prussian Academy of Sciences. GW150914 is 99 years, 9 months, and 20 days away
- **April 15, 1972:** at MIT Rai Weiss' Publication of Quarterly Progress Report No. 105 outlines the concept behind LIGO
- **1992:** The epoch of LIGO construction begins, leading to the realisation of the two observatories LIGO Livingston (LLO) and LIGO Hanford (LHO).
- **mid-late 90s:** Some of this audience are born.
- **2002:** The two initial LIGO detectors and the GEO 600 detector start their first period of scientific data taking, 'Science Run 1'.
- ...

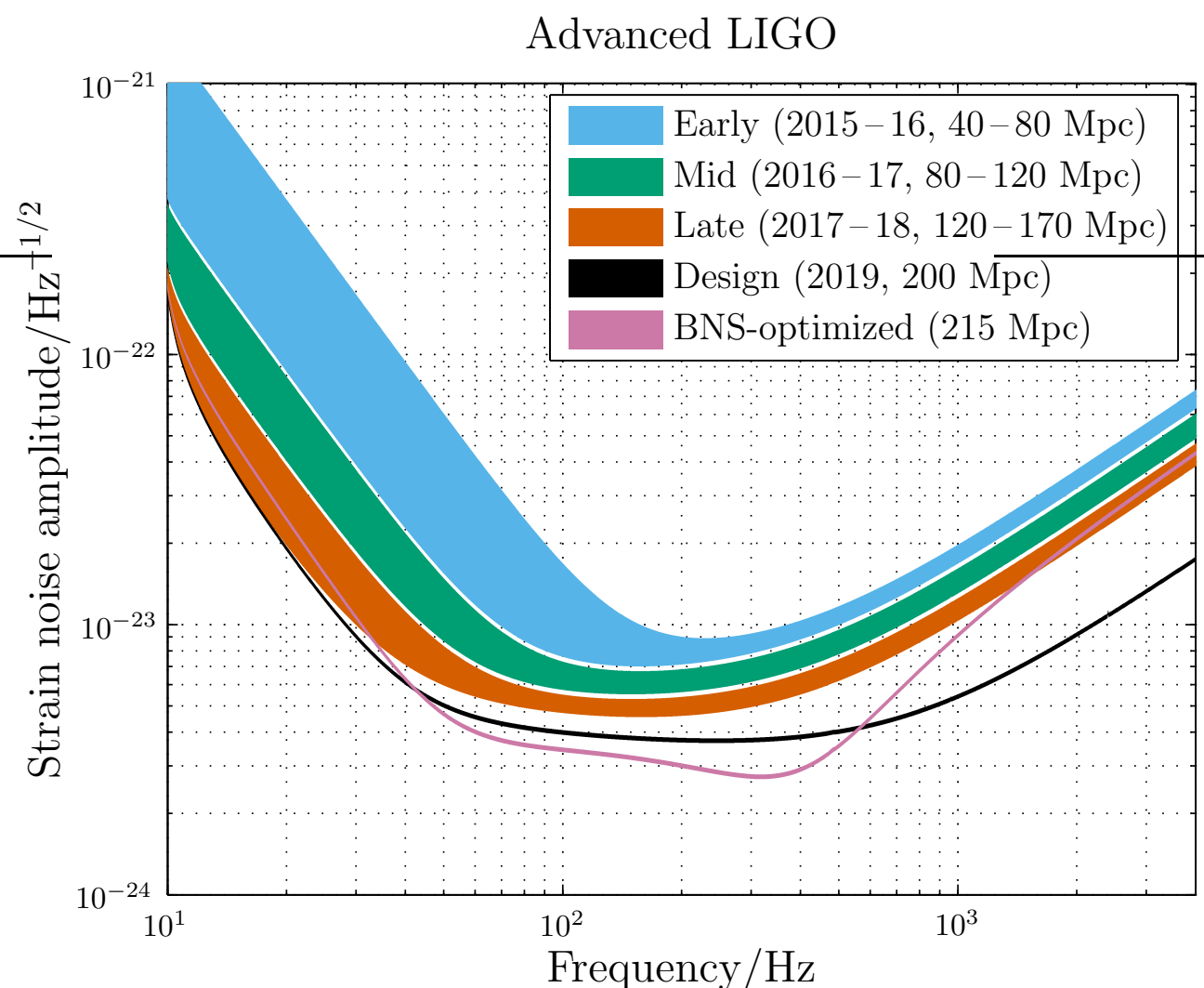
# The rest of the 1st observing run (O1)

---

GW151012 (formerly LVT151012), and GW151226

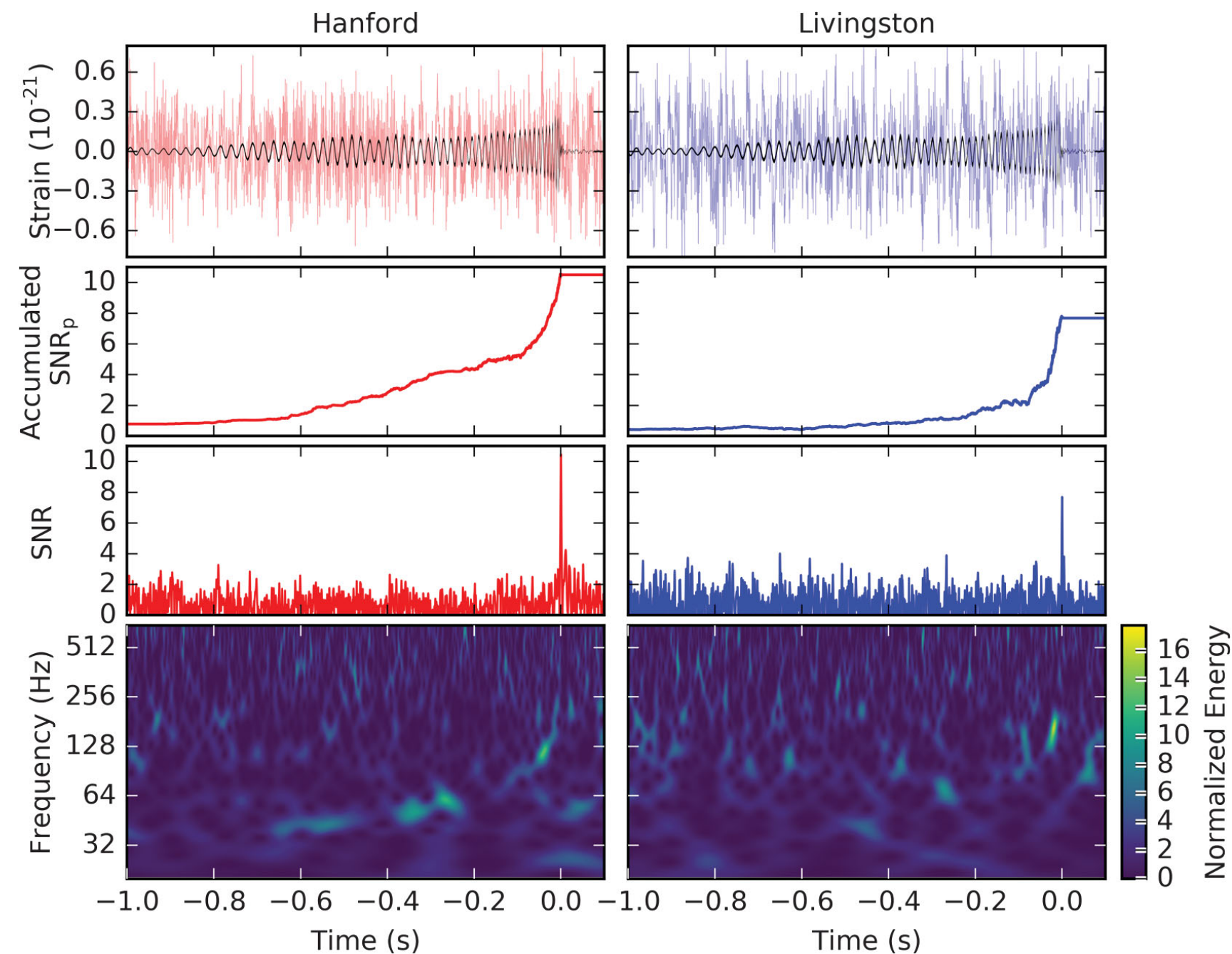
# The O1 run (Sep 2015 - Jan 2016)

- Initial LIGO and Virgo successfully completed their operations with the S6/VSR2,3 runs in 2011.
- Advanced LIGO began operation in September 2015 with the first “Observing” run O1 spanning 12th Sep - 19th Jan.
- This accumulated 51.5 days of coincident data.

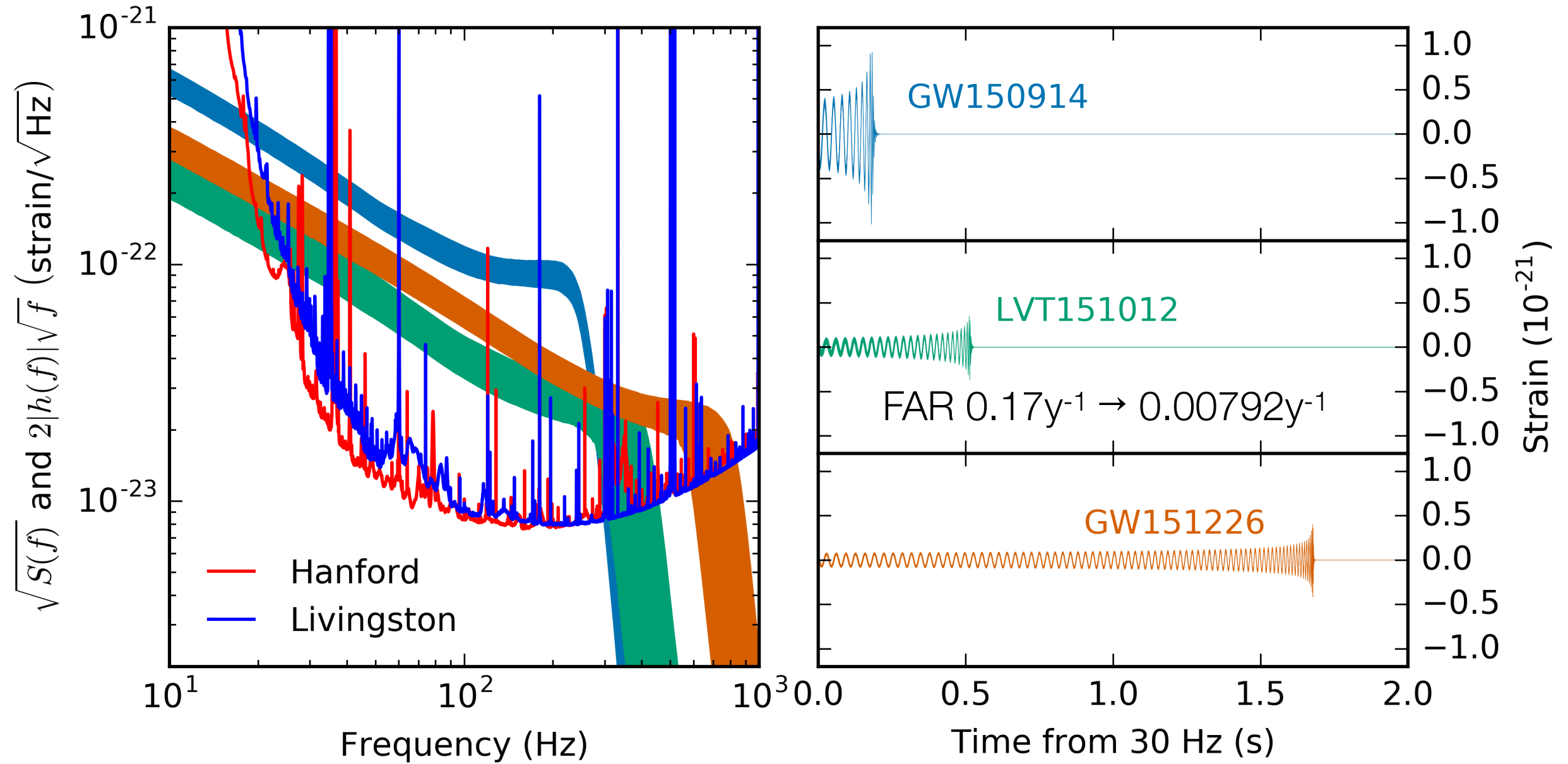


# GW151226 (Boxing Day event)

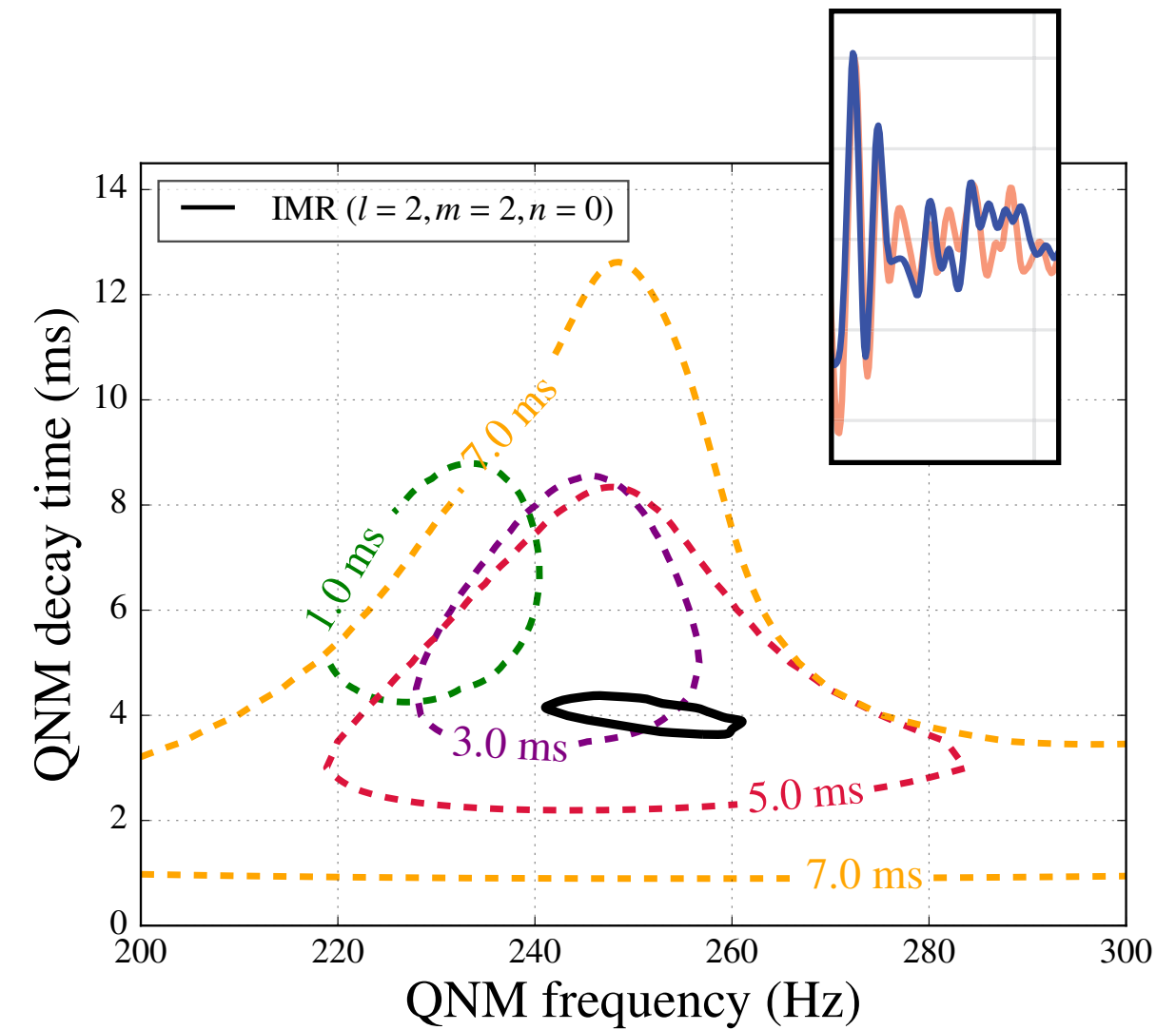
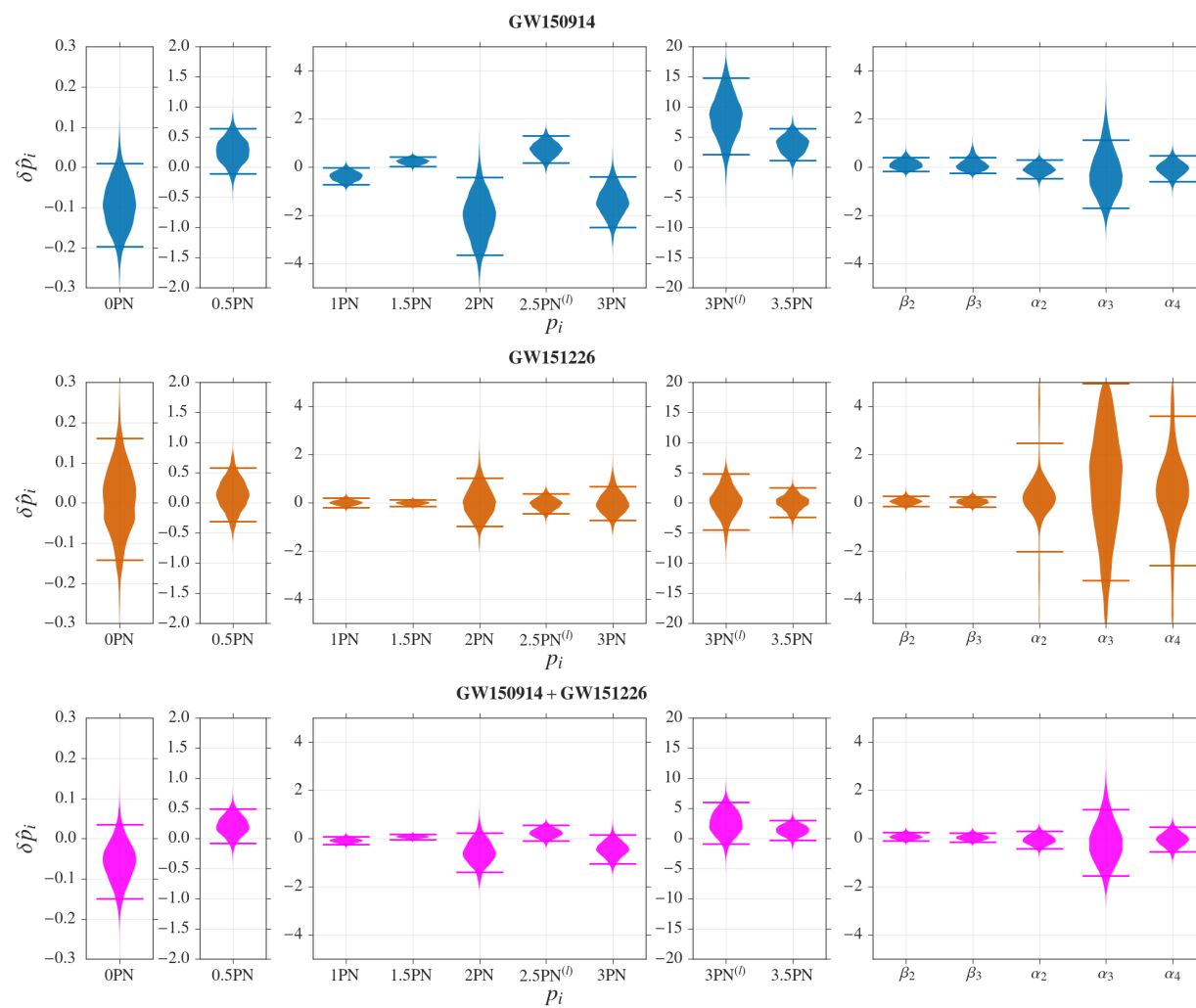
3rd



# O1 Waveform comparison



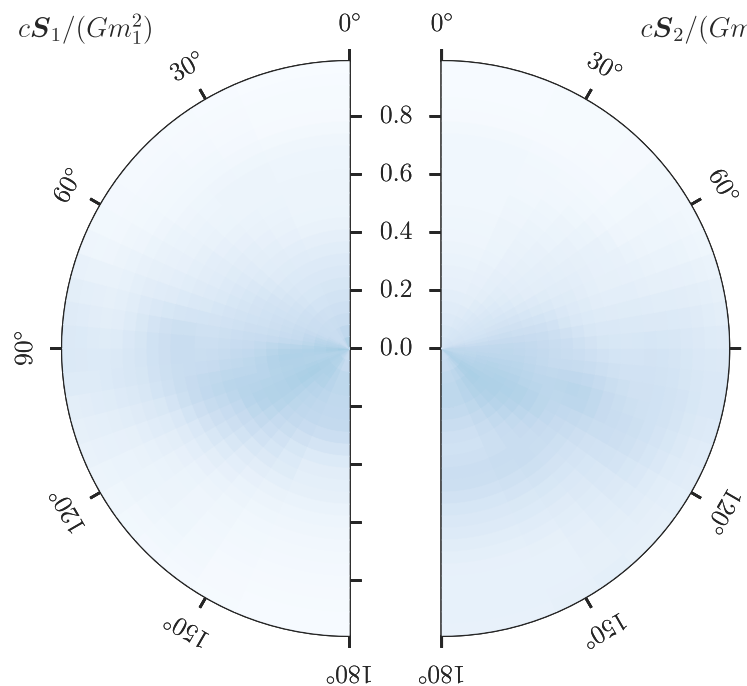
# Is general relativity right?



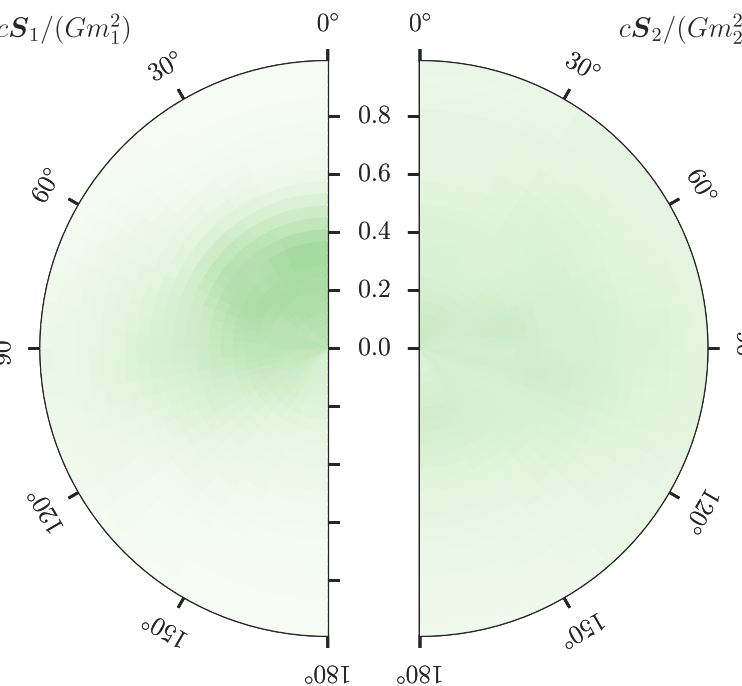
# O1 Spins

---

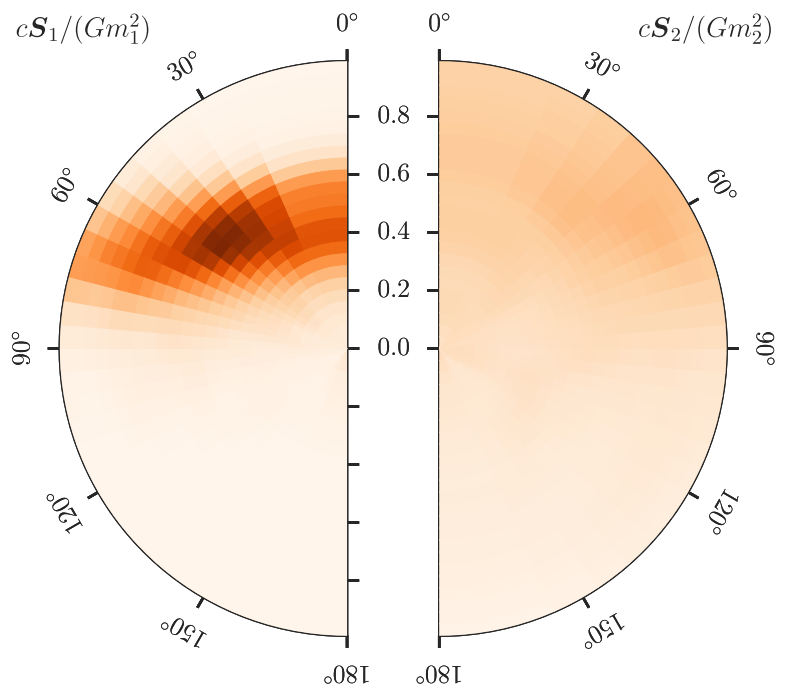
GW150914



GW151012



GW151226



## The 2nd observing run (O2)

---

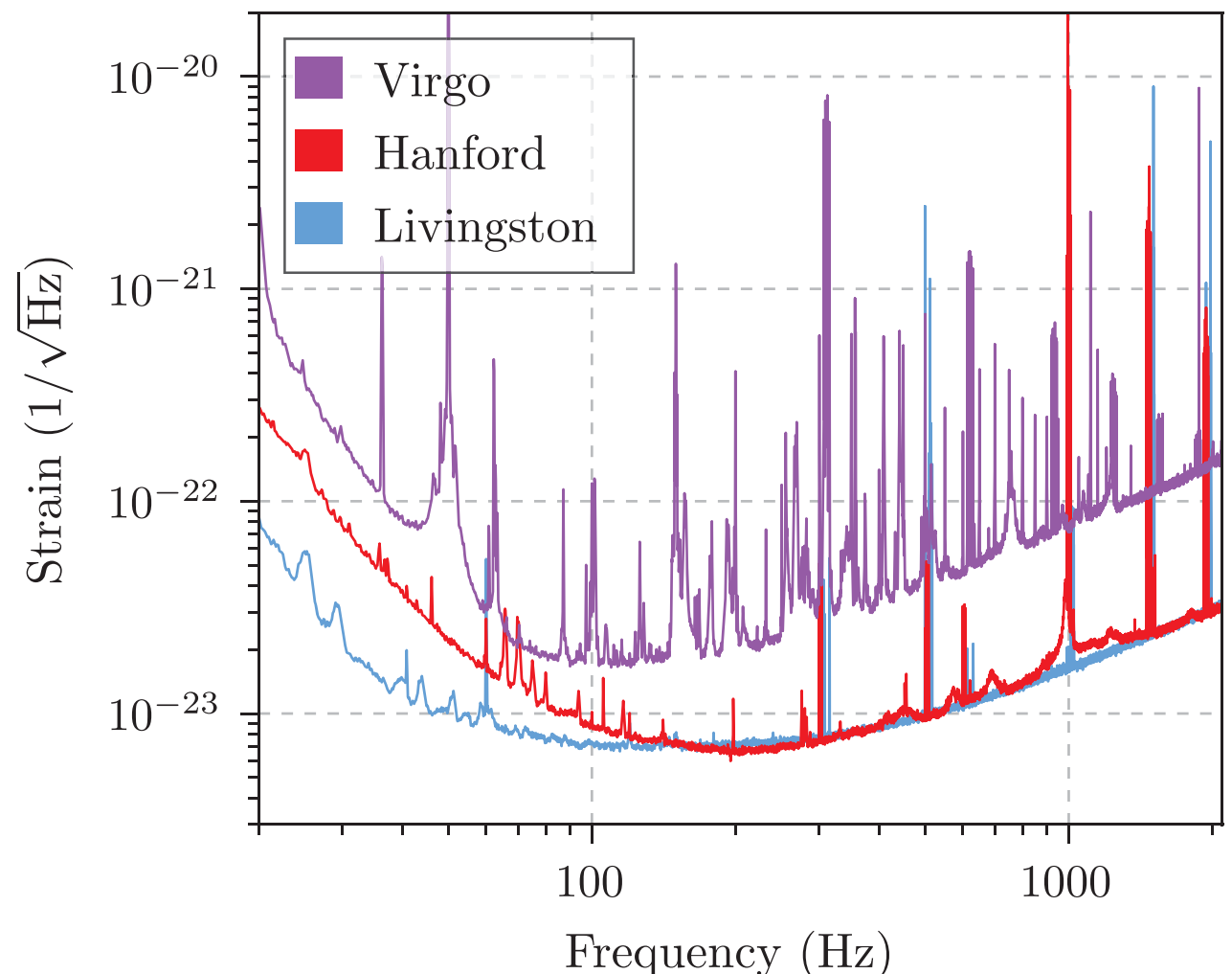
[ONLINE] GW170104, GW170608, GW170814, (the BNS GW170817),

and...

[OFFLINE] GW170729, GW170819, GW170818, and GW170823

# The O2 run (Nov 2016 - Sep 2017)

- The Advanced LIGO O2 run began in November 2016 and ended in September 2017.
- Sensitivity was marginally improved but most importantly, Virgo joined in September 2017.
- From this data we have published 3 BBH detections and 1 BNS detection (GW170817).



# GW170104

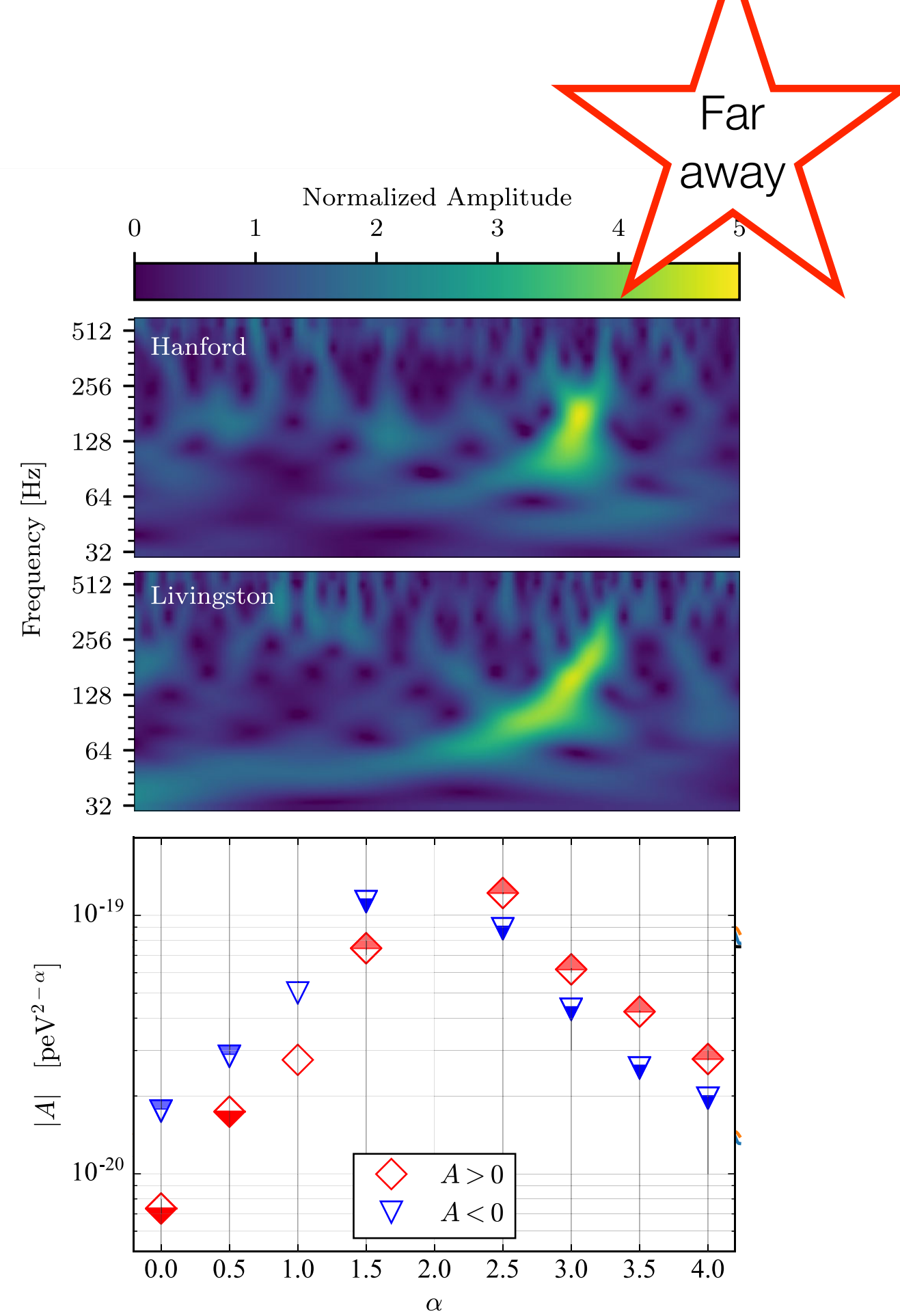
- This event had component masses of  $31^{+8.4}_{-6.0}$  and  $19^{+5.3}_{-5.9} M_{\odot}$ .
- This event was at redshift 0.2 and had SNR 13.
- Combining this event with previous detections allows us to constrain the graviton mass and wavelength

$$m_g \leq 7.7 \times 10^{-23} \text{ eV}/c^2$$

$$\lambda_g > 1.6 \times 10^{13} \text{ km}$$

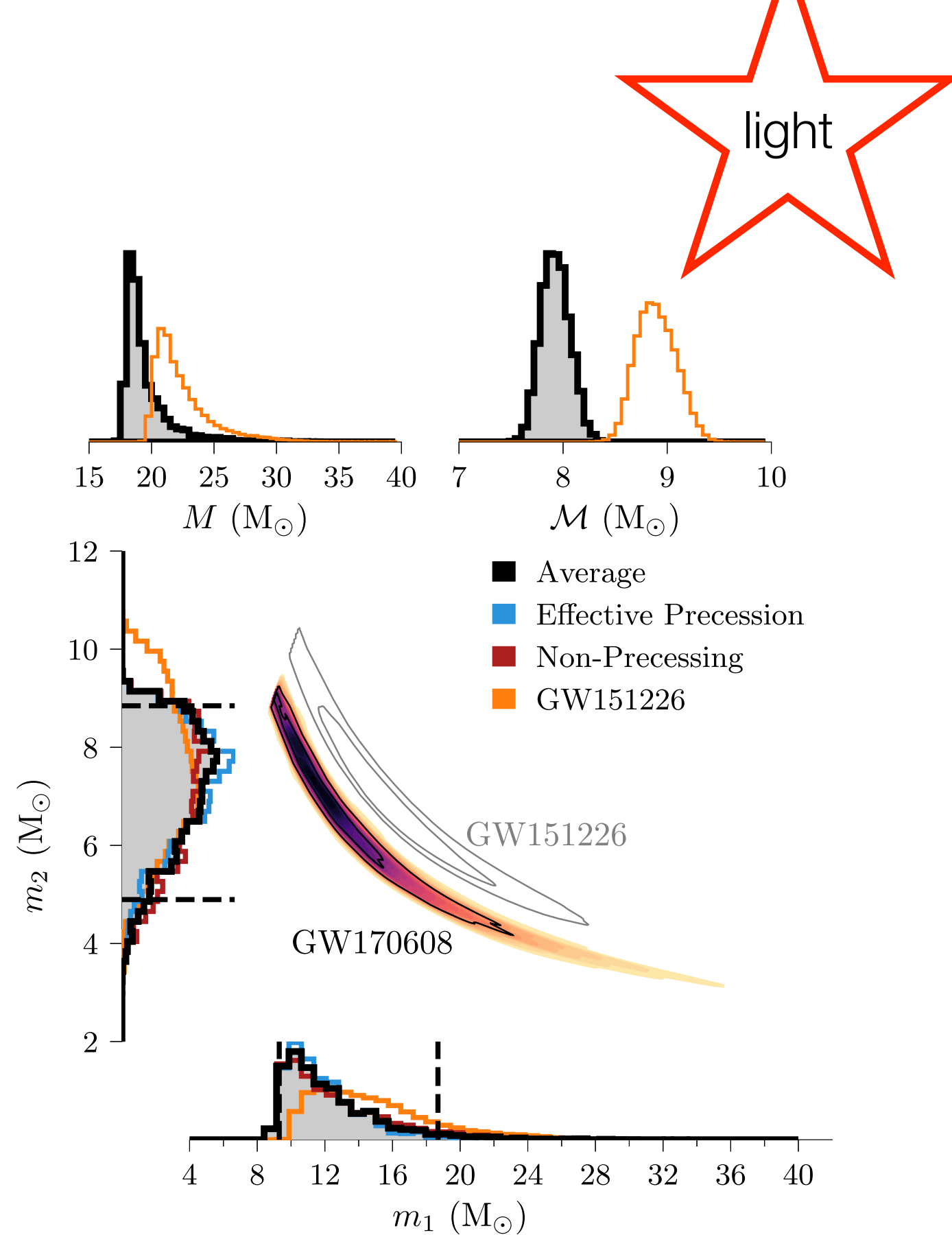
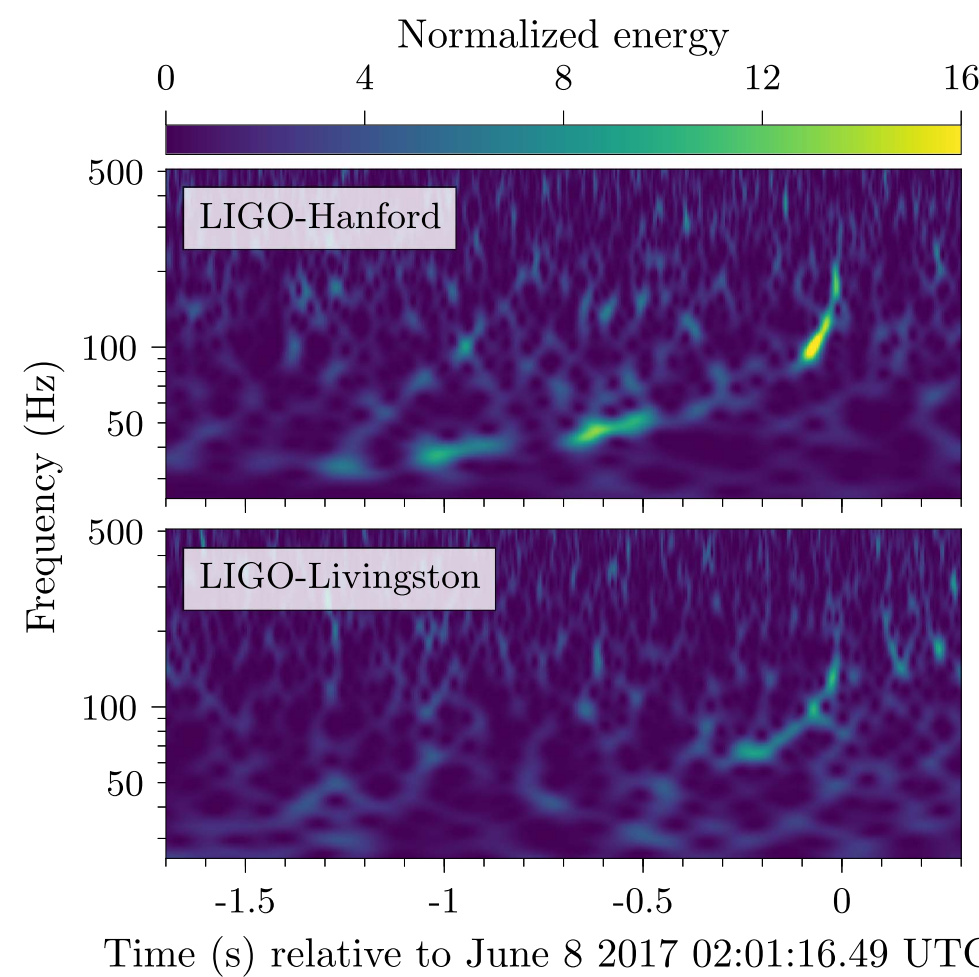
- Using a modified dispersion relation the group velocity of the GWs becomes

$$\frac{v_g}{c} = 1 + \frac{1}{2}(\alpha - 1)AE^{\alpha-2}$$



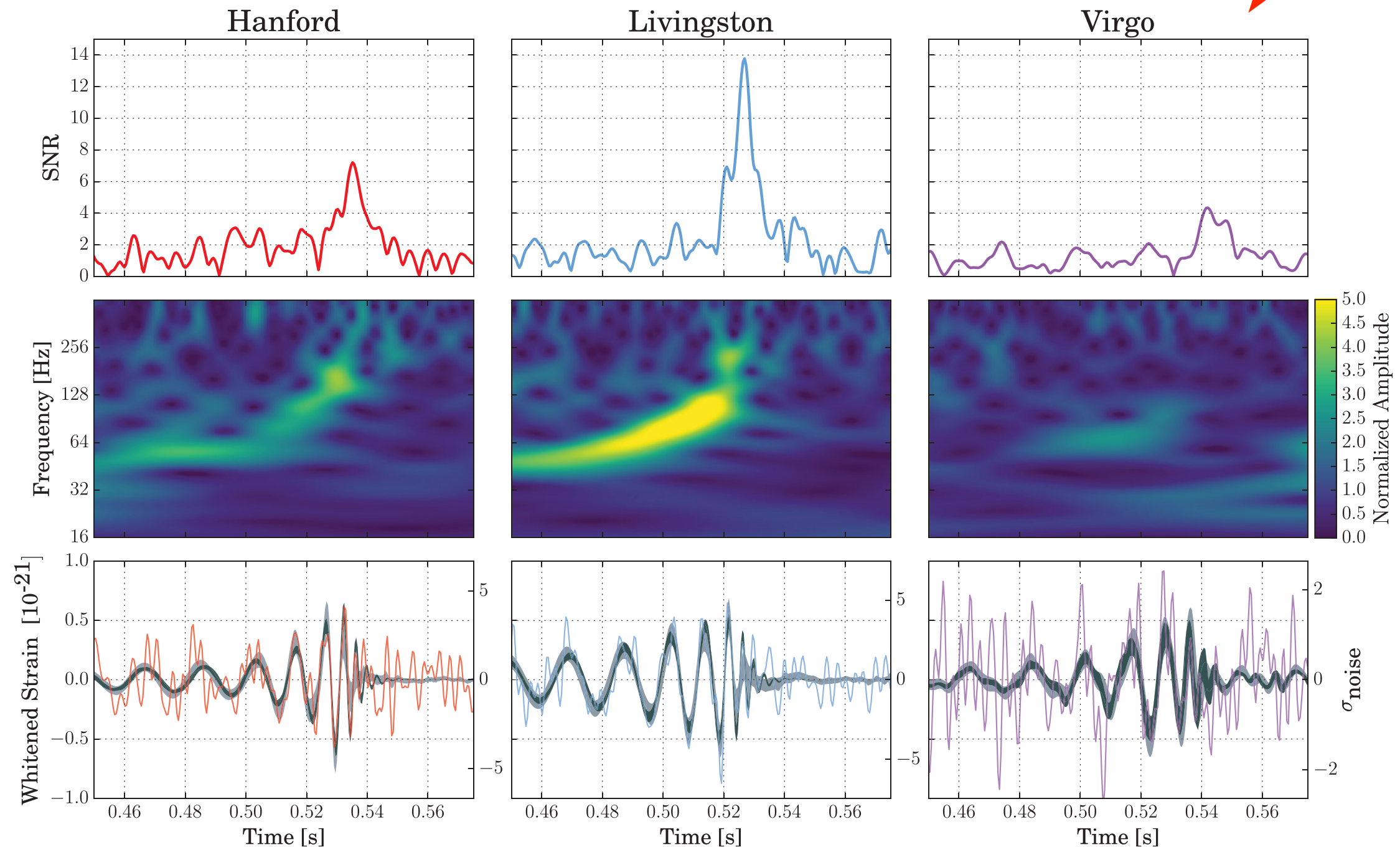
# GW170608

- This event had component masses of  $12^{+7}_{-2}$  and  $7^{+2}_{-2} M_{\odot}$ .
- This event was at redshift 0.07 and had SNR 13.

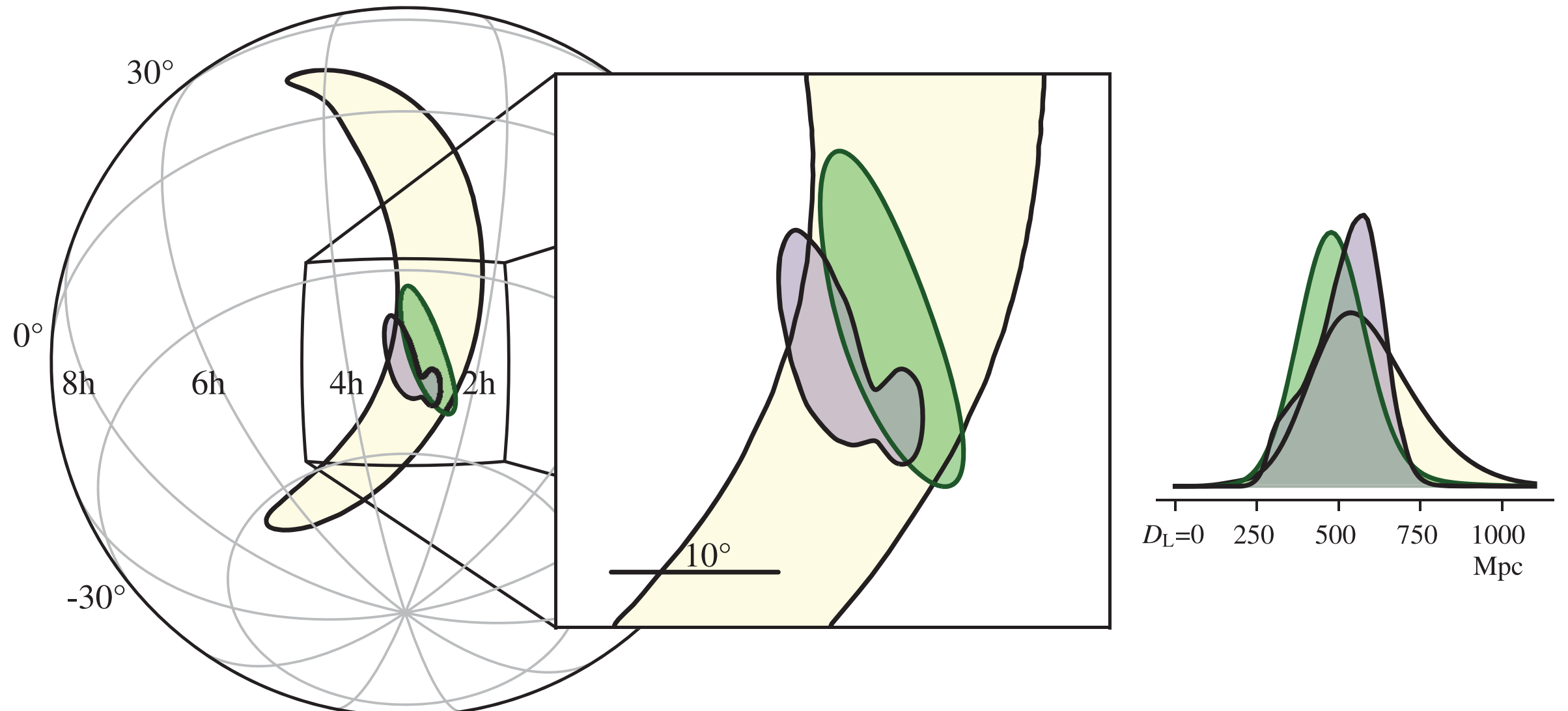


# GW170814

LIGO &  
Virgo



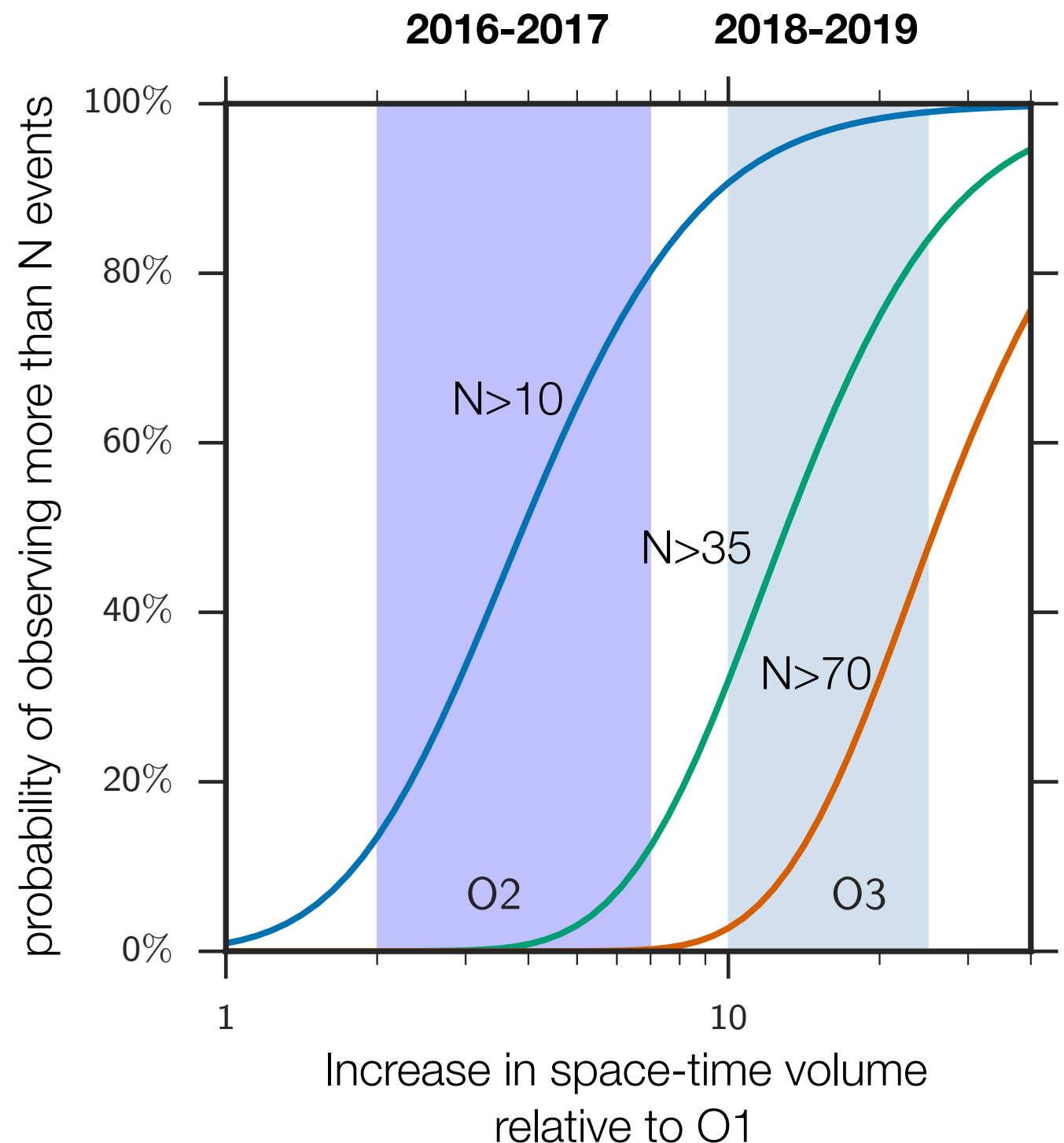
# GW170814



- This event had component masses of  $31$  and  $19 M_{\odot}$ .
- This event was at redshift  $0.2$  and had SNR  $13$ .

# What happens next?

- The first observing runs O1 and O2 are the first of many as the detectors improve in sensitivity.
- O3 will have  $\sim$ 50 times the sensitivity of O1.
- There **will be** many more detections.
- We must also not forget binary neutron stars, unmodelled transients, stochastic background, continuous signals, ...



# Additional properties

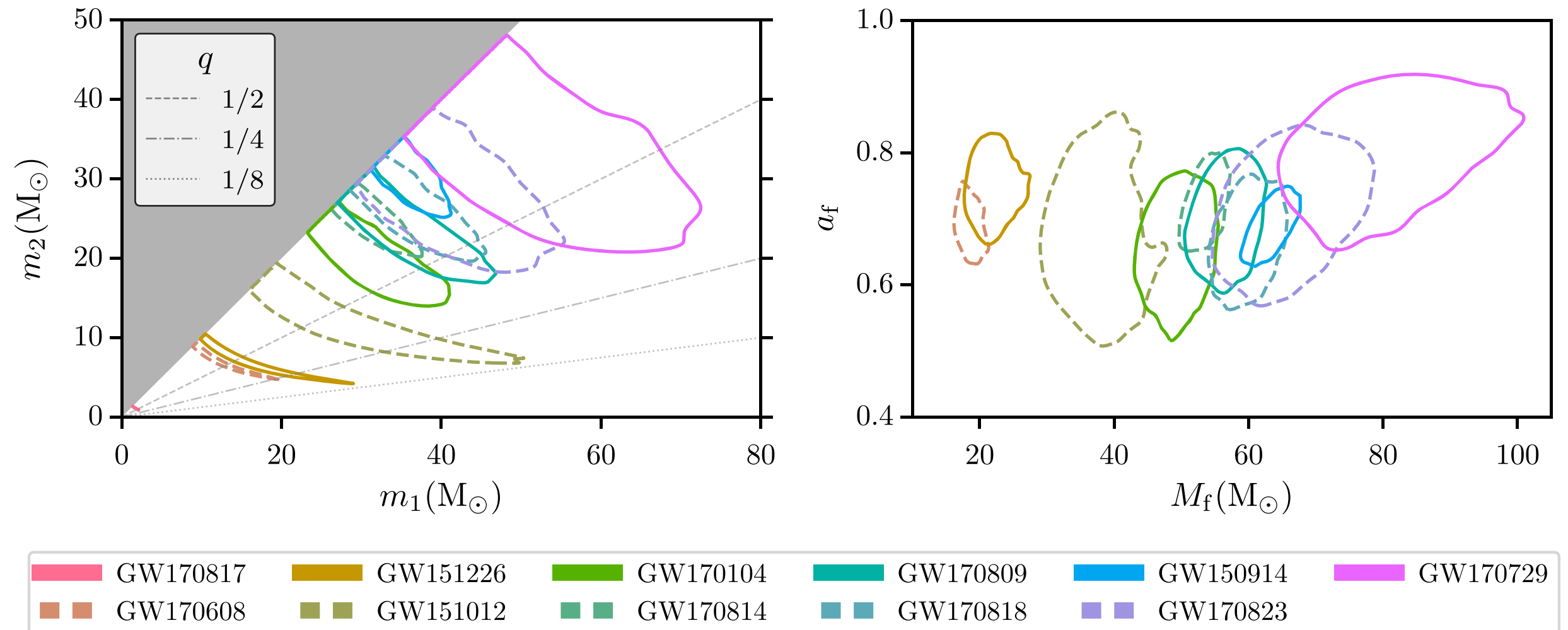
---

Characteristics of the ensemble

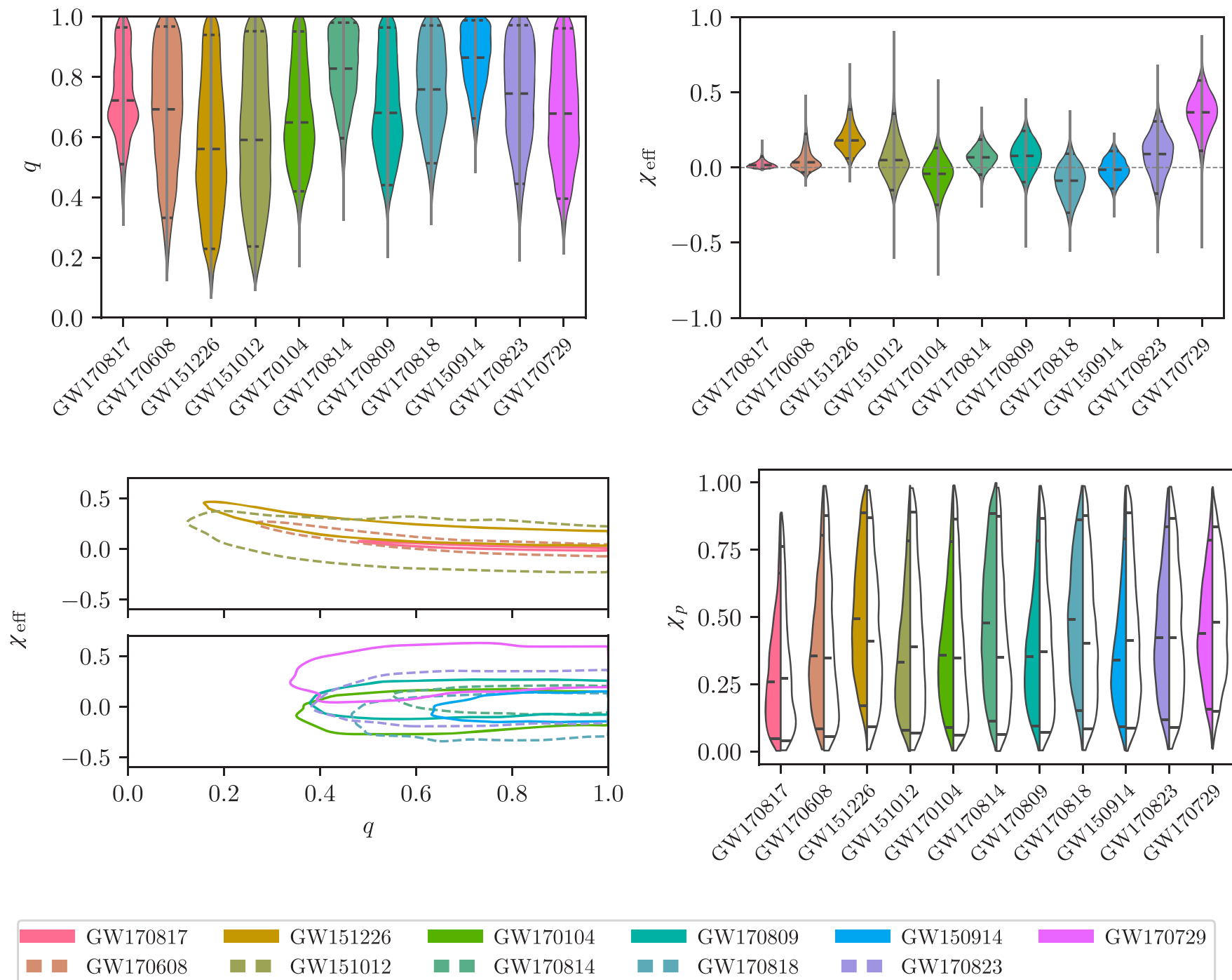
# The big table of O1/O2 BBH properties

| Event    | $m_1/M_\odot$          | $m_2/M_\odot$          | $\mathcal{M}/M_\odot$     | $\chi_{\text{eff}}$     | $M_f/M_\odot$          | $a_f$                  | $E_{\text{rad}}/(M_\odot c^2)$ | $\ell_{\text{peak}}/(\text{erg s}^{-1})$ | $d_L/\text{Mpc}$       | $z$                    | $\Delta\Omega/\text{deg}^2$ |
|----------|------------------------|------------------------|---------------------------|-------------------------|------------------------|------------------------|--------------------------------|--|------------------------|------------------------|-----------------------------|
| GW150914 | $35.6^{+4.7}_{-3.1}$   | $30.6^{+3.0}_{-4.4}$   | $28.6^{+1.7}_{-1.5}$      | $-0.01^{+0.12}_{-0.13}$ | $63.1^{+3.4}_{-3.0}$   | $0.69^{+0.05}_{-0.04}$ | $3.1^{+0.4}_{-0.4}$            | $3.6^{+0.4}_{-0.4} \times 10^{56}$       | $440^{+150}_{-170}$    | $0.09^{+0.03}_{-0.03}$ | 182                         |
| GW151012 | $23.2^{+14.9}_{-5.5}$  | $13.6^{+4.1}_{-4.8}$   | $15.2^{+2.1}_{-1.2}$      | $0.05^{+0.31}_{-0.20}$  | $35.6^{+10.8}_{-3.8}$  | $0.67^{+0.13}_{-0.11}$ | $1.6^{+0.6}_{-0.5}$            | $3.2^{+0.8}_{-1.7} \times 10^{56}$       | $1080^{+550}_{-490}$   | $0.21^{+0.09}_{-0.09}$ | 1523                        |
| GW151226 | $13.7^{+8.8}_{-3.2}$   | $7.7^{+2.2}_{-2.5}$    | $8.9^{+0.3}_{-0.3}$       | $0.18^{+0.20}_{-0.12}$  | $20.5^{+6.4}_{-1.5}$   | $0.74^{+0.07}_{-0.05}$ | $1.0^{+0.1}_{-0.2}$            | $3.4^{+0.7}_{-1.7} \times 10^{56}$       | $450^{+180}_{-190}$    | $0.09^{+0.04}_{-0.04}$ | 1033                        |
| GW170104 | $30.8^{+7.3}_{-5.6}$   | $20.0^{+4.9}_{-4.6}$   | $21.4^{+2.2}_{-1.8}$      | $-0.04^{+0.17}_{-0.21}$ | $48.9^{+5.1}_{-4.0}$   | $0.66^{+0.08}_{-0.11}$ | $2.2^{+0.5}_{-0.5}$            | $3.3^{+0.6}_{-1.0} \times 10^{56}$       | $990^{+440}_{-430}$    | $0.20^{+0.08}_{-0.08}$ | 921                         |
| GW170608 | $11.0^{+5.5}_{-1.7}$   | $7.6^{+1.4}_{-2.2}$    | $7.9^{+0.2}_{-0.2}$       | $0.03^{+0.19}_{-0.07}$  | $17.8^{+3.4}_{-0.7}$   | $0.69^{+0.04}_{-0.04}$ | $0.9^{+0.0}_{-0.1}$            | $3.5^{+0.4}_{-1.3} \times 10^{56}$       | $320^{+120}_{-110}$    | $0.07^{+0.02}_{-0.02}$ | 392                         |
| GW170729 | $50.2^{+16.2}_{-10.2}$ | $34.0^{+9.1}_{-10.1}$  | $35.4^{+6.5}_{-4.8}$      | $0.37^{+0.21}_{-0.25}$  | $79.5^{+14.7}_{-10.2}$ | $0.81^{+0.07}_{-0.13}$ | $4.8^{+1.7}_{-1.7}$            | $4.2^{+0.9}_{-1.5} \times 10^{56}$       | $2840^{+1400}_{-1360}$ | $0.49^{+0.19}_{-0.21}$ | 1041                        |
| GW170809 | $35.0^{+8.3}_{-5.9}$   | $23.8^{+5.1}_{-5.2}$   | $24.9^{+2.1}_{-1.7}$      | $0.08^{+0.17}_{-0.17}$  | $56.3^{+5.2}_{-3.8}$   | $0.70^{+0.08}_{-0.09}$ | $2.7^{+0.6}_{-0.6}$            | $3.5^{+0.6}_{-0.9} \times 10^{56}$       | $1030^{+320}_{-390}$   | $0.20^{+0.05}_{-0.07}$ | 308                         |
| GW170814 | $30.6^{+5.6}_{-3.0}$   | $25.2^{+2.8}_{-4.0}$   | $24.1^{+1.4}_{-1.1}$      | $0.07^{+0.12}_{-0.12}$  | $53.2^{+3.2}_{-2.4}$   | $0.72^{+0.07}_{-0.05}$ | $2.7^{+0.4}_{-0.3}$            | $3.7^{+0.4}_{-0.5} \times 10^{56}$       | $600^{+150}_{-220}$    | $0.12^{+0.03}_{-0.04}$ | 87                          |
| GW170817 | $1.46^{+0.12}_{-0.10}$ | $1.27^{+0.09}_{-0.09}$ | $1.186^{+0.001}_{-0.001}$ | $0.00^{+0.02}_{-0.01}$  | $\leq 2.8$             | $\leq 0.89$            | $\geq 0.04$                    | $\geq 0.1 \times 10^{56}$                | $40^{+7}_{-15}$        | $0.01^{+0.00}_{-0.00}$ | 16                          |
| GW170818 | $35.4^{+7.5}_{-4.7}$   | $26.7^{+4.3}_{-5.2}$   | $26.5^{+2.1}_{-1.7}$      | $-0.09^{+0.18}_{-0.21}$ | $59.4^{+4.9}_{-3.8}$   | $0.67^{+0.07}_{-0.08}$ | $2.7^{+0.5}_{-0.5}$            | $3.4^{+0.5}_{-0.7} \times 10^{56}$       | $1060^{+420}_{-380}$   | $0.21^{+0.07}_{-0.07}$ | 39                          |
| GW170823 | $39.5^{+11.2}_{-6.7}$  | $29.0^{+6.7}_{-7.8}$   | $29.2^{+4.6}_{-3.6}$      | $0.09^{+0.22}_{-0.26}$  | $65.4^{+10.1}_{-7.4}$  | $0.72^{+0.09}_{-0.12}$ | $3.3^{+1.0}_{-0.9}$            | $3.6^{+0.7}_{-1.1} \times 10^{56}$       | $1940^{+970}_{-900}$   | $0.35^{+0.15}_{-0.15}$ | 1666                        |

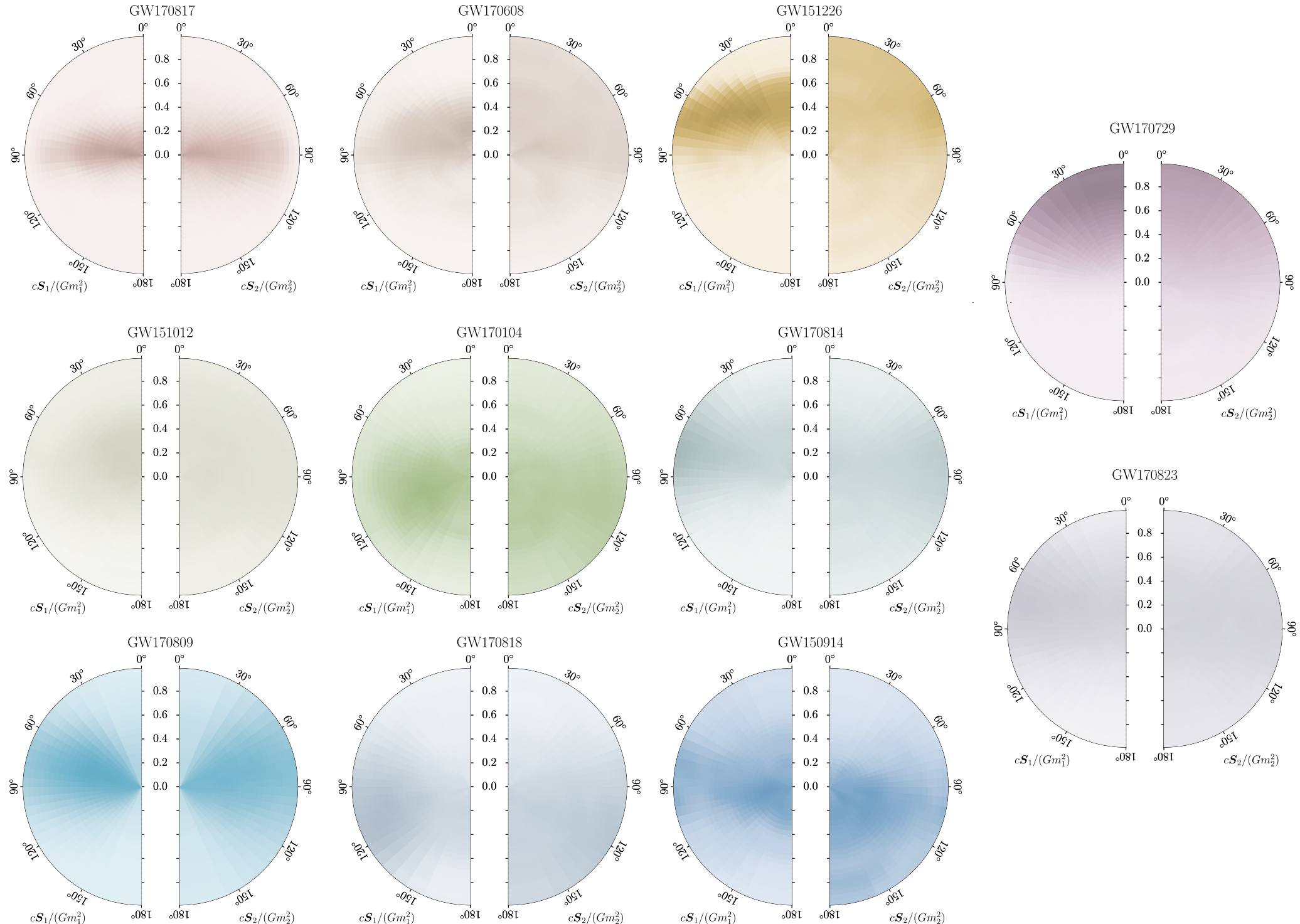
# Masses and spins



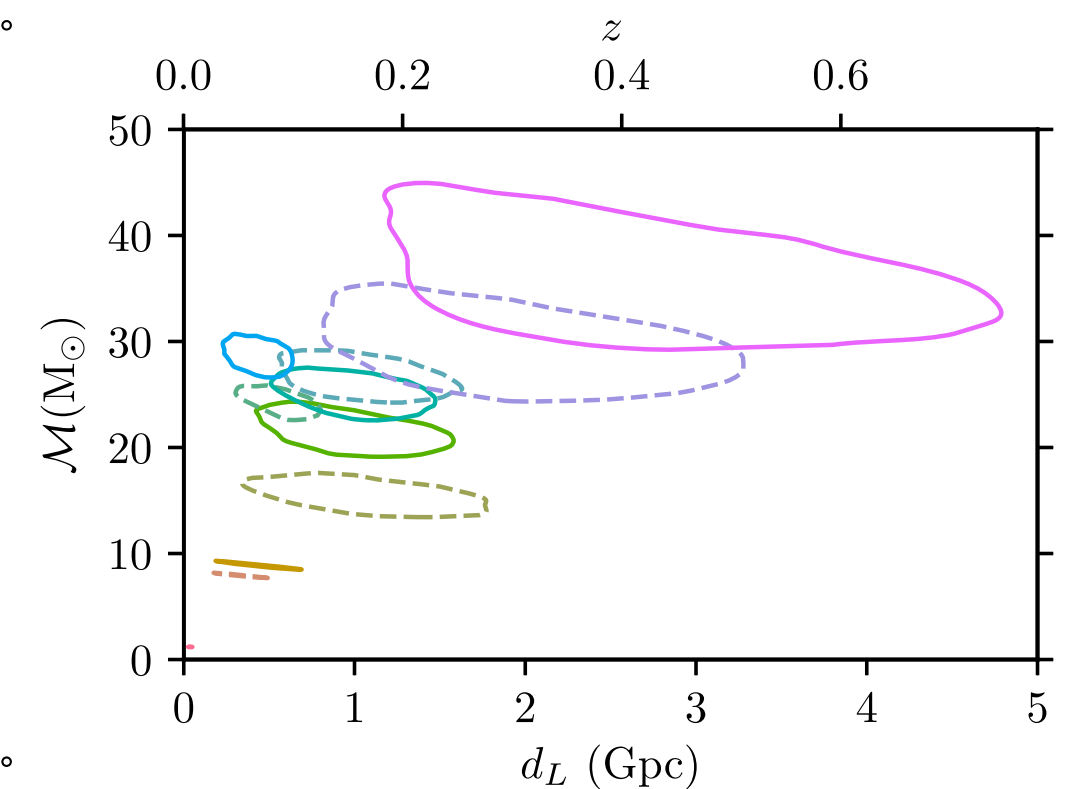
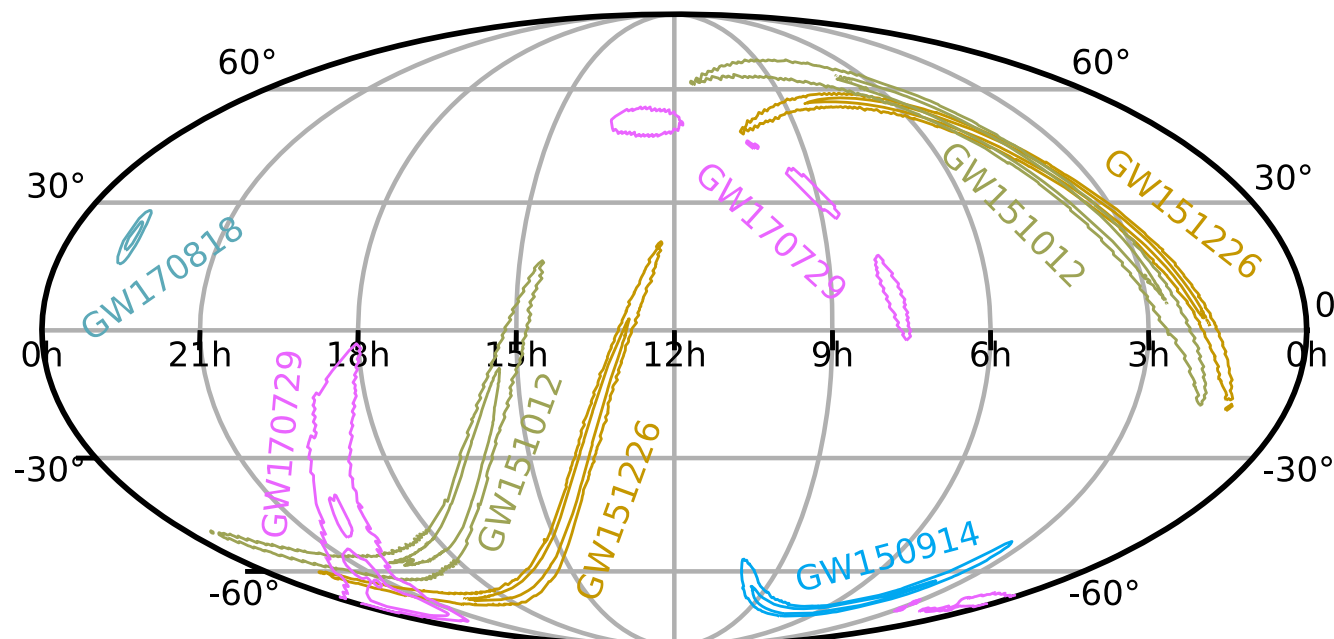
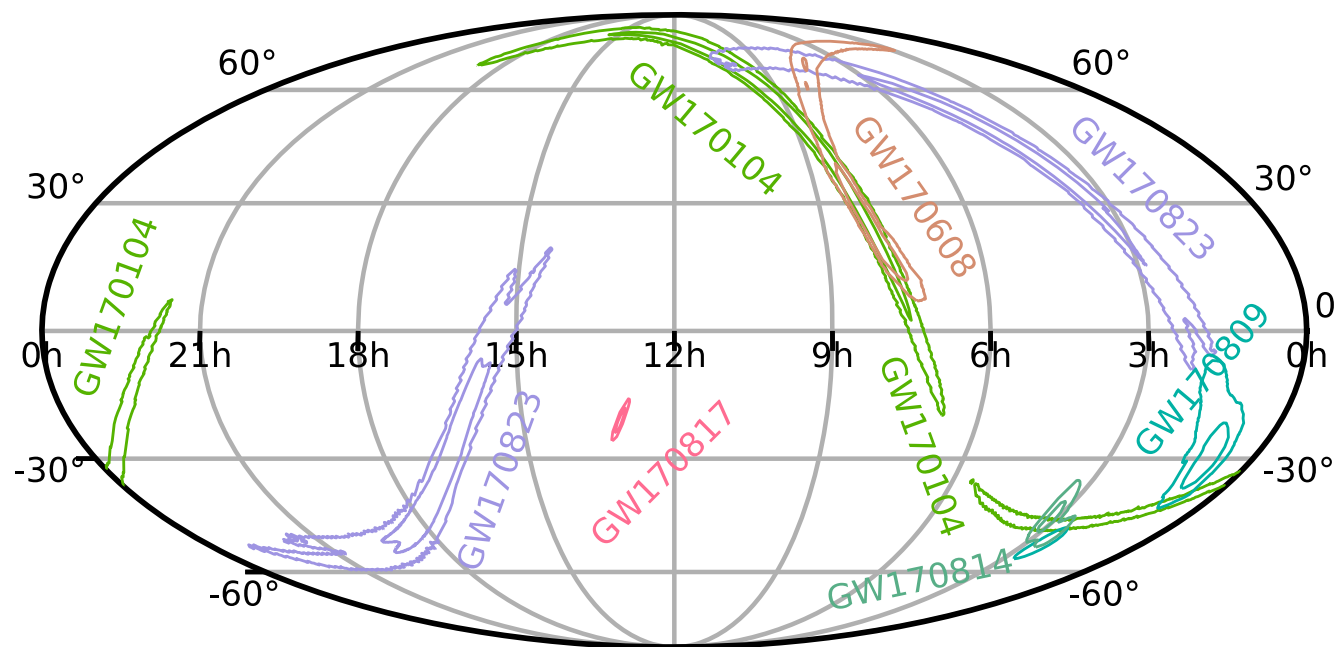
# Masses and spins



# Spins

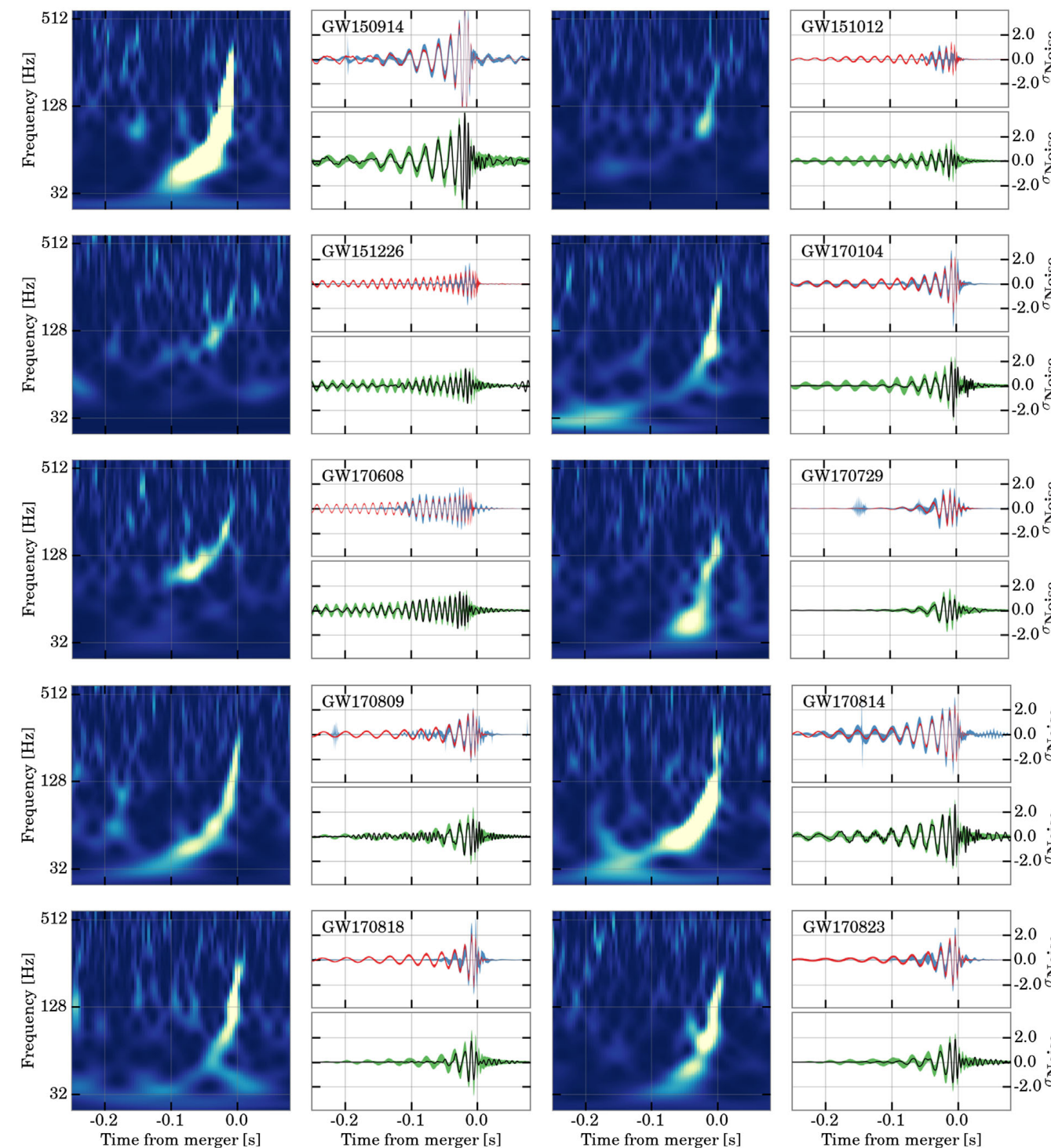


# Sky localisation



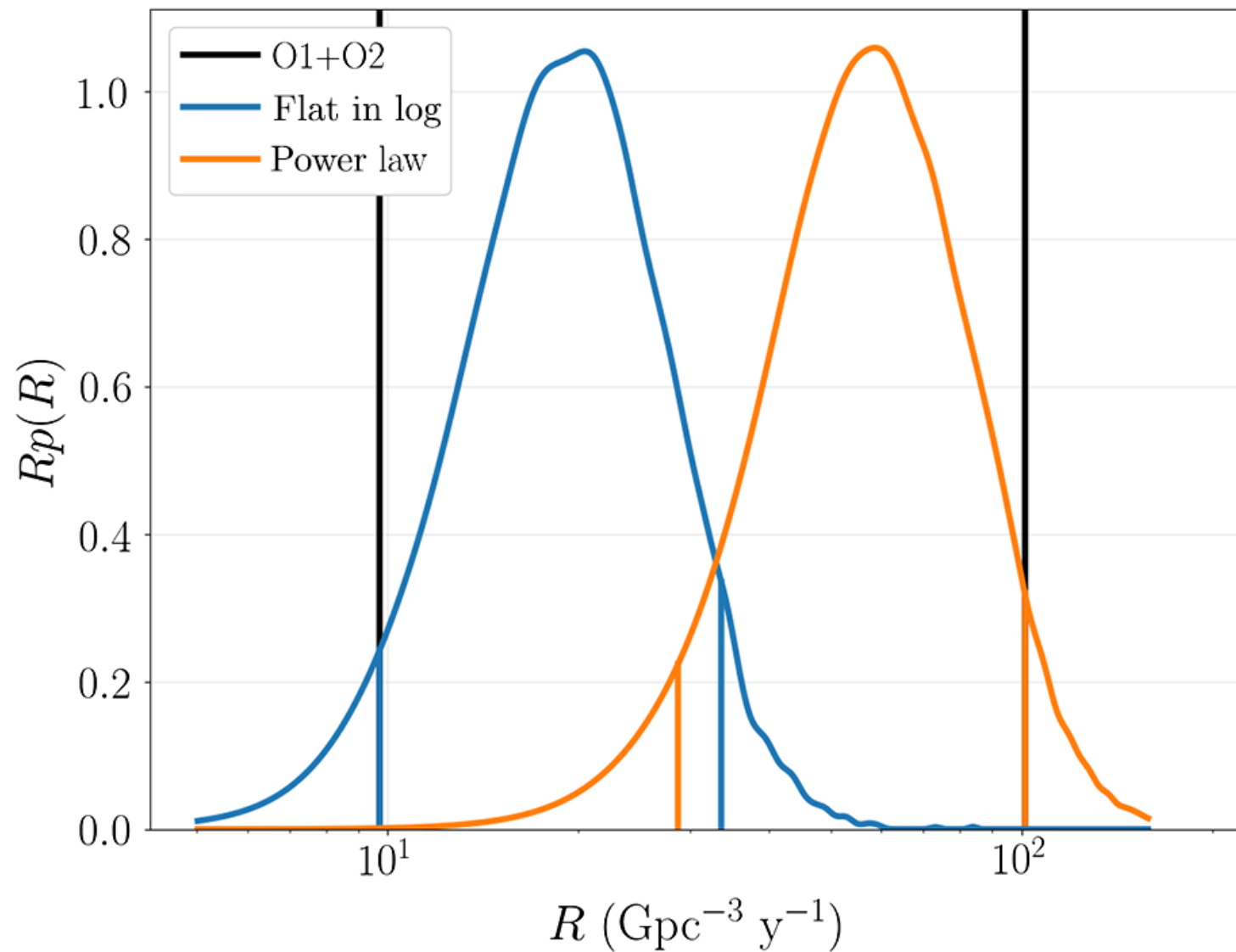
# Waveforms

---



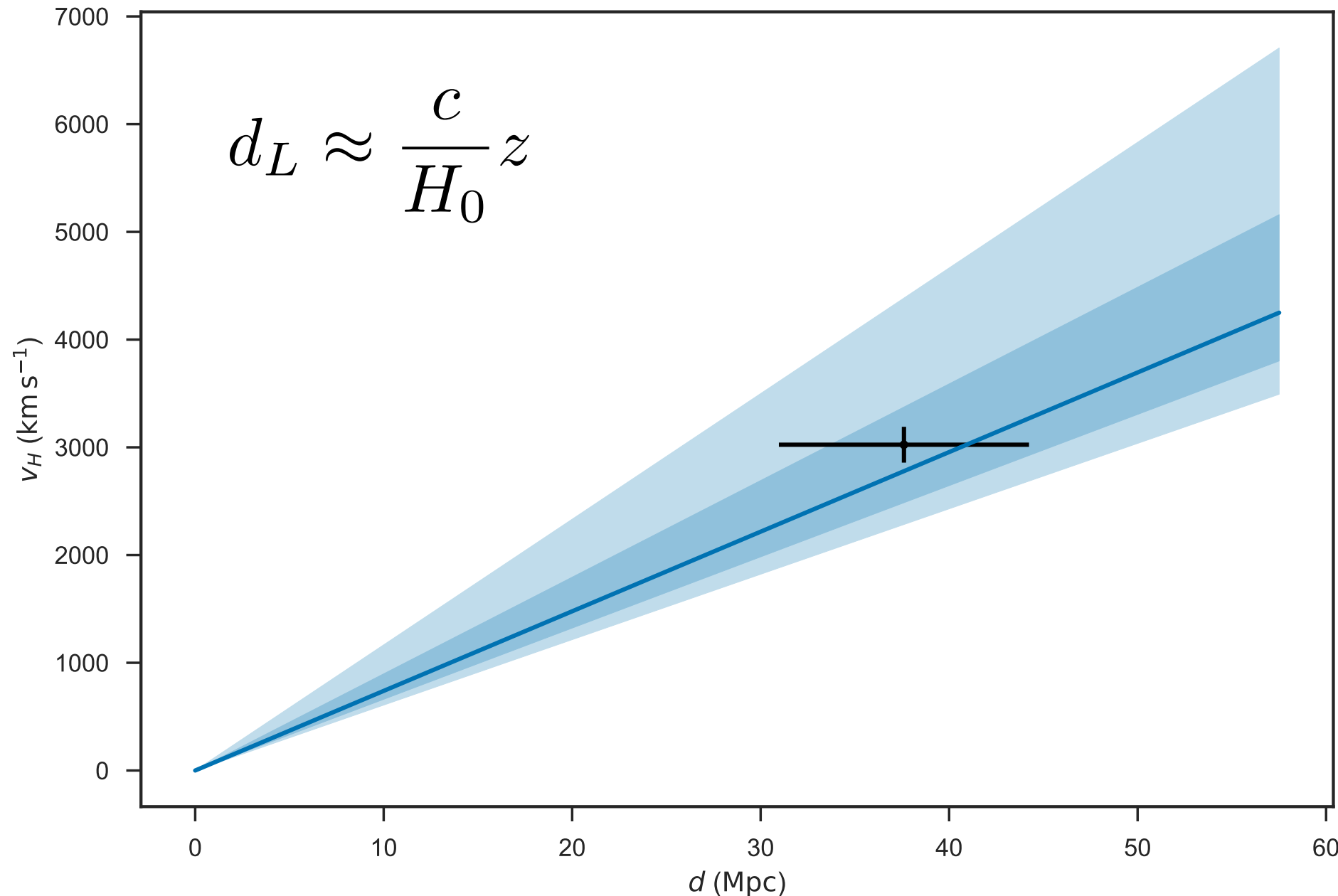
# Astrophysical Event Rate

---



# Cosmology

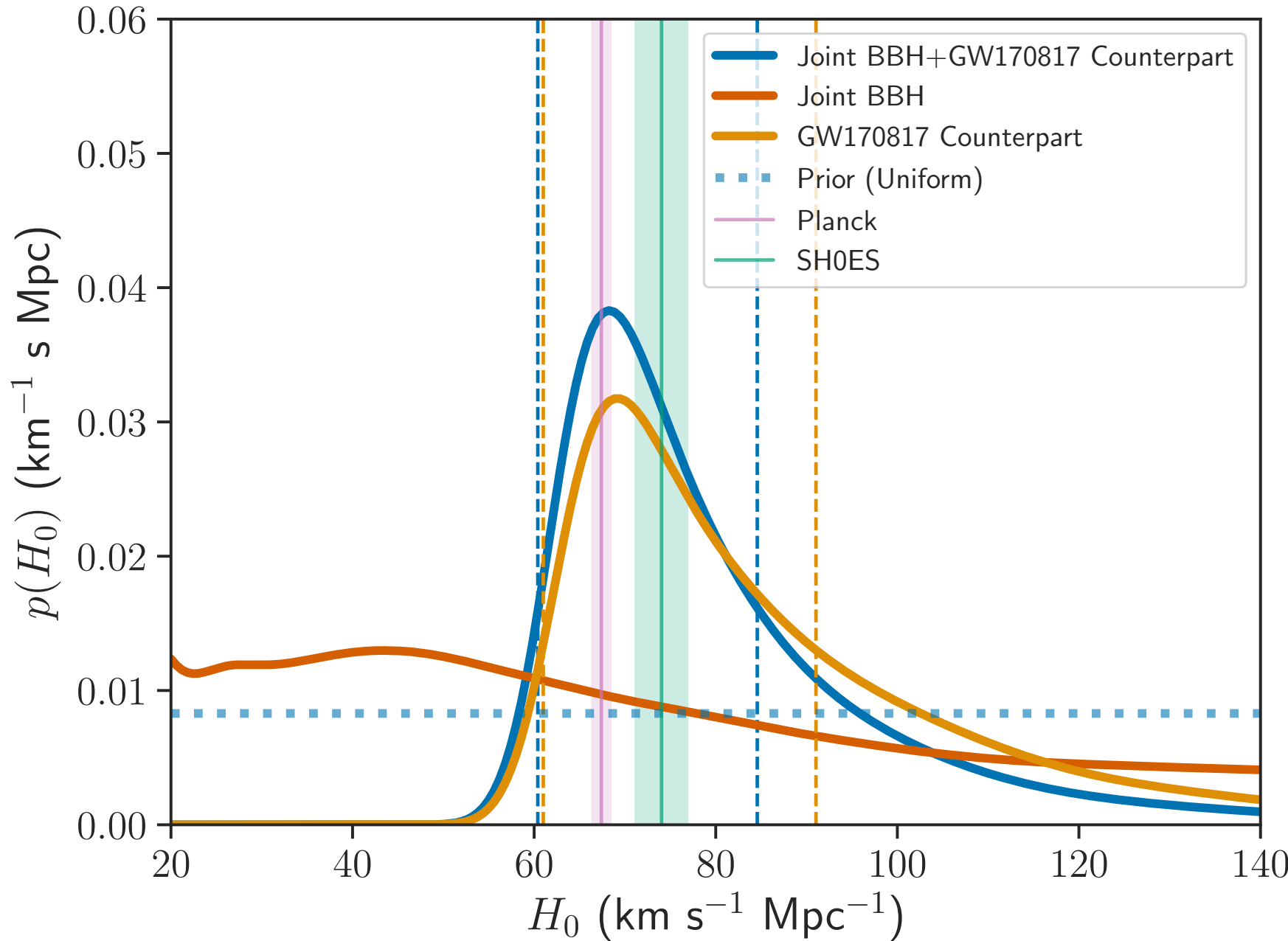
---



Credit: Will Farr

# The Hubble constant

---



# A distance limit

---

- The strain at the source can at most be  $\sim 1$  at the Schwarzschild radius. Since the amplitude decreases as

$$h \sim R/d_L$$

- Therefore we can set an upper-limit on the distance based on the measured peak strain amplitude

$$d_L \leq 10^{21} \times 100 \text{ km} \sim 3 \text{ Gpc}$$

- This is very rough. See problems for an opportunity to refine it.

# A rough luminosity

---

- By Setting

$$\omega \sim c/r \text{ and } r \sim GM/c^2 \text{ and } M\omega \sim c^3/G$$

- By dimensional analysis of the quadrupole formula

$$L \sim \frac{G}{c^5} M^2 r^4 \omega^6$$

- We get the following universal approximation

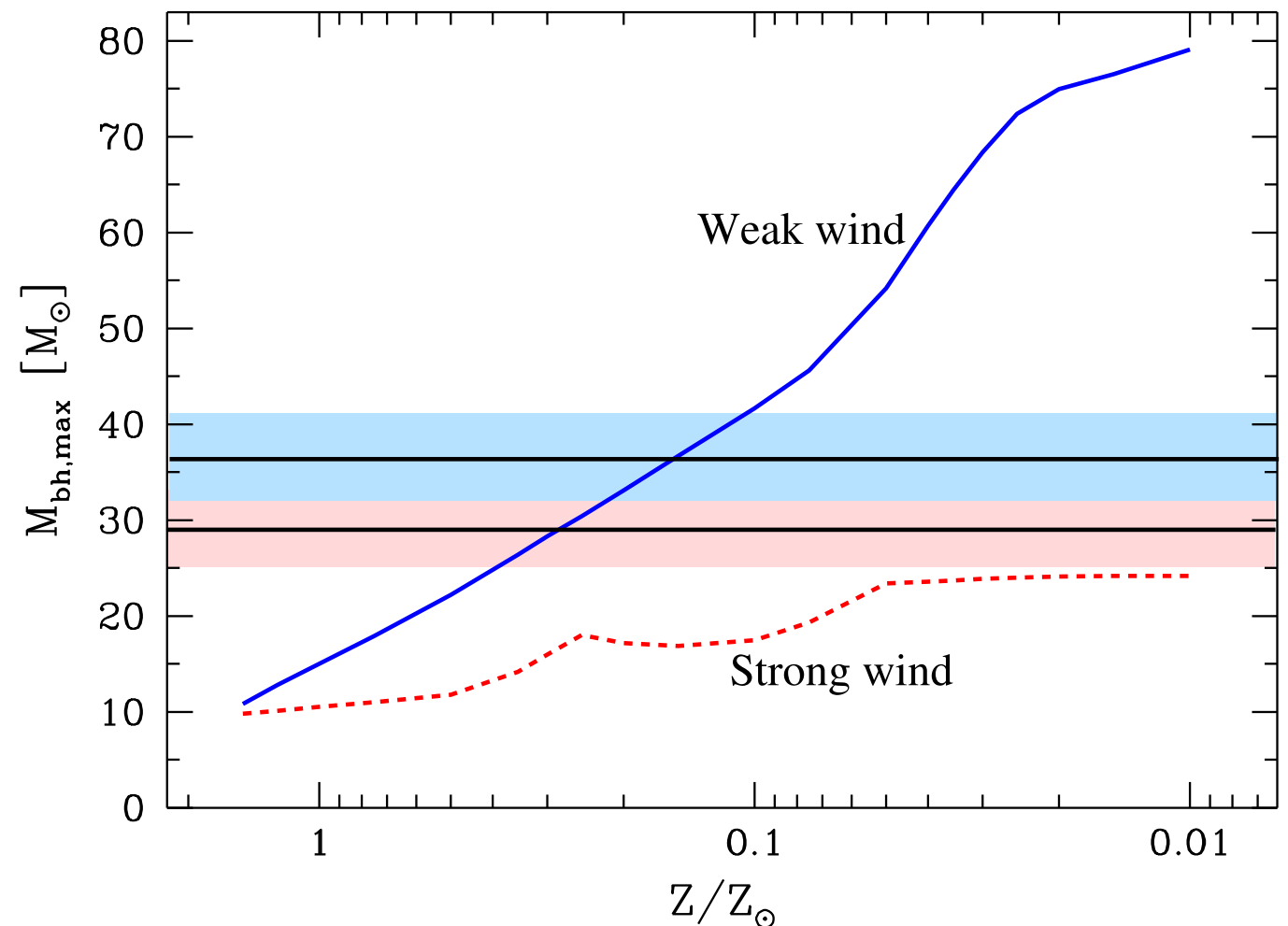
$$L \sim L_{\text{Planck}} = c^5/G.$$

- Hence, to within factors of a few, all CBC events are equally luminous ( $3 \times 10^{56}$  ergs/sec) since the mass sets both the characteristic energy and time scale of the event.

- However, a more slightly refined analysis gives  $L \sim \frac{c^3 d_L^2}{4G} |\dot{h}|^2 \sim \frac{c^5}{4G} \left( \frac{\omega_{\text{GW}} d_L h|_{\text{max}}}{c} \right)^2$

# What do the masses tell us?

- The most sensitive feature in determining the mass of a black hole is the metallicity of the star,  $Z$ .
- Low metallicity stars typically have less stellar wind allowing the progenitor star to maintain a higher mass.
- GW150914 comprised the heaviest known\* black-hole ( $\sim 35 M_{\odot}$ ) and indicates a possible low metallicity.



# The effect of spin

---

- We define the dimensionless spin parameter  $\chi = \frac{c}{G} \frac{S}{m^2}$
- This modifies the gravitational radii (as well as orbital dynamics) such that the radius of an extremal Kerr black hole is

$$r_{\text{EK}}(m) = \frac{1}{2} r_{\text{Schwarz}}(m) = Gm/c^2.$$

- Hence we can get a lower limit on the Newtonian separation of 2 black holes

$$r_{\text{EK}}(m_1) + r_{\text{EK}}(m_2) = \frac{1}{2} r_{\text{Schwarz}}(M) = \frac{GM}{c^2} \approx 1.5 \left( \frac{M}{M_{\odot}} \right) \text{ km.}$$

- The orbital compactness (with eccentricity, unequal masses, spin) is

$$\mathcal{R} = \frac{r_{\text{sep}}(M)}{r_{\text{EK}}(M)} \leq \frac{R(M)}{r_{\text{EK}}(M)} = \frac{c^2}{(GM\omega_{\text{Kep}})^{2/3}} \leq \frac{c^2}{(2^{6/5} G \mathcal{M} \omega_{\text{Kep}})^{2/3}} = \frac{c^2}{(2^{6/5} \pi G \mathcal{M} f_{\text{GW}}|_{\text{max}})^{2/3}} \simeq 3.4,$$

# Really? Black-holes?

---

- We've shown that the system must have a compactness ratio <3.4.

- Therefore the Newtonian density scale is

$$\rho \geq \frac{m}{(4\pi/3)R^3} = 3 \times 10^{15} \left( \frac{3.4}{\mathcal{R}} \right)^3 \left( \frac{35M_\odot}{m} \right)^2 \frac{\text{kg}}{\text{m}^3}$$

- This is less dense than NS densities but... again using the approximation

$$\omega \sim c/r \text{ and } r \sim GM/c^2 \text{ and } M\omega \sim c^3/G$$

- We can derive the following limit

$$\left( \frac{M_{\text{max}}}{\mathcal{M}} \right) \simeq 3.4^{3/2} \times 2^{6/5} \simeq 14.4$$

- From which it follows that the max mass is  $432M_\odot$  with  $q=83$ . Leading to a lowest component mass of  $5M_\odot$ , far greater than the max NS mass.

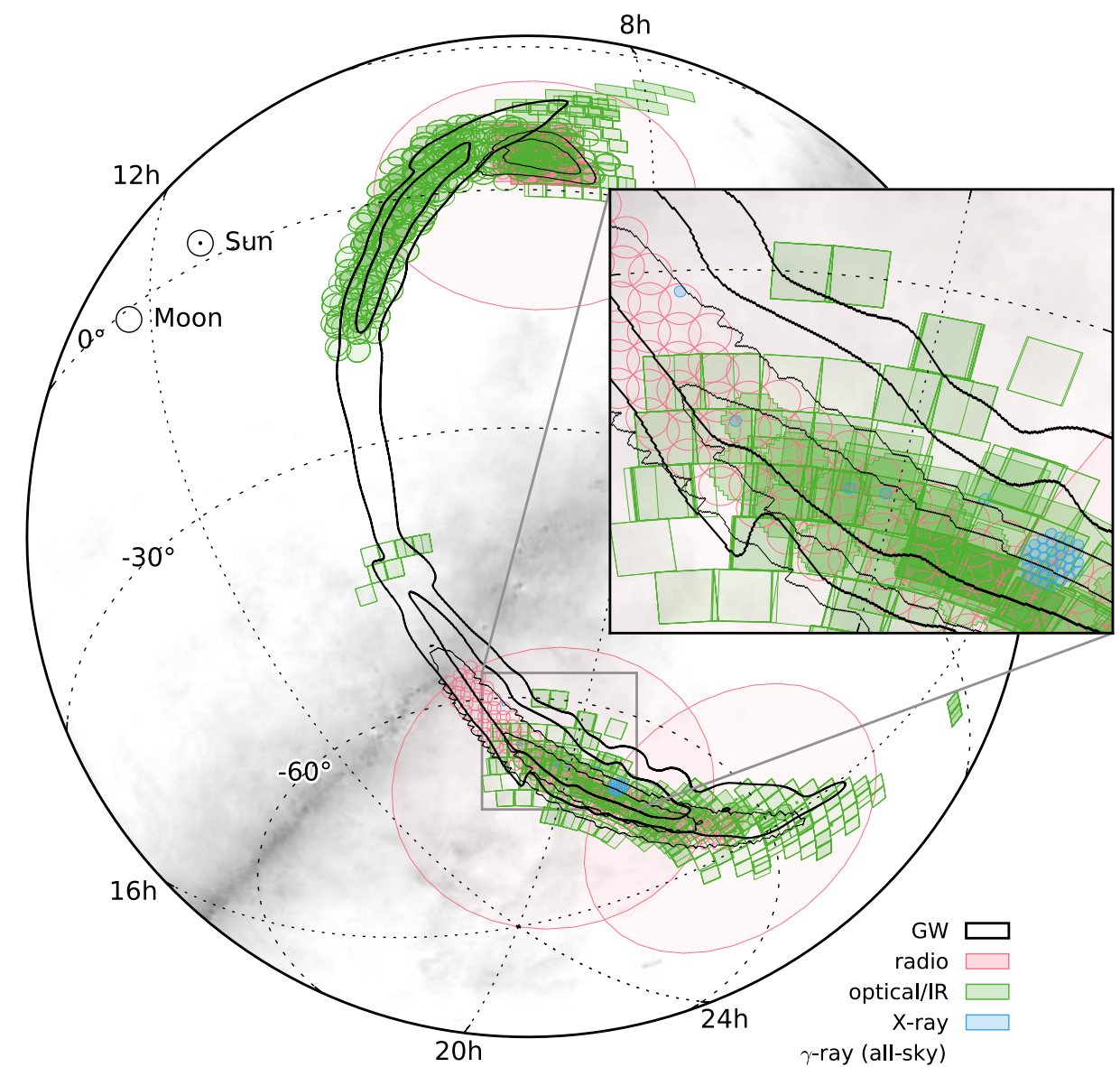
# Formation channels

---

- Possible BBH formation channels include:
  - Dynamical formation in a dense stellar environment (possibly assisted by gas drag in galactic nuclear disks).
  - Or isolated binary evolution
    - either the classical variant via a common-envelope phase (possibly from population III binaries).
    - or chemically homogeneous evolution in close tidally locked binaries.
- All of these channels have been shown to be consistent with the GW150914 discovery.
- The low masses of GW151226 are probably inconsistent with the chemically homogeneous evolution model.
- **A larger population (masses and spins) will help identify the correct channel(s).**

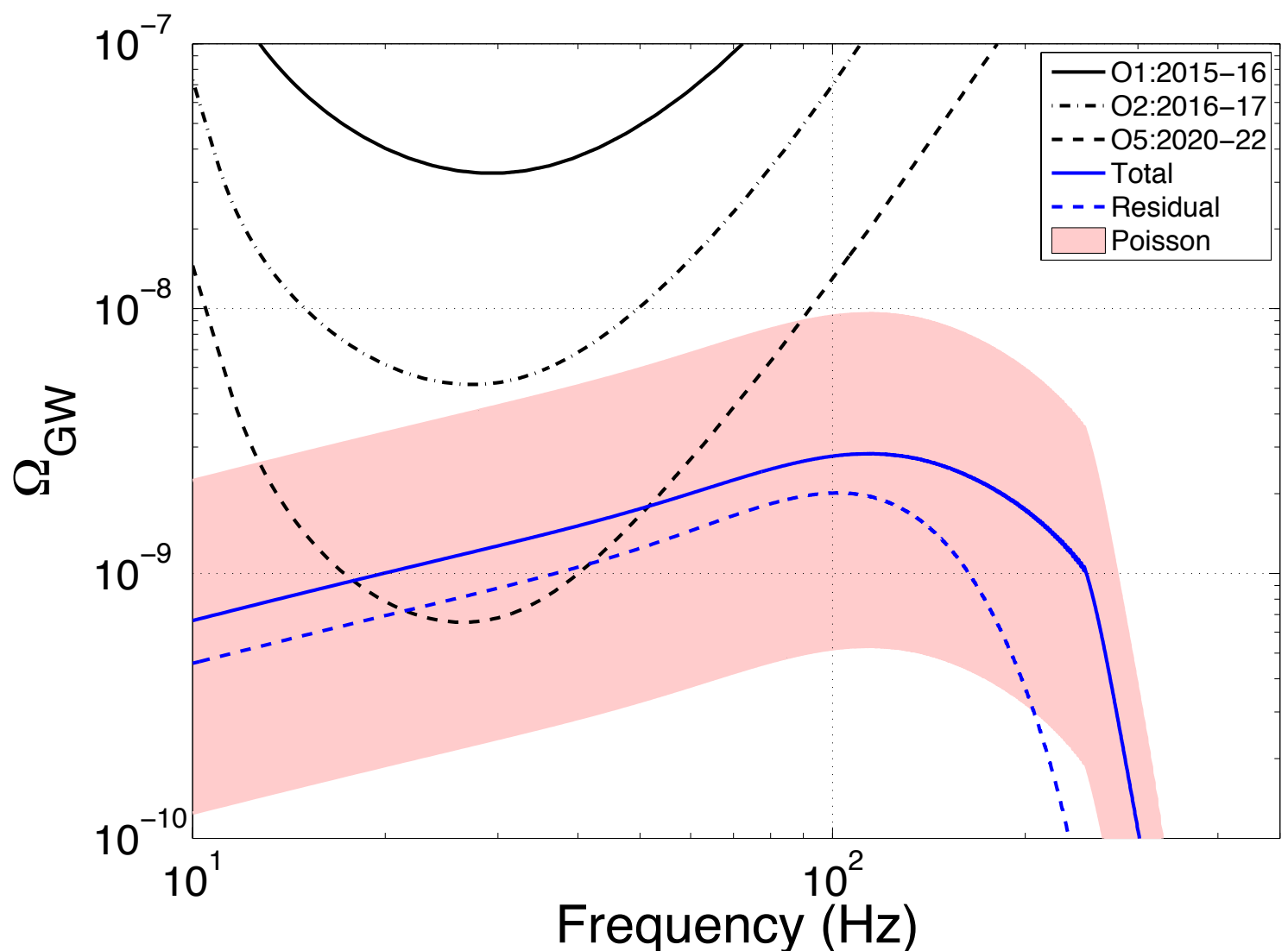
# Were there EM counterparts?

- The event time and location was shared with 63 teams of observers covering radio, optical, near-infrared, X-ray, and gamma-ray wavelengths with ground- and space-based facilities (**multi-messenger astronomy**).
- As this event turned out to be a binary black hole merger, there is little expectation of a detectable electromagnetic signature.
- There was a reported Fermi GBM trigger for GW150914 but...



# Too many to count

- The ensemble of all binary black hole mergers form an **astrophysical stochastic background**.
- This would inform us on the evolution of such binary systems over the history of the universe
- This has implications for space based detectors (eLISA) and for ultra-low frequency waves detectable with pulsar timing arrays.



# Problems

---

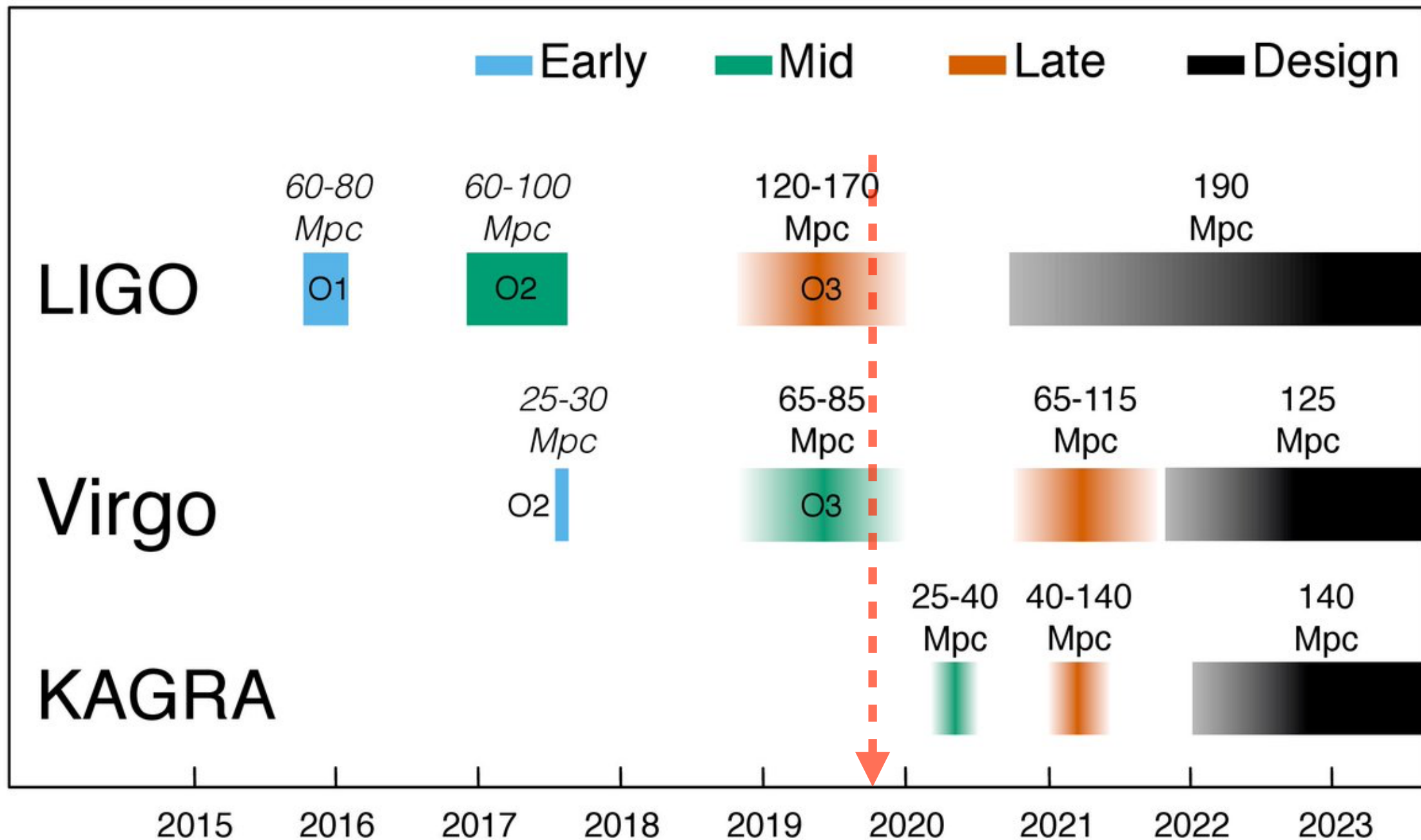
1. Show that an asymmetric mass ratio would lead to a more compact system.
2. Derive an expression for the distance to a CBC event as a function of its frequency at peak strain and the peak strain.
3. Show that  $\sim 3M_{\odot}$  of energy were emitted during the merger of GW150914.
4. Repeat all calculations for GW151226 and LVT151012.

# Conclusions

---

Extra things and a summary

# What's happening now?



# GraceDB [https://gracedb.ligo.org]

## GraceDB – Gravitational-Wave Candidate Event Database

| HOME | PUBLIC ALERTS | SEARCH | LATEST | DOCUMENTATION |  |  | LOGIN |
|------|---------------|--------|--------|---------------|--|--|-------|
|------|---------------|--------|--------|---------------|--|--|-------|

Latest – as of 18 November 2019 08:07:59 UTC

Test and MDC events and superevents are not included in the search results by default; see the [query help](#) for information on how to search for events and superevents in those categories.

Query:

Search for:

| UID       | Labels   | t_start           | t_0               | t_end             | FAR (Hz)  | UTC                     | Created |
|-----------|--|-------------------|-------------------|-------------------|-----------|-------------------------|---------|
| S191117j  | ADVNO EM_Selected SKYMAP_READY EMBRIGHT_READY PASTRO_READY DQOK GCN_PRELIM_SENT          | 1258006119.454868 | 1258006120.454868 | 1258006121.454868 | 1.114e-18 | 2019-11-17 06:08:46 UTC |         |
| S191110af | ADVNO EM_Selected SKYMAP_READY DQOK GCN_PRELIM_SENT                                      | 1257462422.079116 | 1257462422.183200 | 1257462422.287284 | 2.499e-09 | 2019-11-10 23:10:59 UTC |         |
| S191110x  | PE_READY ADVNO EM_Selected SKYMAP_READY EMBRIGHT_READY PASTRO_READY DQOK GCN_PRELIM_SENT | 1257444539.210120 | 1257444540.210120 | 1257444541.210120 | 2.930e-11 | 2019-11-10 18:09:05 UTC |         |
| S191109d  | PE_READY ADVOK EM_Selected SKYMAP_READY EMBRIGHT_READY PASTRO_READY DQOK GCN_PRELIM_SENT | 1257296854.204590 | 1257296855.220703 | 1257296856.278186 | 1.537e-13 | 2019-11-09 01:07:46 UTC |         |
| S191105e  | PE_READY ADVOK EM_Selected SKYMAP_READY EMBRIGHT_READY PASTRO_READY DQOK GCN_PRELIM_SENT | 1256999738.931152 | 1256999739.933105 | 1256999740.933105 | 2.283e-08 | 2019-11-05 14:35:45 UTC |         |
| S190930t  | ADVOK EM_Selected SKYMAP_READY EMBRIGHT_READY PASTRO_READY DQOK GCN_PRELIM_SENT          | 1253889264.685342 | 1253889265.685342 | 1253889266.685342 | 1.543e-08 | 2019-09-30 14:34:30 UTC |         |
| S190930s  | PE_READY ADVOK EM_Selected SKYMAP_READY EMBRIGHT_READY PASTRO_READY DQOK GCN_PRELIM_SENT | 1253885758.235347 | 1253885759.246810 | 1253885760.253734 | 3.008e-09 | 2019-09-30 13:36:04 UTC |         |
| S190928c  | ADVNO EM_Selected SKYMAP_READY DQOK GCN_PRELIM_SENT                                      | 1253671923.328316 | 1253671923.364500 | 1253671923.400684 | 6.729e-09 | 2019-09-28 02:14:18 UTC |         |
| S190924h  | PE_READY ADVOK EM_Selected SKYMAP_READY EMBRIGHT_READY PASTRO_READY DQOK GCN_PRELIM_SENT | 1253326743.785645 | 1253326744.846654 | 1253326745.876674 | 8.928e-19 | 2019-09-24 02:19:25 UTC |         |
| S190923y  | ADVOK EM_Selected SKYMAP_READY EMBRIGHT_READY PASTRO_READY DQOK GCN_PRELIM_SENT          | 1253278576.645077 | 1253278577.645508 | 1253278578.654868 | 4.783e-08 | 2019-09-23 12:56:22 UTC |         |
| S190915ak | PE_READY ADVOK SKYMAP_READY EMBRIGHT_READY PASTRO_READY DQOK GCN_PRELIM_SENT             | 1252627039.685111 | 1252627040.690891 | 1252627041.730049 | 9.735e-10 | 2019-09-15 23:57:25 UTC |         |
| S190910h  | PE_READY ADVOK SKYMAP_READY EMBRIGHT_READY PASTRO_READY DQOK GCN_PRELIM_SENT             | 1252139415.544299 | 1252139416.544448 | 1252139417.544448 | 3.584e-08 | 2019-09-10 08:30:21 UTC |         |
| S190910d  | PE_READY ADVOK SKYMAP_READY EMBRIGHT_READY PASTRO_READY DQOK GCN_PRELIM_SENT             | 1252113996.241211 | 1252113997.242676 | 1252113998.264918 | 3.717e-09 | 2019-09-10 01:26:35 UTC |         |
| S190901ap | PE_READY ADVOK SKYMAP_READY EMBRIGHT_READY PASTRO_READY DQOK GCN_PRELIM_SENT             | 1251415878.837767 | 1251415879.837767 | 1251415880.838844 | 7.027e-09 | 2019-09-01 23:31:24 UTC |         |
| S190829u  | PE_READY ADVNO SKYMAP_READY EMBRIGHT_READY PASTRO_READY DQOK GCN_PRELIM_SENT             | 1251147973.281494 | 1251147974.283940 | 1251147975.283940 | 5.151e-09 | 2019-08-29 21:06:19 UTC |         |
| S190828l  | PE_READY ADVOK SKYMAP_READY EMBRIGHT_READY PASTRO_READY DQOK GCN_PRELIM_SENT             | 1251010526.884921 | 1251010527.886557 | 1251010528.913573 | 4.629e-11 | 2019-08-28 06:55:26 UTC |         |
| S190828j  | PE_READY ADVOK SKYMAP_READY EMBRIGHT_READY PASTRO_READY DQOK GCN_PRELIM_SENT             | 1251009262.739486 | 1251009263.756472 | 1251009264.796332 | 8.474e-22 | 2019-08-28 06:34:21 UTC |         |
| S190822c  | ADVNO SKYMAP_READY EMBRIGHT_READY PASTRO_READY DQOK GCN_PRELIM_SENT                      | 1250472616.589125 | 1250472617.589203 | 1250472618.589203 | 6.145e-18 | 2019-08-22 01:30:23 UTC |         |
| S190816i  | PE_READY ADVNO SKYMAP_READY EMBRIGHT_READY PASTRO_READY DQOK GCN_PRELIM_SENT             | 1249995888.757789 | 1249995889.757789 | 1249995890.757789 | 1.436e-08 | 2019-08-16 13:05:12 UTC |         |
| S190814bv | PE_READY ADVOK SKYMAP_READY EMBRIGHT_READY PASTRO_READY DQOK GCN_PRELIM_SENT             | 1249852255.996787 | 1249852257.012957 | 1249852258.021731 | 2.033e-33 | 2019-08-14 21:11:18 UTC |         |
| S190808ae | ADVNO SKYMAP_READY EMBRIGHT_READY PASTRO_READY DQOK GCN_PRELIM_SENT                      | 1249338098.496141 | 1249338099.496141 | 1249338100.496141 | 3.366e-08 | 2019-08-08 22:21:45 UTC |         |
| S190728q  | PE_READY ADVOK SKYMAP_READY EMBRIGHT_READY PASTRO_READY DQOK GCN_PRELIM_SENT             | 1248331527.497344 | 1248331528.546797 | 1248331529.706055 | 2.527e-23 | 2019-07-28 06:45:27 UTC |         |
| S190727h  | PE_READY ADVOK SKYMAP_READY EMBRIGHT_READY PASTRO_READY DQOK GCN_PRELIM_SENT             | 1248242630.976288 | 1248242631.985887 | 1248242633.180176 | 1.378e-10 | 2019-07-27 06:03:51 UTC |         |
| S190720a  | PE_READY ADVOK SKYMAP_READY EMBRIGHT_READY PASTRO_READY DQOK GCN_PRELIM_SENT             | 1247616533.703127 | 1247616534.704102 | 1247616535.860840 | 3.801e-09 | 2019-07-20 00:08:53 UTC |         |
| S190718y  | ADVOK SKYMAP_READY EMBRIGHT_READY PASTRO_READY DQOK GCN_PRELIM_SENT                      | 1247495729.067865 | 1247495730.067865 | 1247495731.067865 | 3.648e-08 | 2019-07-18 14:35:34 UTC |         |
| S190707q  | PE_READY ADVOK SKYMAP_READY EMBRIGHT_READY PASTRO_READY DQOK GCN_PRELIM_SENT             | 1246527223.118398 | 1246527224.181226 | 1246527225.284180 | 5.265e-12 | 2019-07-07 09:33:44 UTC |         |

# GraceDB [https://gracedb.ligo.org]

## GraceDB – Gravitational-Wave Candidate Event Database

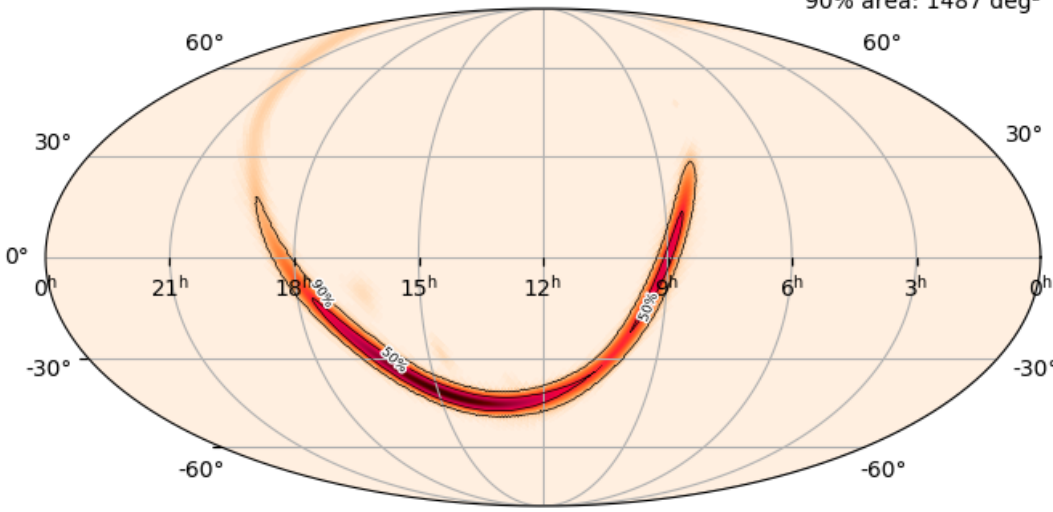
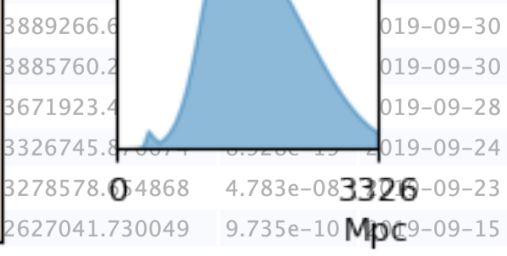
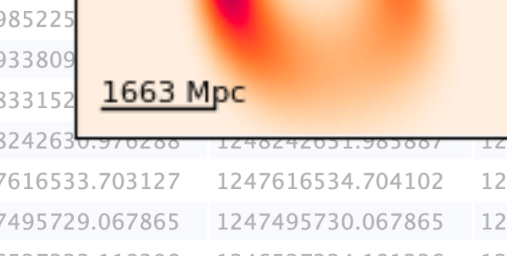
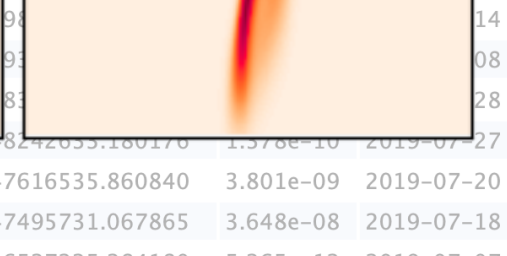
| HOME | PUBLIC ALERTS | SEARCH | LATEST | DOCUMENTATION | LOGIN |
|------|---------------|--------|--------|---------------|-------|
|------|---------------|--------|--------|---------------|-------|

Latest – as of 18 November 2019 08:07:59 UTC

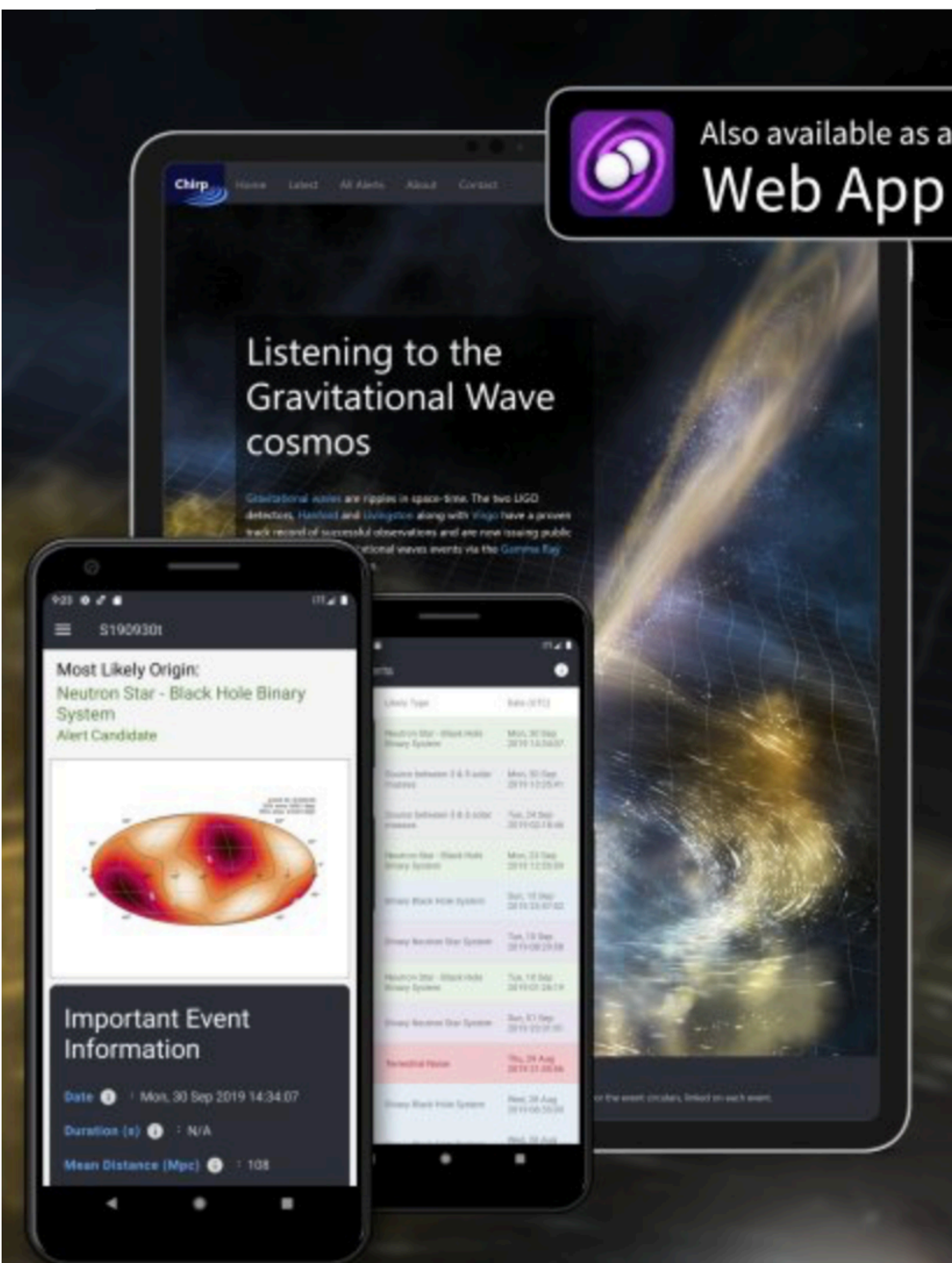
Test and MDC events and superevents are not included in the search results by default; see the [query help](#) for information on how to search for events and superevents in those categories.

Query:

Search for:  Superevent

| UID       | Labels   | t_start           | t_0   | t_end             | FAR (Hz)  | Created                 |
|-----------|--|-------------------|---|-------------------|-----------|-------------------------|
| S191117j  | ADVNO EM_Selected SKYMAP_READY EMBRIGHT_READY PASTRO_READY DQOK GCN_PRELIM_SENT          | 125800611         |   | 8006121.454868    | 1.114e-18 | 2019-11-17 06:08:46 UTC |
| S191110af | ADVNO EM_Selected SKYMAP_READY DQOK GCN_PRELIM_SENT                                      | 125746242         |  | 7462422.287294    | 2.109e-09 | 2019-11-10 23:10:59 UTC |
| S191110x  | PE_READY ADVNO EM_Selected SKYMAP_READY EMBRIGHT_READY PASTRO_READY DQOK GCN_PRELIM_SENT | 125744453         |  | 7444541.2         | 4.783e-08 | 2019-11-10 18:09:05 UTC |
| S191109d  | PE_READY   | 125729685         |  | 7296856.2         | 9.735e-10 | 2019-11-09 01:07:46 UTC |
| S191105e  | PE_READY   | 125699973         |  | 6999740.9         | 1.568e-10 | 2019-11-05 14:35:45 UTC |
| S190930t  | ADVNO  | 125388926         |  | 3889266.6         | 1.568e-10 | 2019-09-30 14:34:30 UTC |
| S190930s  | PE_READY   | 125388575         |  | 3885760.2         | 1.568e-10 | 2019-09-30 13:36:04 UTC |
| S190928c  | ADVNO  | 125367192         |  | 3671923.4         | 1.568e-10 | 2019-09-28 02:14:18 UTC |
| S190924h  | PE_READY   | 125332674         |  | 3326745.8         | 1.568e-10 | 2019-09-24 02:19:25 UTC |
| S190923y  | ADVNO  | 125327857         |  | 3278578.0         | 4.783e-08 | 2019-09-23 12:56:22 UTC |
| S190915ak | PE_READY   | 125262703         |  | 2627041.730049    | 9.735e-10 | 2019-09-15 23:57:25 UTC |
| S190910h  | PE_READY   | 125213941         |  | 213941.2          | 1.114e-18 | 2019-09-10 08:30:21 UTC |
| S190910d  | PE_READY   | 125211399         |  | 211399.2          | 1.114e-18 | 2019-09-10 01:26:35 UTC |
| S190901ap | PE_READY   | 125141587         |  | 141587.2          | 1.114e-18 | 2019-09-01 23:31:24 UTC |
| S190829u  | PE_READY   | 125114797         |  | 114797.2          | 1.114e-18 | 2019-08-29 21:06:19 UTC |
| S190828l  | PE_READY   | 125101052         |  | 101052.2          | 1.114e-18 | 2019-08-28 06:55:26 UTC |
| S190828j  | PE_READY   | 125100926         |  | 100926.2          | 1.114e-18 | 2019-08-28 06:34:21 UTC |
| S190822c  | ADVNO  | 125047261         |  | 47261.2           | 1.114e-18 | 2019-08-22 01:30:23 UTC |
| S190816i  | PE_READY   | 124999588         |  | 99588.2           | 1.114e-18 | 2019-08-16 13:05:12 UTC |
| S190814bv | PE_READY ADVNO SKYMAP_READY EMBRIGHT_READY PASTRO_READY DQOK GCN_PRELIM_SENT             | 124985225         |  | 85225.2           | 1.114e-18 | 2019-08-14 21:11:18 UTC |
| S190808ae | ADVNO SKYMAP_READY EMBRIGHT_READY PASTRO_READY DQOK GCN_PRELIM_SENT                      | 124933809         |  | 93809.2           | 1.114e-18 | 2019-08-08 22:21:45 UTC |
| S190728q  | PE_READY ADVOK SKYMAP_READY EMBRIGHT_READY PASTRO_READY DQOK GCN_PRELIM_SENT             | 124833152         |  | 83152.2           | 1.114e-18 | 2019-08-28 06:45:27 UTC |
| S190727h  | PE_READY ADVOK SKYMAP_READY EMBRIGHT_READY PASTRO_READY DQOK GCN_PRELIM_SENT             | 1248242630.570268 |  | 1248242630.570268 | 1.114e-18 | 2019-07-27 06:03:51 UTC |
| S190720a  | PE_READY ADVOK SKYMAP_READY EMBRIGHT_READY PASTRO_READY DQOK GCN_PRELIM_SENT             | 1247616533.703127 |  | 1247616533.703127 | 3.801e-09 | 2019-07-20 00:08:53 UTC |
| S190718y  | ADVOK SKYMAP_READY EMBRIGHT_READY PASTRO_READY DQOK GCN_PRELIM_SENT                      | 1247495729.067865 |  | 1247495729.067865 | 3.648e-08 | 2019-07-18 14:35:34 UTC |
| S190707g  | PE_READY ADVOK SKYMAP_READY EMBRIGHT_READY PASTRO_READY DQOK GCN_PRELIM_SENT             | 1246527223.118398 |  | 1246527223.118398 | 5.265e-12 | 2019-07-07 09:33:44 UTC |

# Mobile alerts



# Chirp

Keep track of the latest gravitational wave alerts.



GET IT ON  
**Google Play**



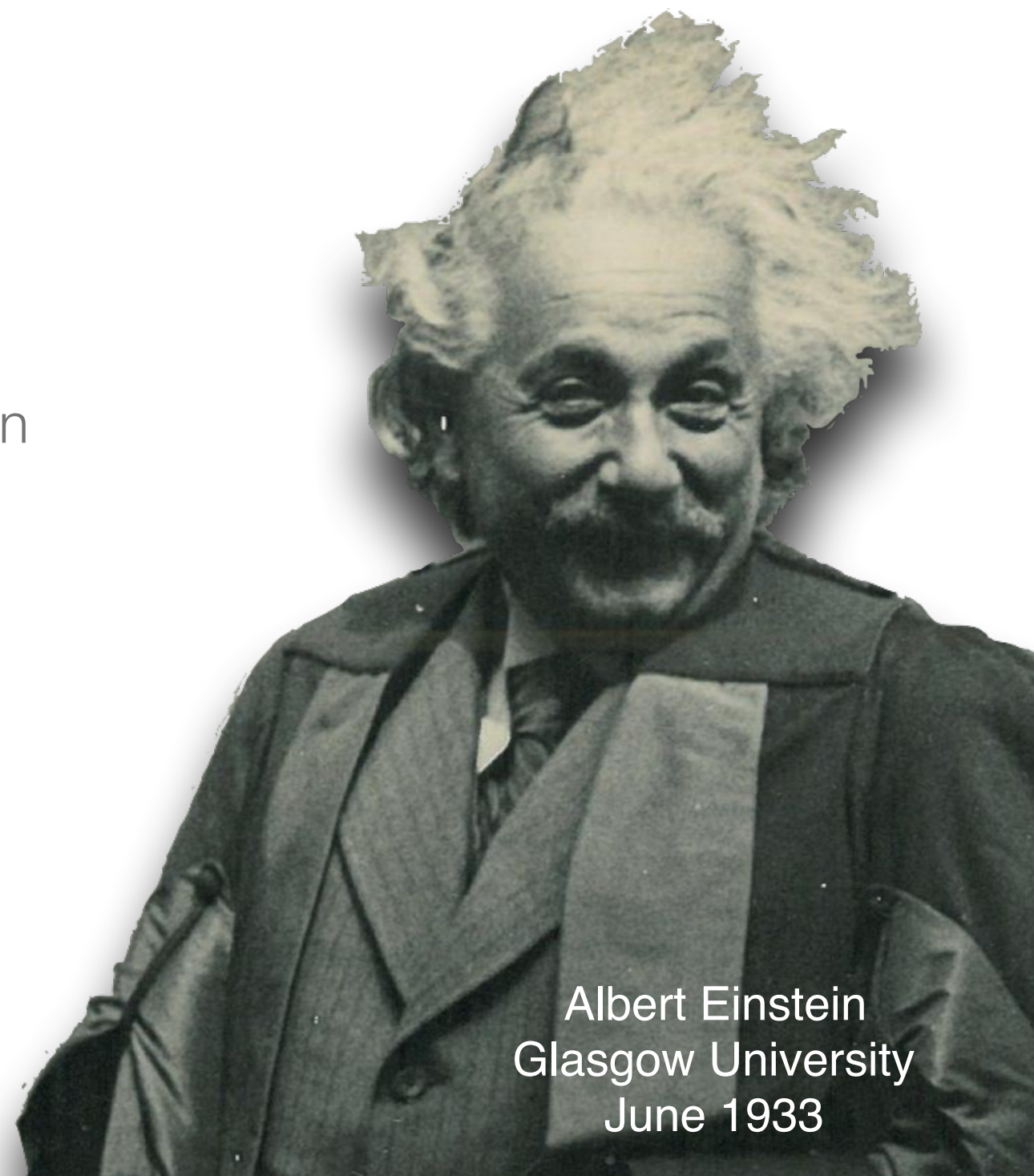
Download on the  
**App Store**

## LASER LABS

# Summary

---

- As the director of LIGO Lab put it “We did it! We detected gravitational waves!” (Dave Reitze)
- Our very first discovery has provided the first observation of binary black holes.
- Our 9 additional BBH and a BNS detection has proved that it wasn’t a fluke!
- This is just the beginning of a completely new era of observational astronomy.
- We are in a uniquely exciting time for gravitational research (LISA PathFinder, LIGO India, Pulsar Timing Arrays).



Albert Einstein  
Glasgow University  
June 1933

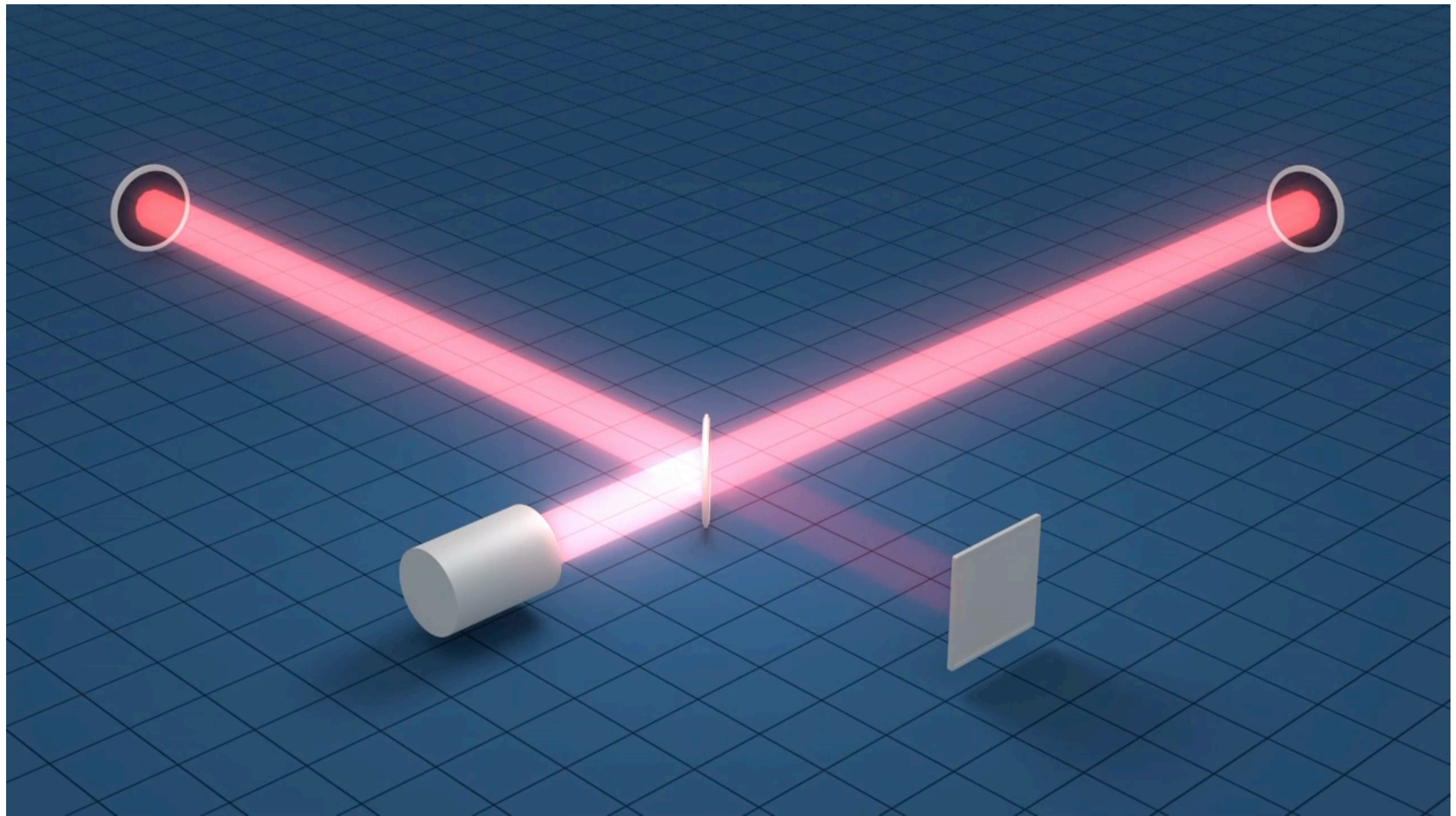
# Extra Slides

---



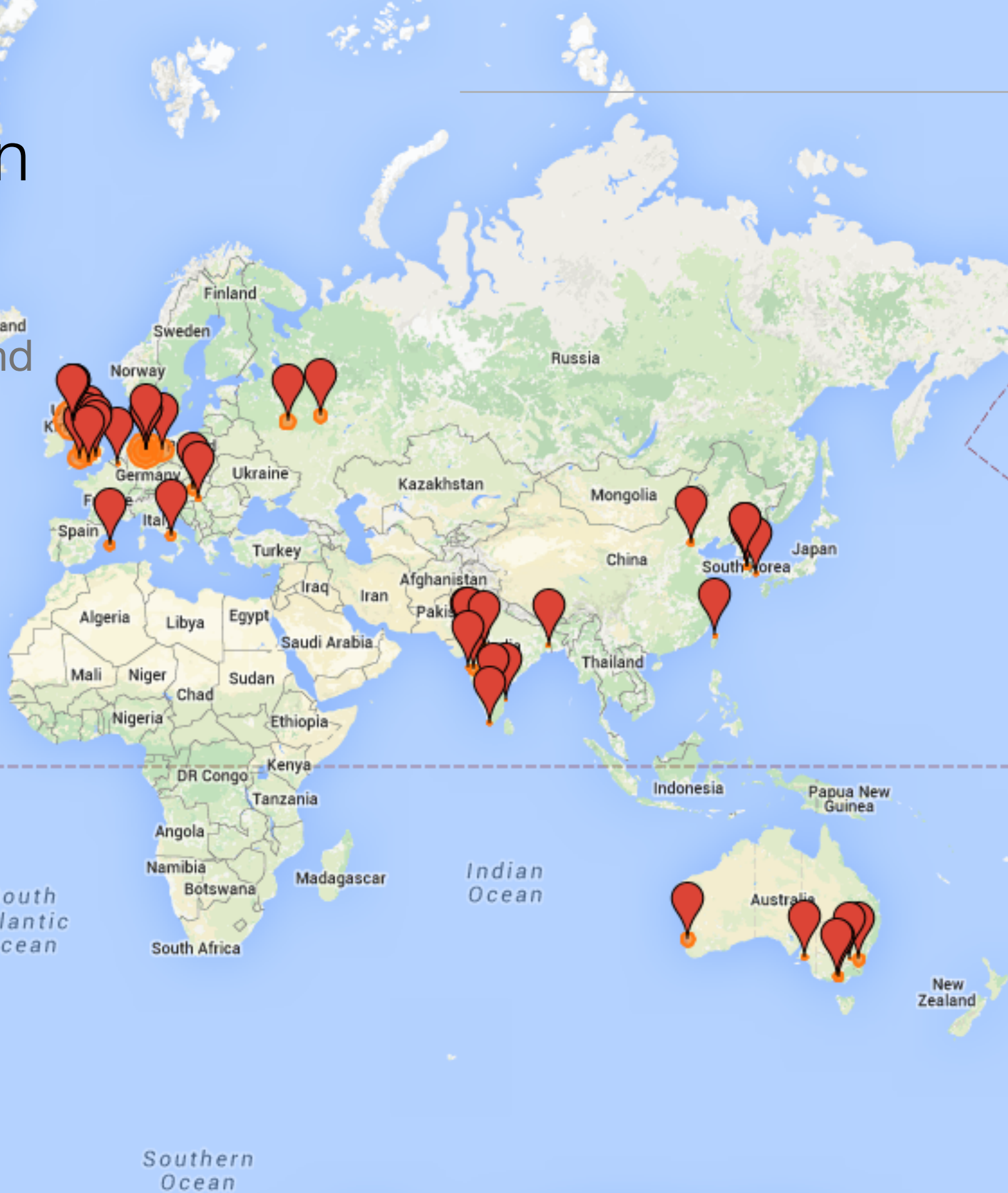
# Interferometric detection

---



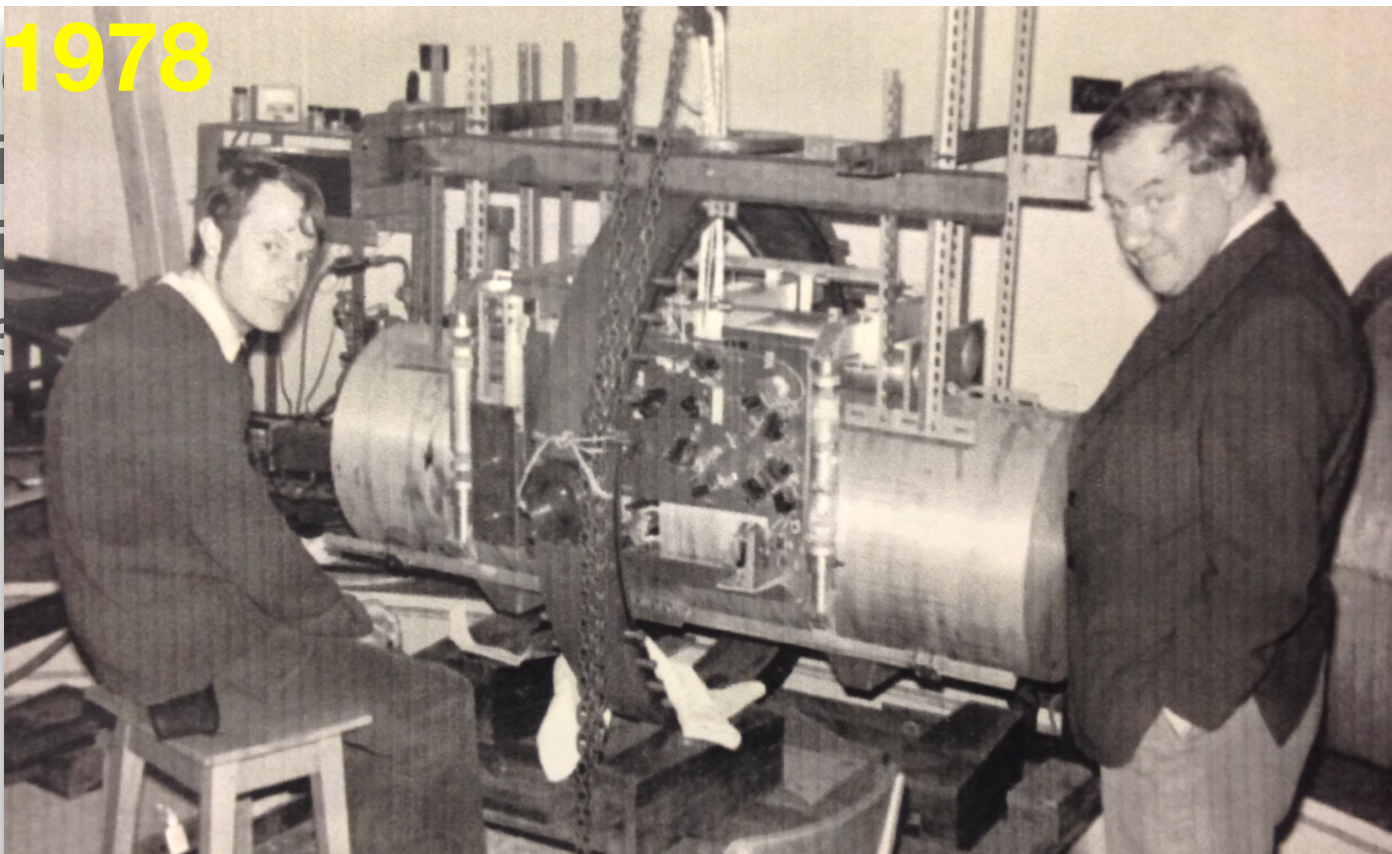
# A global collaboration

- We have over 1000 members spread across 5 continents and over 100 institutions.



# Glasgow's role

- Glasgow's role in stabilising system



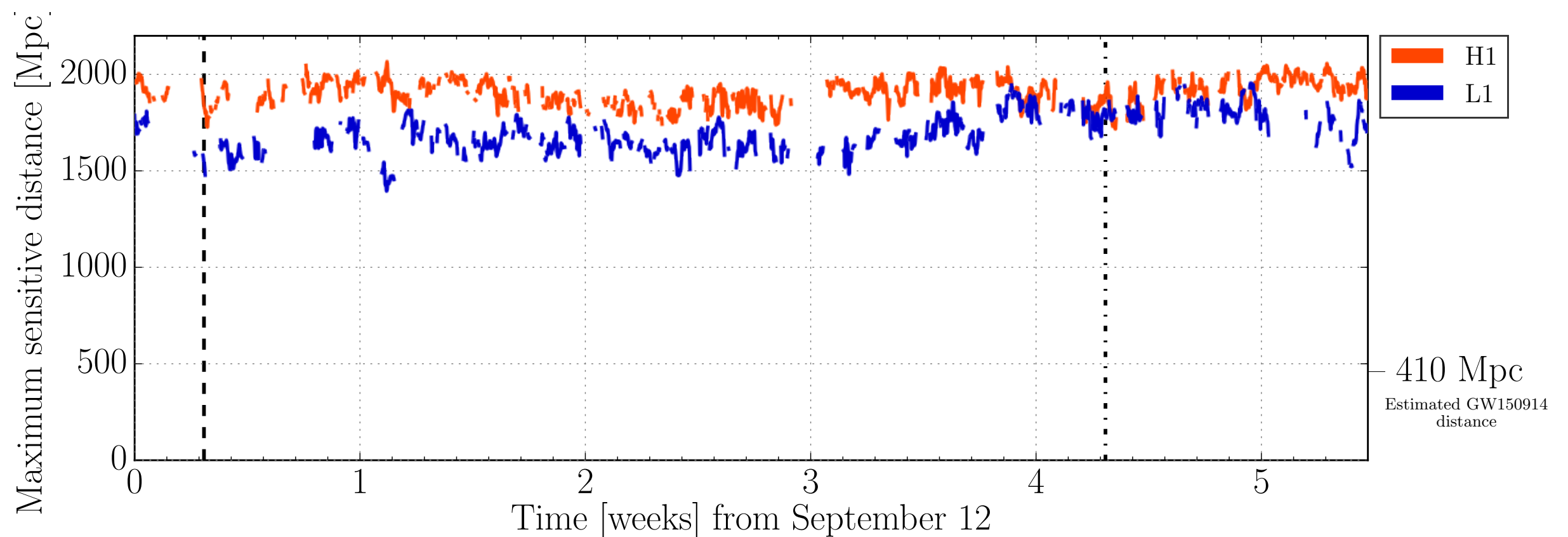
**1978**



**2016**

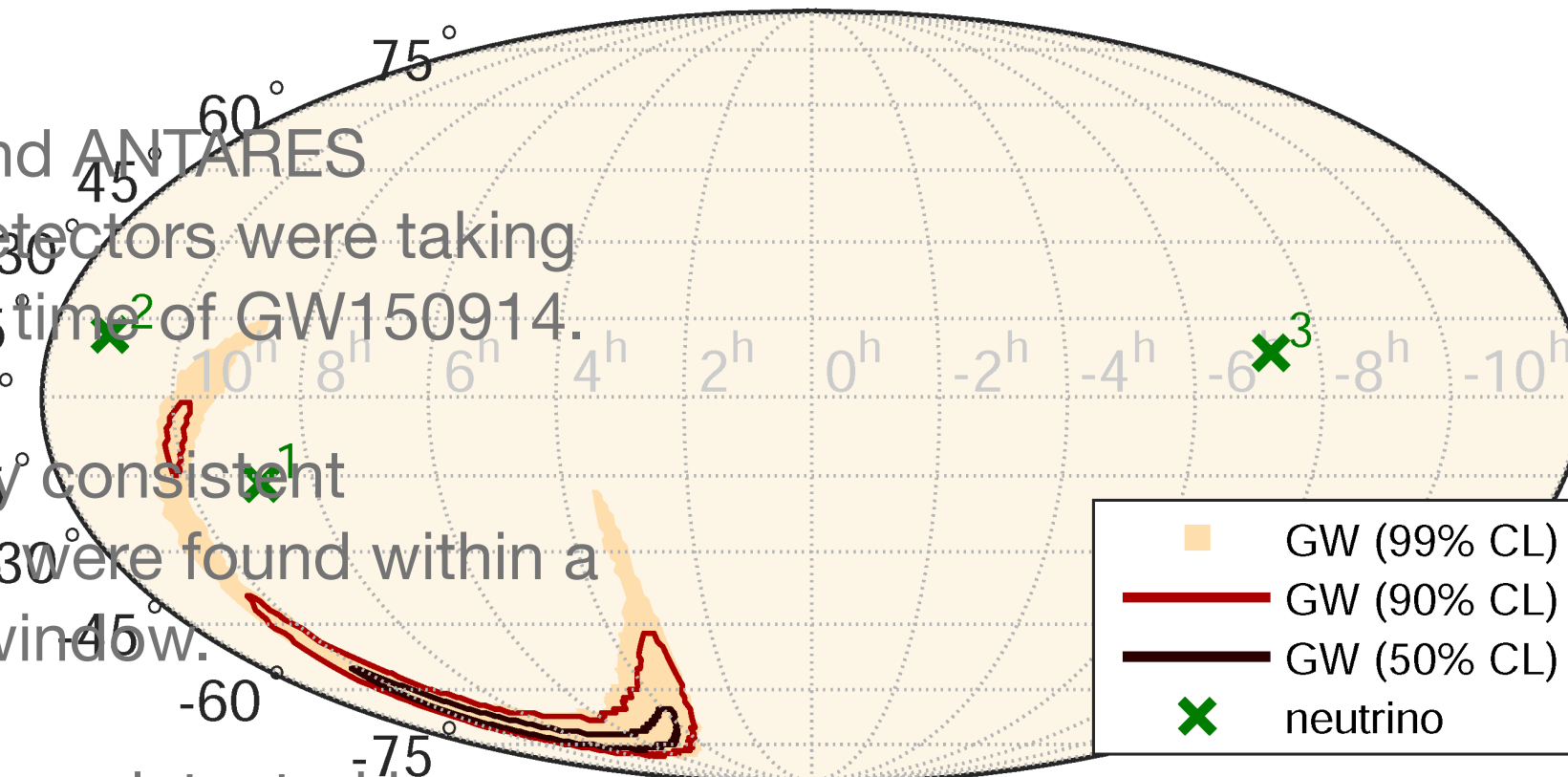
# How far could we hear?

- Our nominal Figure of merit is the binary neutron star range which was  $\sim 70$  Mpc for O1.
- Considering more massive sources similar to GW150914 this distance increases to  $\sim 1.7$



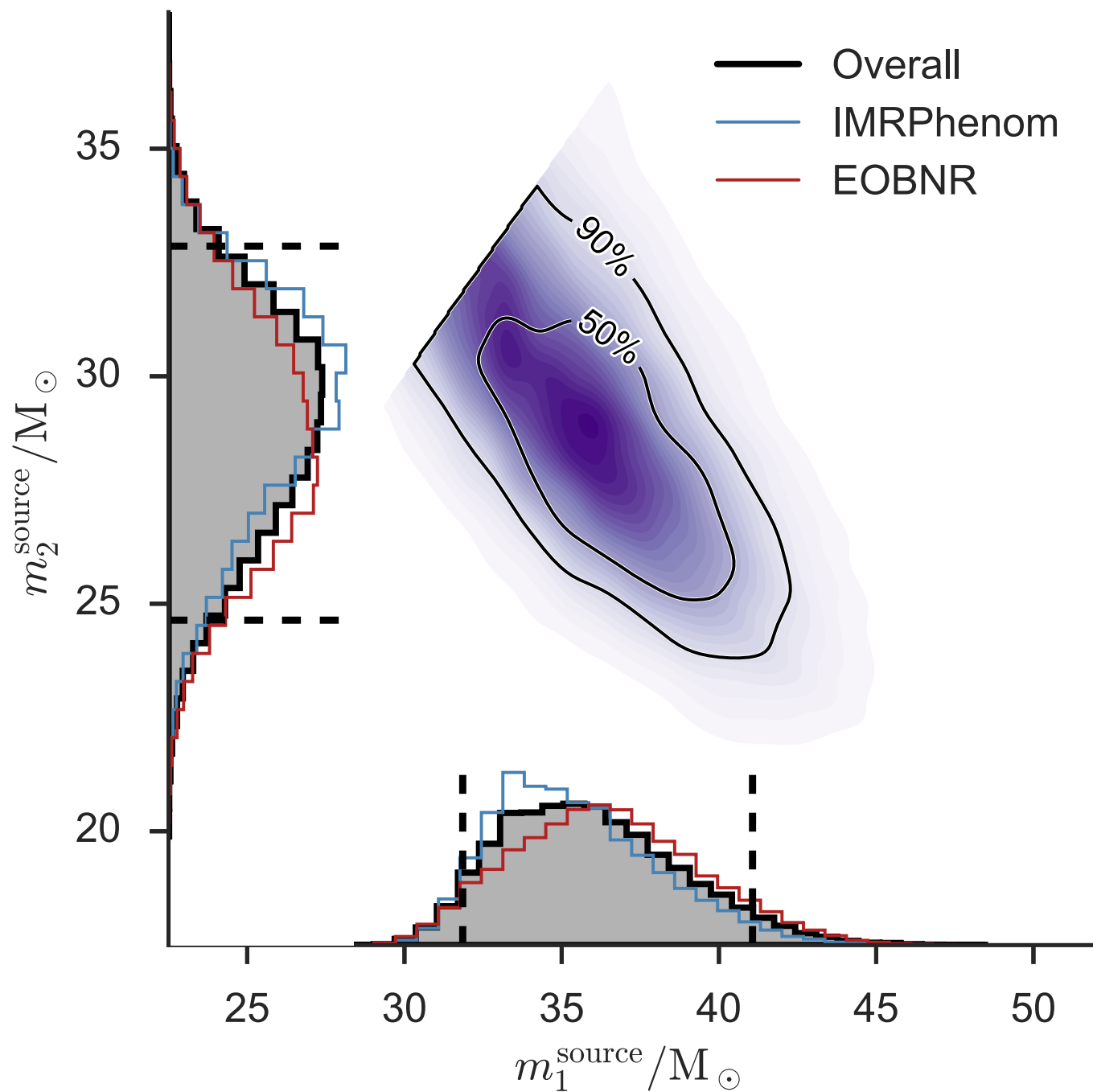
# Any neutrinos?

- IceCube and ANTARES neutrino detectors were taking data at the time of GW150914.
- No spatially consistent candidates were found within a  $\pm 500$  sec window.
- 3 events were detected by IceCube but were consistent with the background.



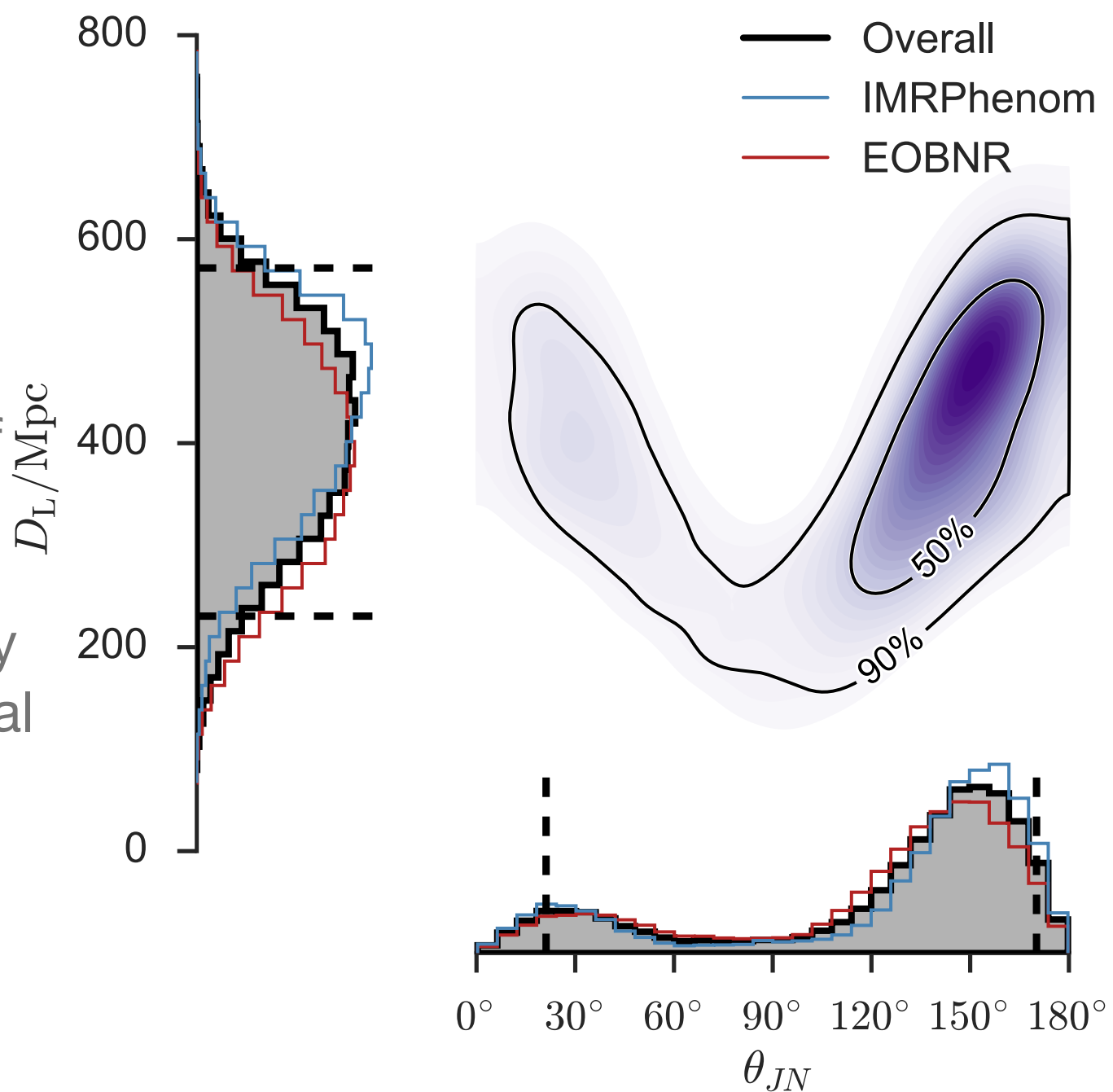
# How heavy?

- The time evolution of the signal frequency tells us the “chirp mass” to  $\pm 10\%$ .
- The component masses are estimated to be  $\sim 36$  and  $29 M_\odot$ .
- The result black hole has an estimated mass of  $62 M_\odot$ .



# How far?

- The measured amplitude is determined by 4 factors - the mass, distance, orbital inclination, and detector calibration.
- The corresponding redshift of the source is  $z \sim 0.1$ .
- In principle we can use galaxy catalogues to identify potential host galaxies.



# Other companion papers

---

- In addition to the discovery paper, the second detection paper and the O1 results paper...
- There are 12 companion papers describing the, burst search, the BBH search, the system parameters, the astrophysical rates, implications, tests of GR, stochastic background, calibration, detector characterisation, neutrinos, the detectors, and EM follow-up.

## GW151226 - LIGO's Second Detection

- ["GW151226: Observation of Gravitational Waves from a 22-Solar-Mass Binary Black Hole Coalescence"](#)  
Published in *Phys. Rev. Lett.* **116**, 241103 (2016) -- [Open access article](#)
- ["Binary Black Hole Mergers in the first Advanced LIGO Observing Run"](#)  
Accepted by *Phys. Rev. X*

## GW150914 - LIGO's First Detection

### Discovery Paper

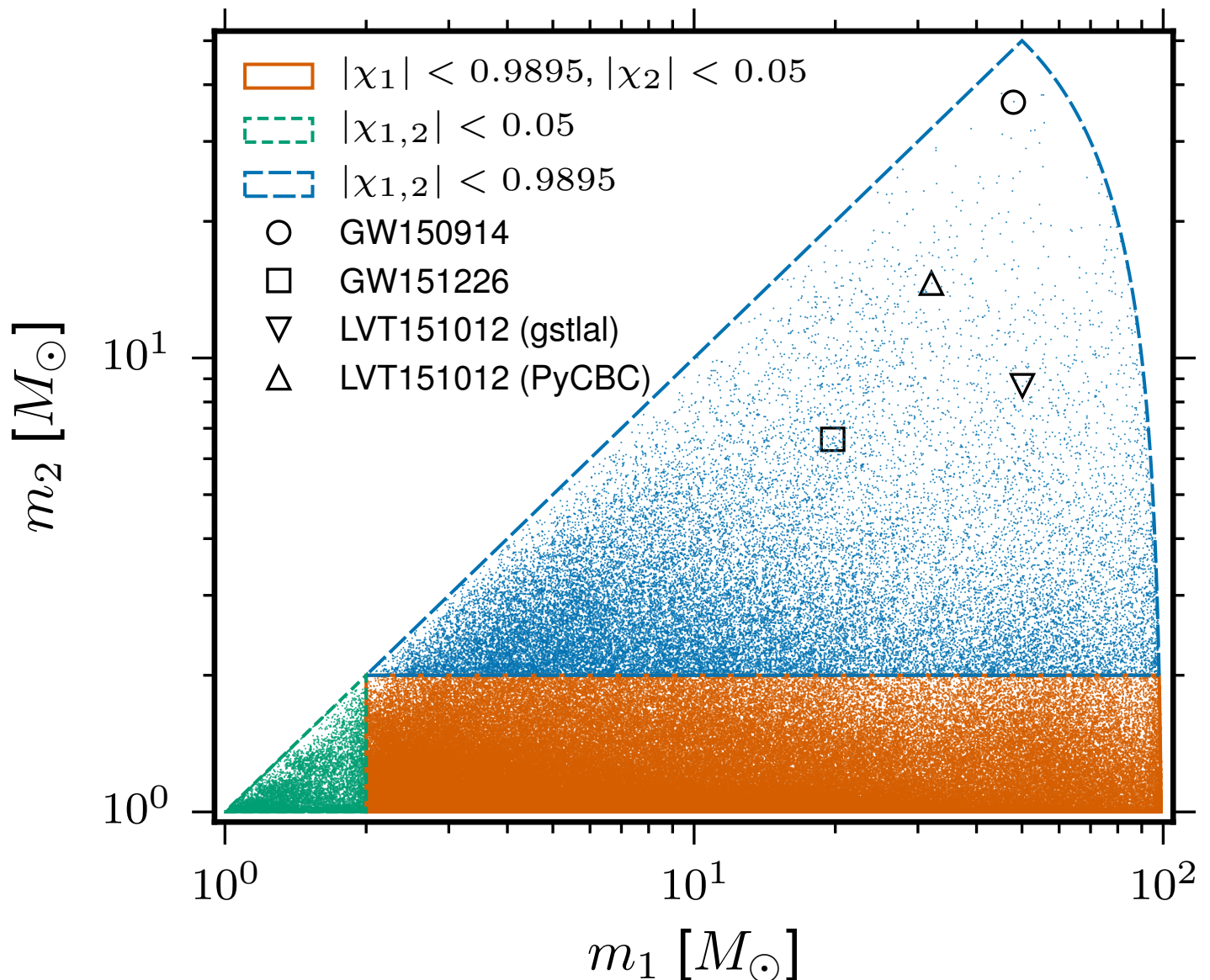
["Observation of Gravitational Waves from a Binary Black Hole Merger"](#)  
Published in *Phys. Rev. Lett.* **116**, 061102 (2016) -- [Open access article](#)

### Related papers

- ["Observing Gravitational-wave Transient GW150914 with Minimal Assumptions"](#)  
Published in *Phys. Rev. D* **93**, 122004 (2016) -- [Abstract](#)
- ["GW150914: First Results from the Search for Binary Black Hole Coalescence with Advanced LIGO"](#)  
Published in *Phys. Rev. D* **93**, 122003 (2016) -- [Abstract](#)
- ["Properties of the Binary Black Hole Merger GW150914"](#)  
Published in *Phys. Rev. Lett.* **116**, 241102 (2016) -- [Open access article](#)
- ["The Rate of Binary Black Hole Mergers Inferred from Advanced LIGO Observations Surrounding GW150914"](#)  
Accepted by *Astrophys. J. Lett.*
- ["Astrophysical Implications of the Binary Black-Hole Merger GW150914"](#)  
Published in *Astrophys. J. Lett.* **818**, L22 (2016) -- [Open access article](#)
- ["Tests of General Relativity with GW150914"](#)  
Published in *Phys. Rev. Lett.* **116**, 221101 (2016) -- [Abstract](#)
- ["GW150914: Implications for the Stochastic Gravitational Wave Background from Binary Black Holes"](#)  
Published in *Phys. Rev. Lett.* **116**, 131102 (2016) -- [Abstract](#)
- ["Calibration of the Advanced LIGO Detectors for the Discovery of the Binary Black-hole Merger GW150914"](#)  
Submitted to *Phys. Rev. Lett.*
- ["Characterization of Transient Noise in Advanced LIGO Relevant to Gravitational Wave Signal GW150914"](#)  
Published in *CQG* **33**, 134001 (2016) -- [Open access article](#)
- ["High-energy Neutrino Follow-up Search of Gravitational Wave Event GW150914 with ANTARES and IceCube"](#)  
Published in *Phys. Rev. D* **93**, 122010 (2016) -- [Abstract](#)
- ["GW150914: The Advanced LIGO Detectors in the Era of First Discoveries"](#)  
Published in *Phys. Rev. Lett.* **116**, 131103 (2016) -- [Abstract](#)
- ["Localization and Broadband Follow-up of the Gravitational-wave Transient GW150914"](#)  
Published in *Astrophys. J. Lett.* **826**, L13 (2016) -- [Open access article](#)

# How do we search?

- Matched filters are correlated with the data to generate time-series of signal-to-noise ratio.
- Templates are placed in the 4-D space of component masses and (anti-)aligned spins.
- We have 2 independent search algorithms in order to verify any candidate signals.
- For GW150914 it was actually a search for un-modelled signals that found it.



# Matched filtering

- For a signal in additive Gaussian noise
- The correlation of a template  $q$  with a dataset  $x$  is (in the frequency domain)

$$c(\tau) = \int_{-\infty}^{\infty} \tilde{x}(f) \tilde{q}^*(f) e^{-2\pi i f \tau} df$$

- For noise with zero mean, the mean and variance of the correlation are

$$\Sigma \equiv \bar{c}(\tau) = \int_{-\infty}^{\infty} \tilde{h}(f) \tilde{q}^*(f) e^{-2\pi i f (\tau - t_a)} df$$

- Where  $N_h^2 = \overline{(c - \bar{c})^2} = \int_{-\infty}^{\infty} S_h(f) |\tilde{q}^*(f)|^2 df$  is the noise spectral density

- This leads to the definition of the signal-to-noise ratio (SNR)

$$x(t) = h(t - t_a) + n(t)$$

$$\rho^2 = \frac{\Sigma^2}{N^2}$$

# Matched filtering

- Let us now define the noise weighted inner product

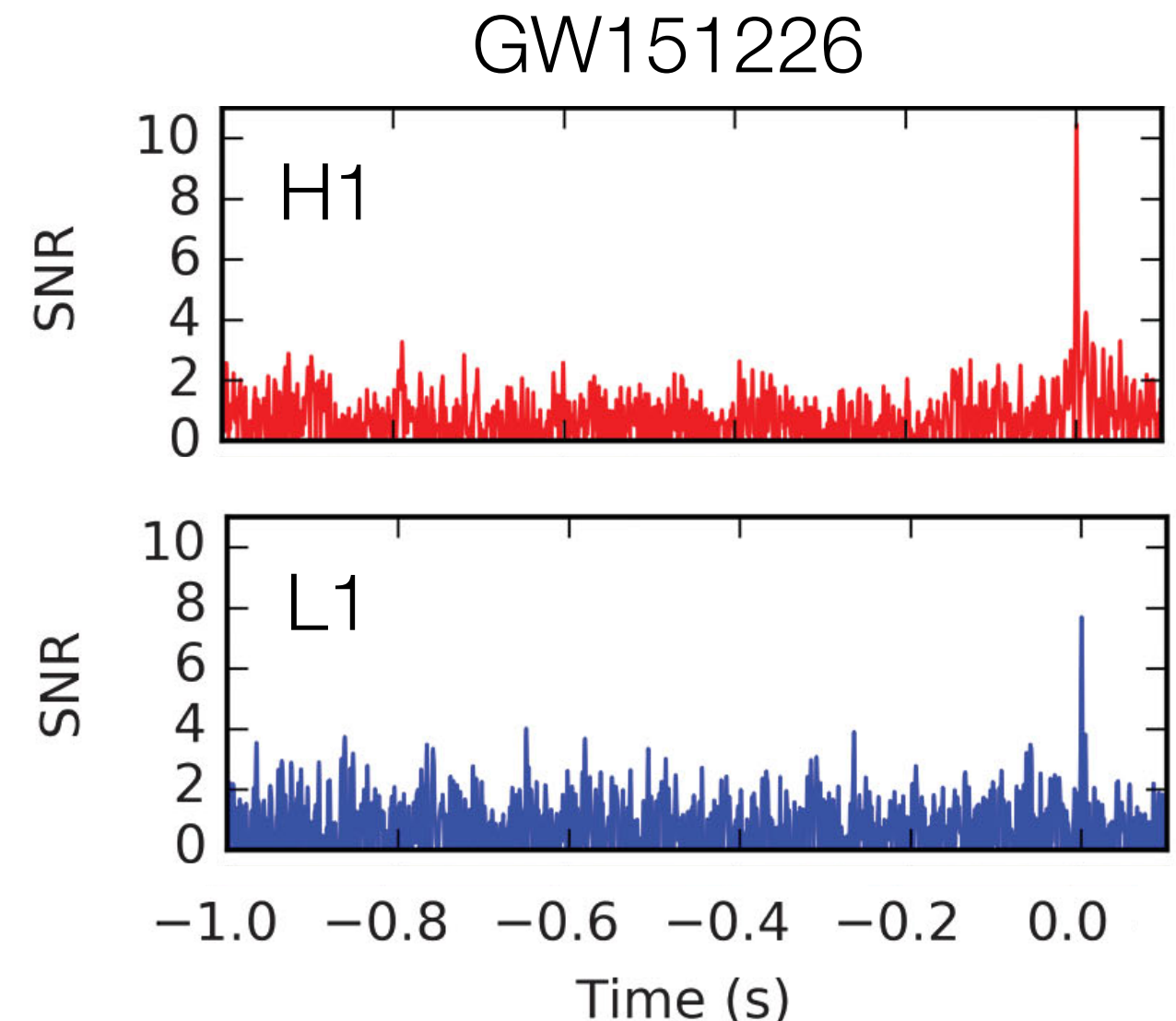
$$\langle a, b \rangle \equiv 2 \int_0^\infty \frac{df}{S_h(f)} [\tilde{a}(f)\tilde{b}^*(f) + \tilde{a}^*(f)\tilde{b}(f)]$$

- This allows us to rewrite the squared SNR as

$$\rho^2 = \frac{\langle h e^{2\pi i f(\tau - t_a)}, S_h q \rangle}{\sqrt{\langle S_h q, S_h q \rangle}}$$

- From which it is clear to see that the optimal filter is

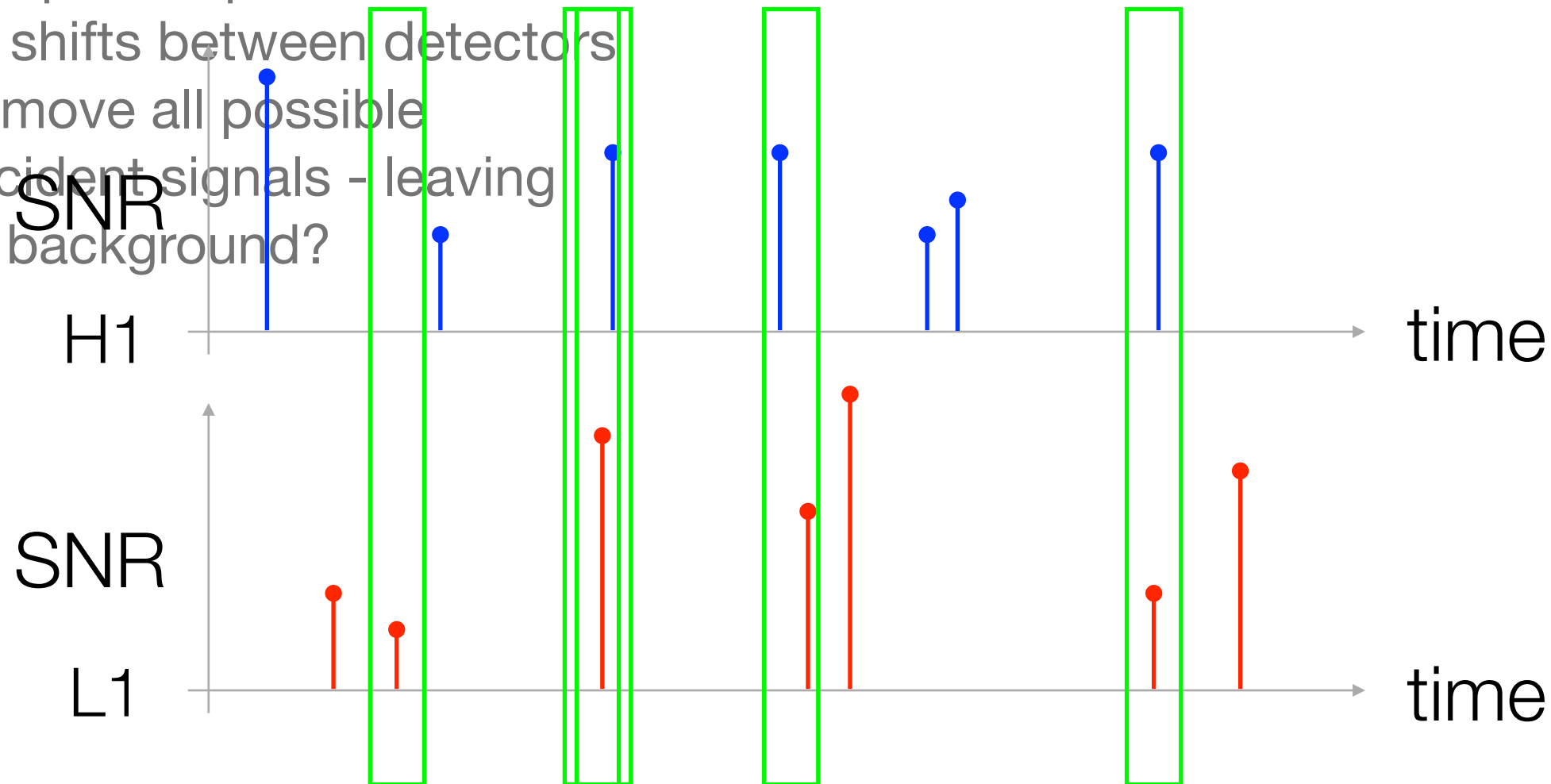
$$\tilde{q}(f) \propto \frac{\tilde{h}(f)e^{2\pi i f(\tau - t_a)}}{S_h(f)}$$



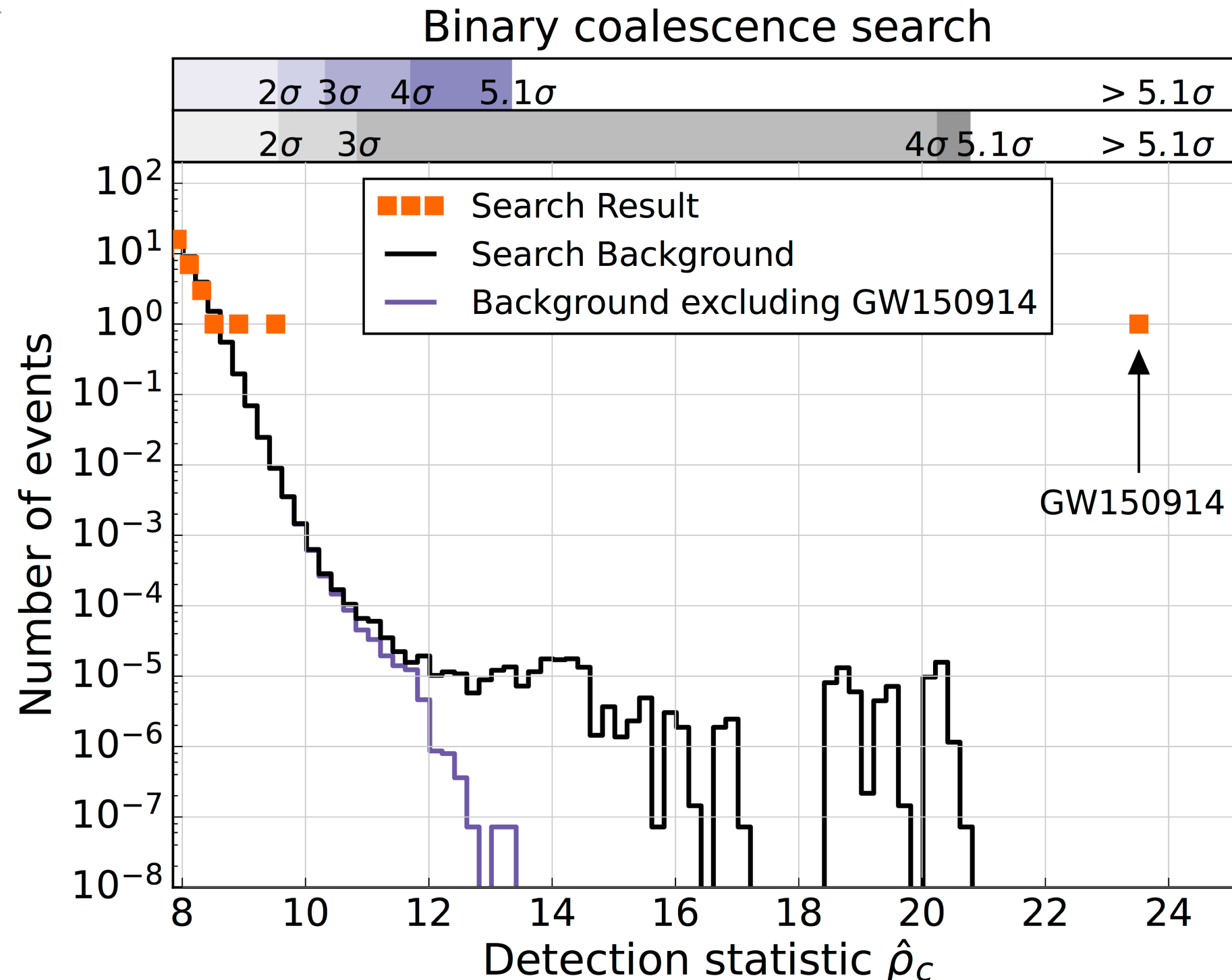
# How can we be sure?

- We use a method known as **time-slides** (or something mathematically equivalent).

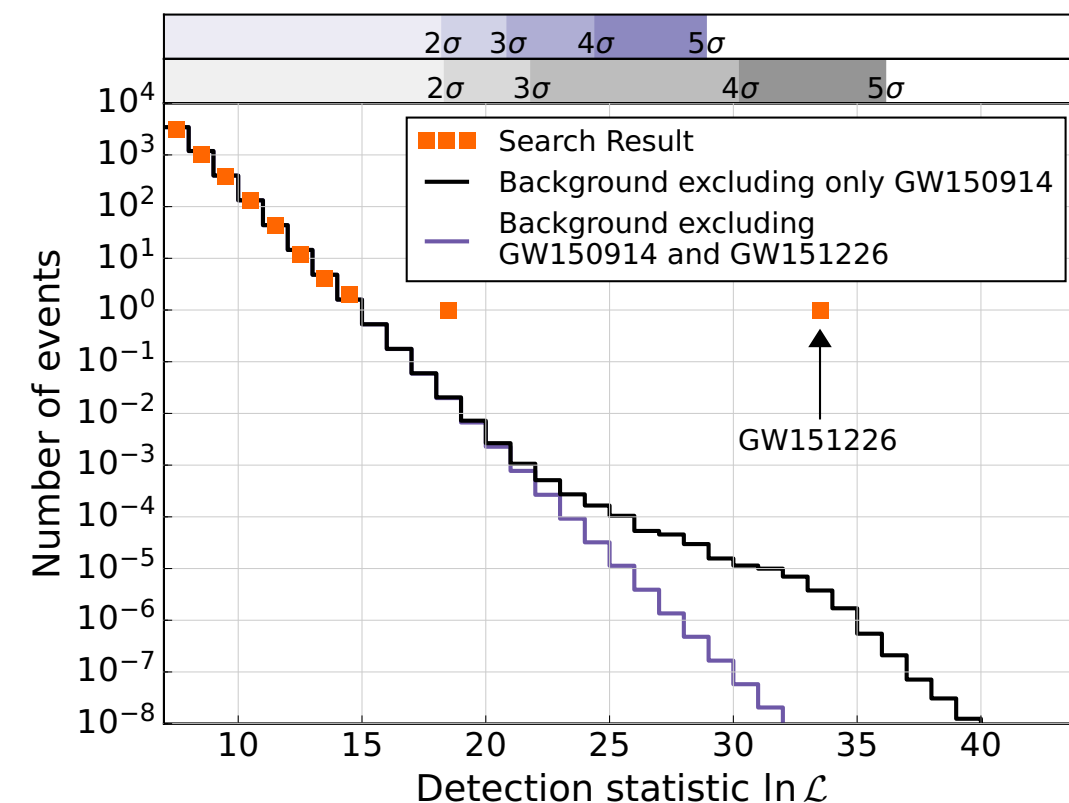
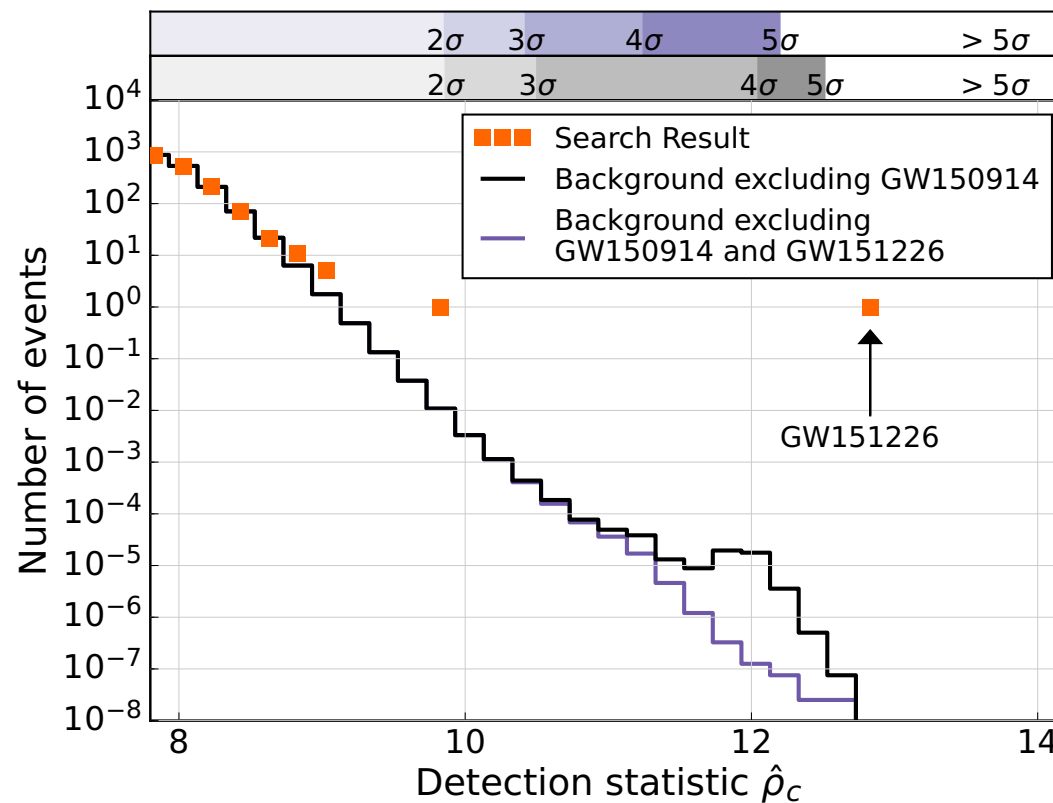
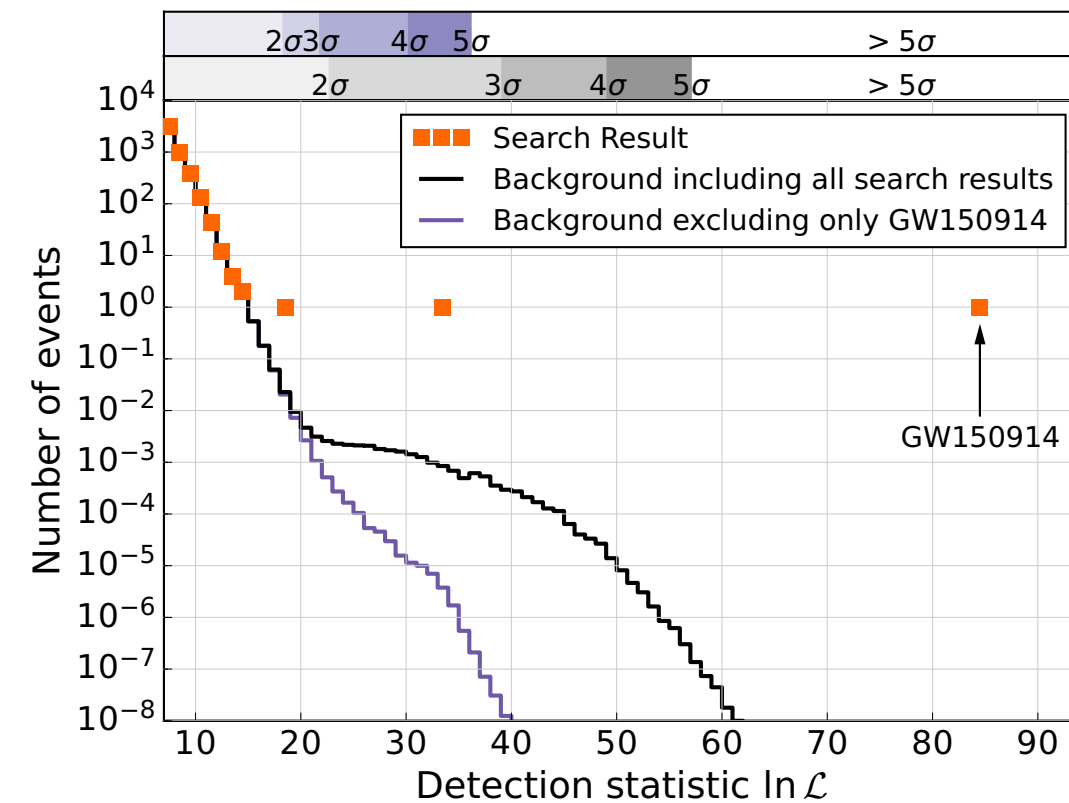
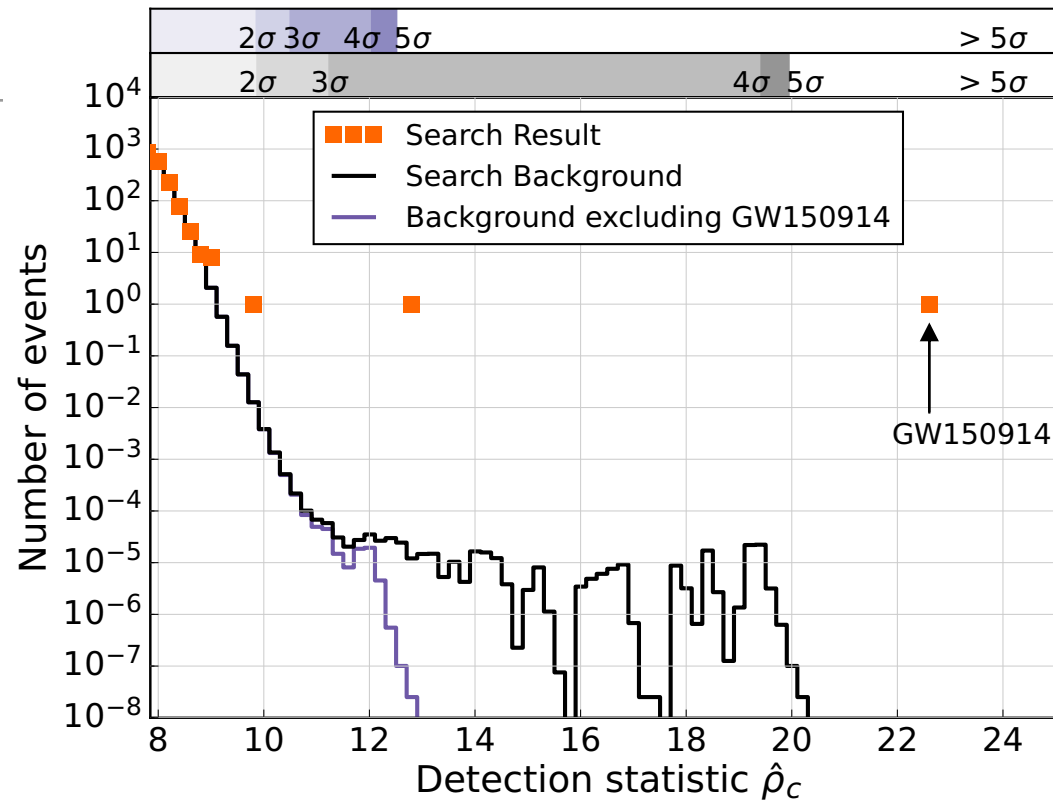
- We impose repeated artificial time shifts between detectors to remove all possible coincident signals - leaving only background?



# Are we sure?

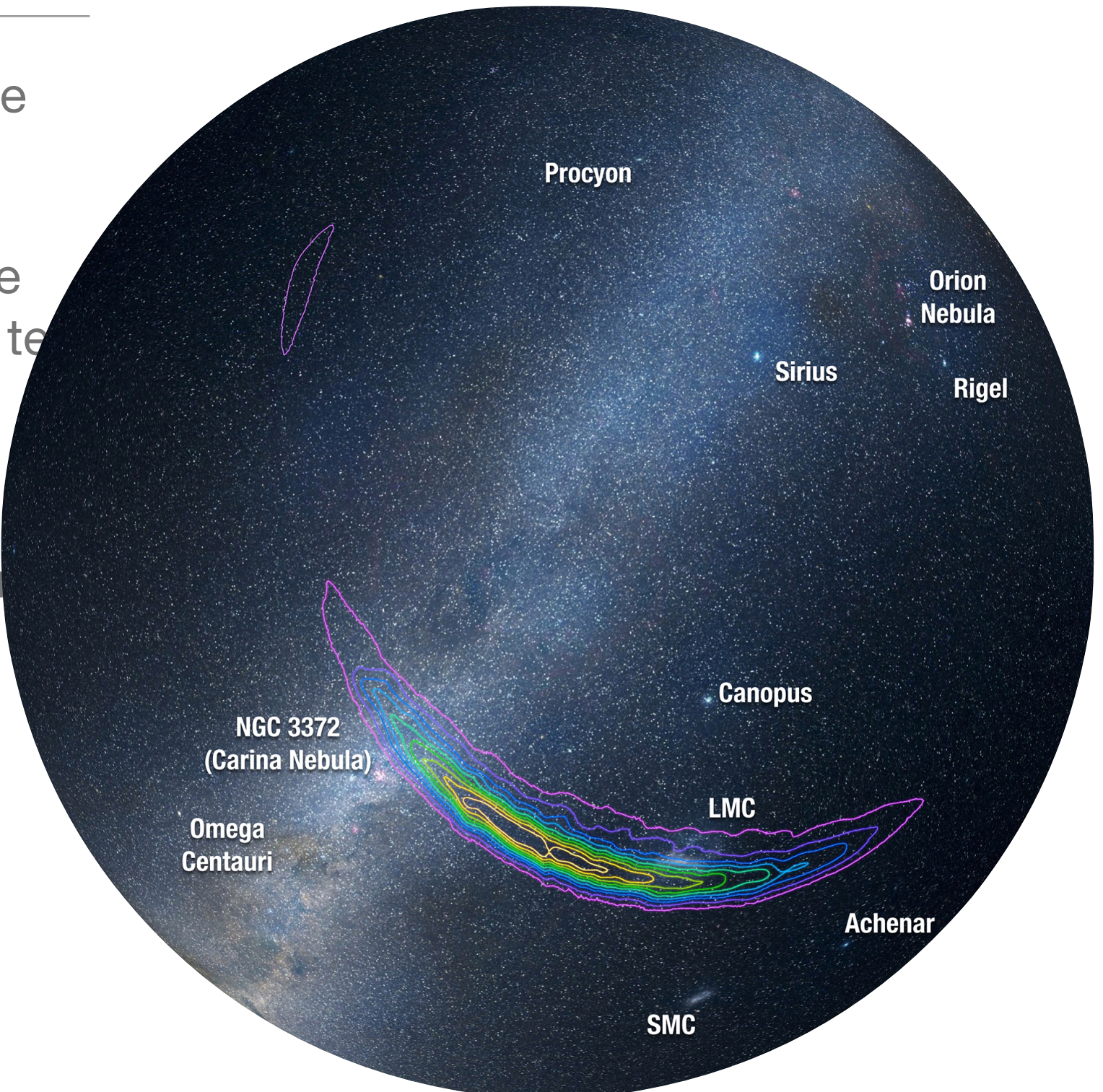


# For both detections?



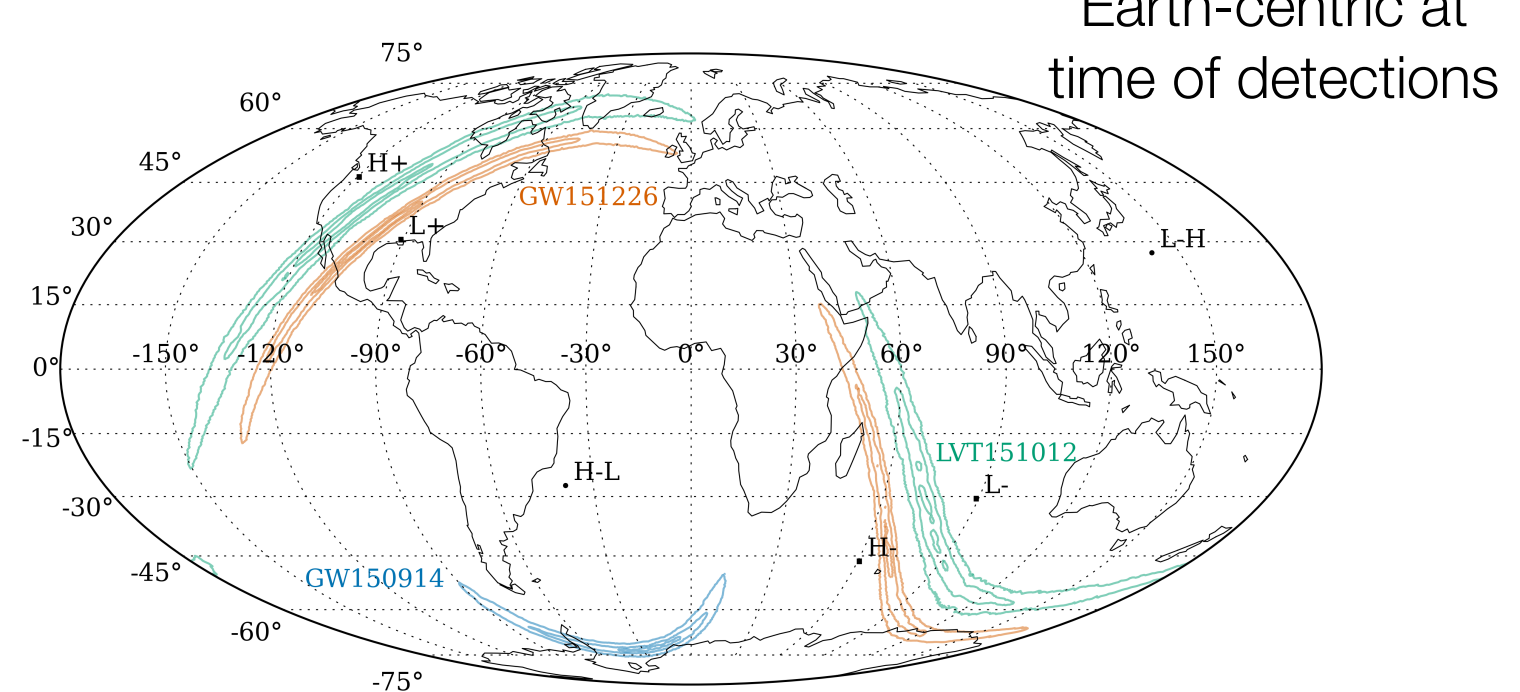
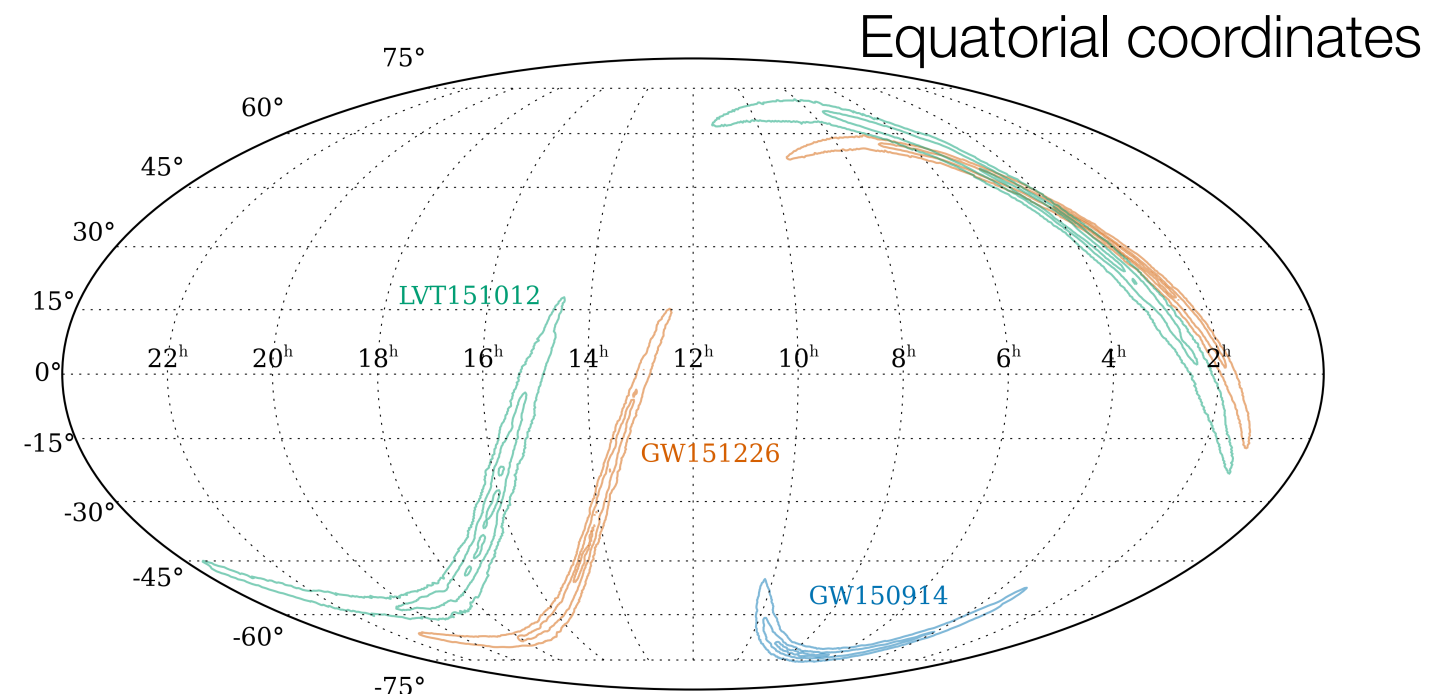
# Where was GW150914?

- Most likely somewhere in the southern hemisphere.
- We can very rapidly estimate the source sky location and tell astronomers to point their telescopes.
- This is relevant to how we first identified this signal. It was found with an **unmodelled** “burst” search.



# Where were the others?

- Notice the typical scale of error-region,  $O(100s)$  square degrees for 2 detectors.
- GW150914, GW151226 and LVT151012 have 230, 850, 1600 sq deg error regions.
- It's low number statistics but also notice the bias towards detection directly over/under the detectors.



# How to measure parameters?

- We rely heavily on **Bayesian parameter estimation**.

$$p(\boldsymbol{\theta}|\mathbf{x}, I) = \frac{p(\mathbf{x}|\boldsymbol{\theta}, I)p(\boldsymbol{\theta}|I)}{p(\mathbf{x}|I)}$$

Diagram illustrating the Bayesian formula:

- posterior** (blue) points to the left term  $p(\boldsymbol{\theta}|\mathbf{x}, I)$ .
- likelihood** (blue) points to the term  $p(\mathbf{x}|\boldsymbol{\theta}, I)$ .
- prior** (blue) points to the term  $p(\boldsymbol{\theta}|I)$ .
- evidence** (blue) points to the term  $p(\mathbf{x}|I)$ .

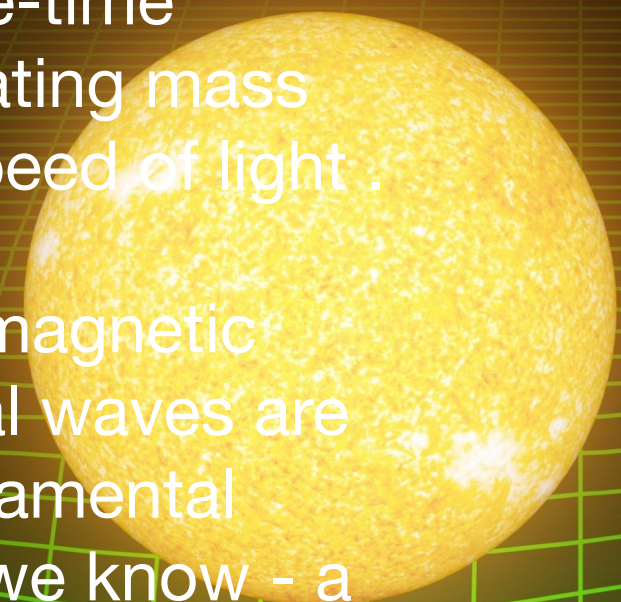
- We must make (motivated) assumptions regarding our noise distribution and the prior values of the parameters.

$$\log p(\mathbf{x}|\boldsymbol{\theta}, I) = \exp \left[ - \sum_{j=0}^{N-1} \frac{|\tilde{x}_j - \tilde{h}_j(\boldsymbol{\theta})|^2}{TS_h(f_j)} \right] + \text{const}$$

- In practice, obtaining posterior probability densities on system parameters is done via **Monte-Carlo techniques** (MCMC, nested sampling).

# Gravitational waves

- “*Mass tells space-time how to curve and spacetime tells mass how to move*”
- 100 years ago Einstein theorised the existence of gravitational waves - tiny distortions in space-time caused by accelerating mass and travel at the speed of light .
- Apart from Electromagnetic waves, gravitational waves are the only other fundamental wave phenomena we know - a new window on the universe.



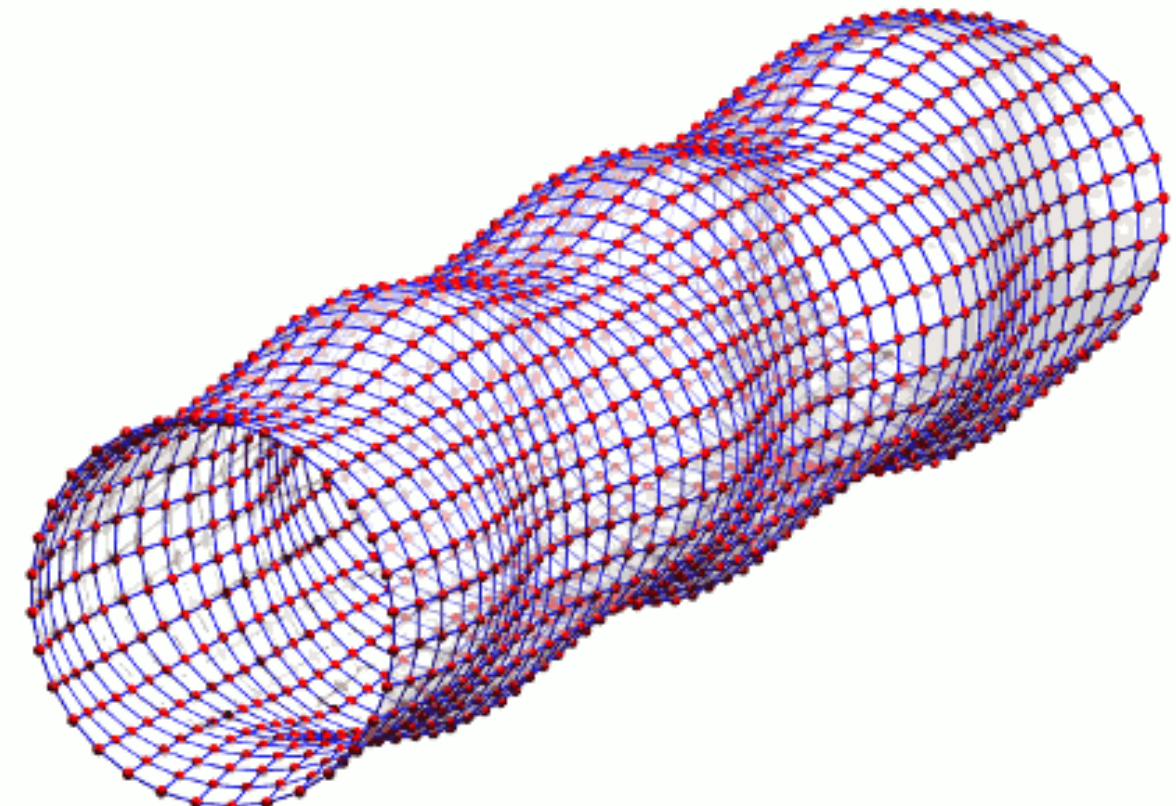
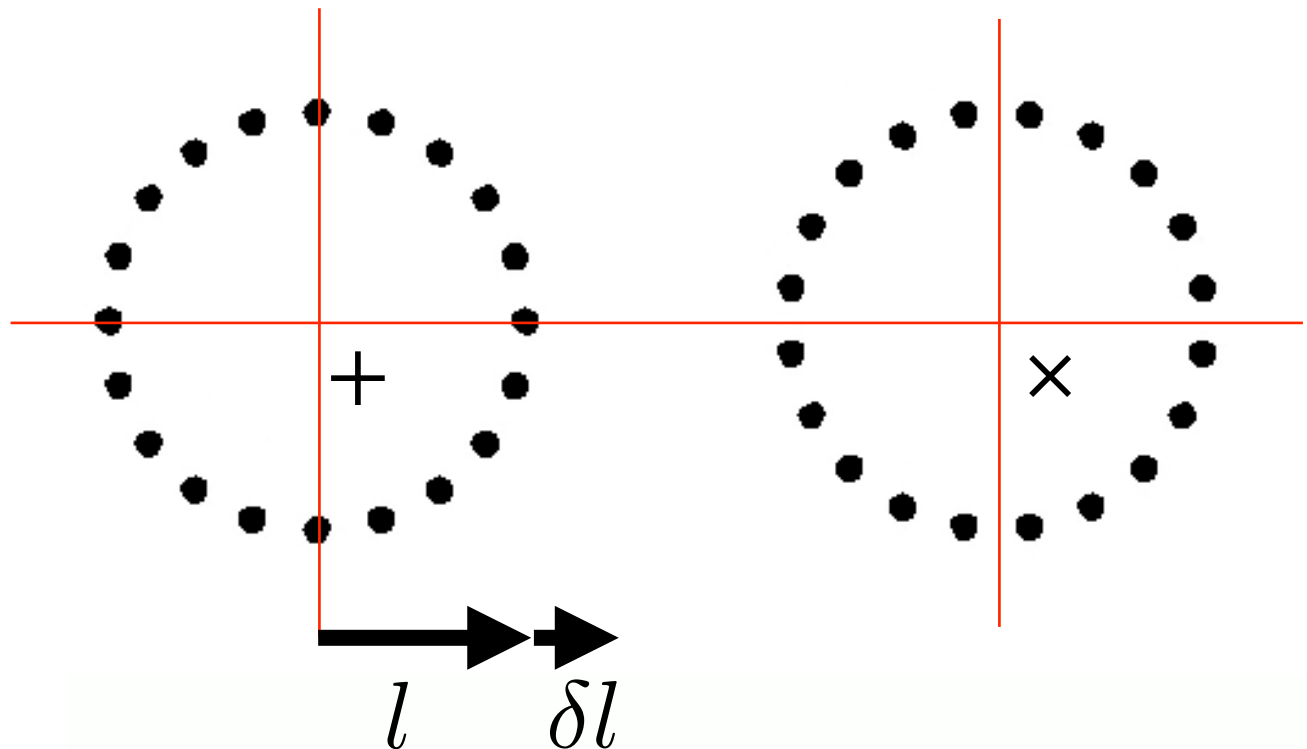
# Measurable effects

- GWs are transverse waves composed of 2 polarisation states.
- Their effect is quantified by the dimensionless strain

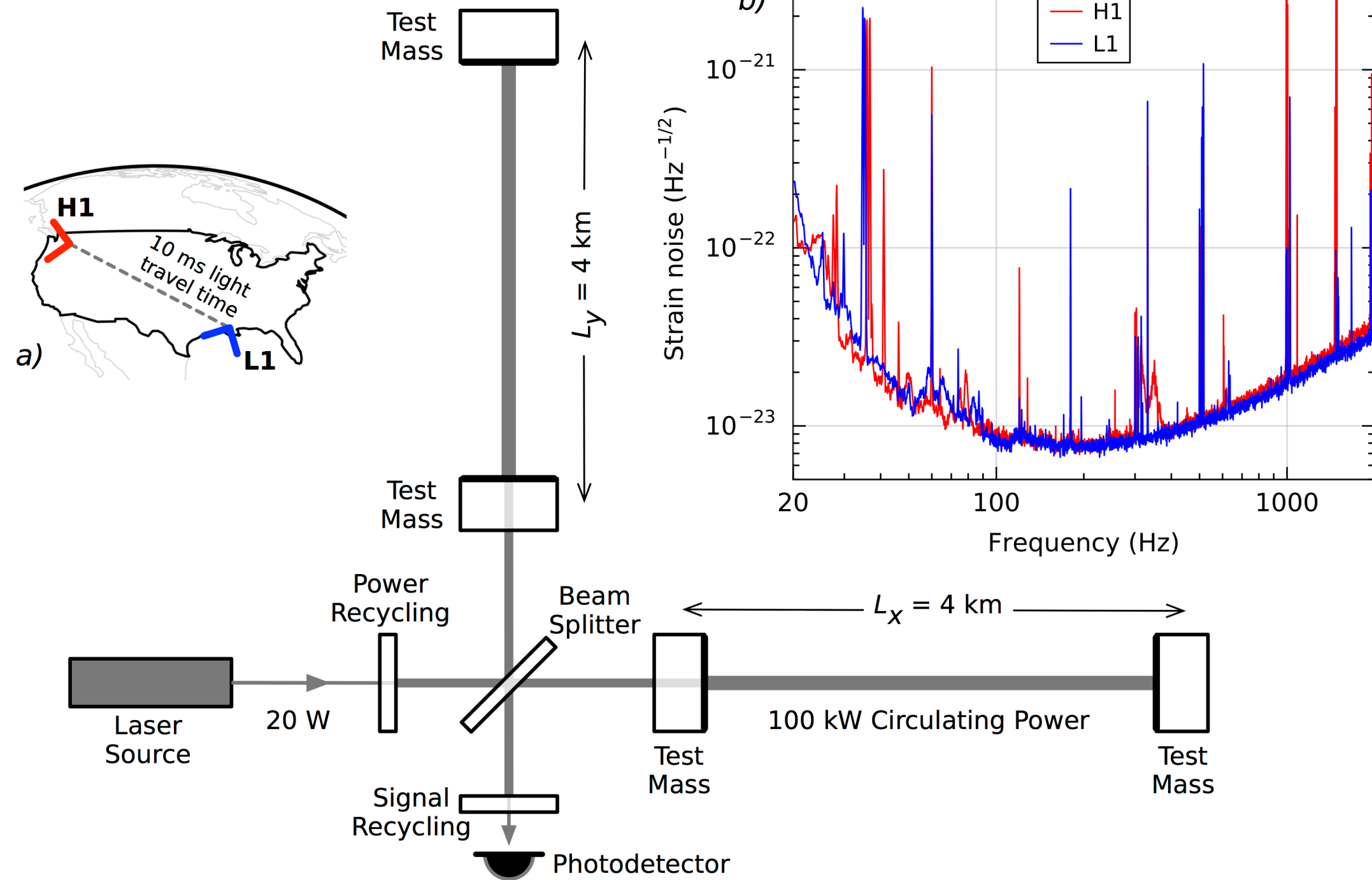
$$h = \frac{\delta l}{l}$$

- Typical levels of strain expected from astrophysical events is

$$\mathcal{O}(10^{-21})$$

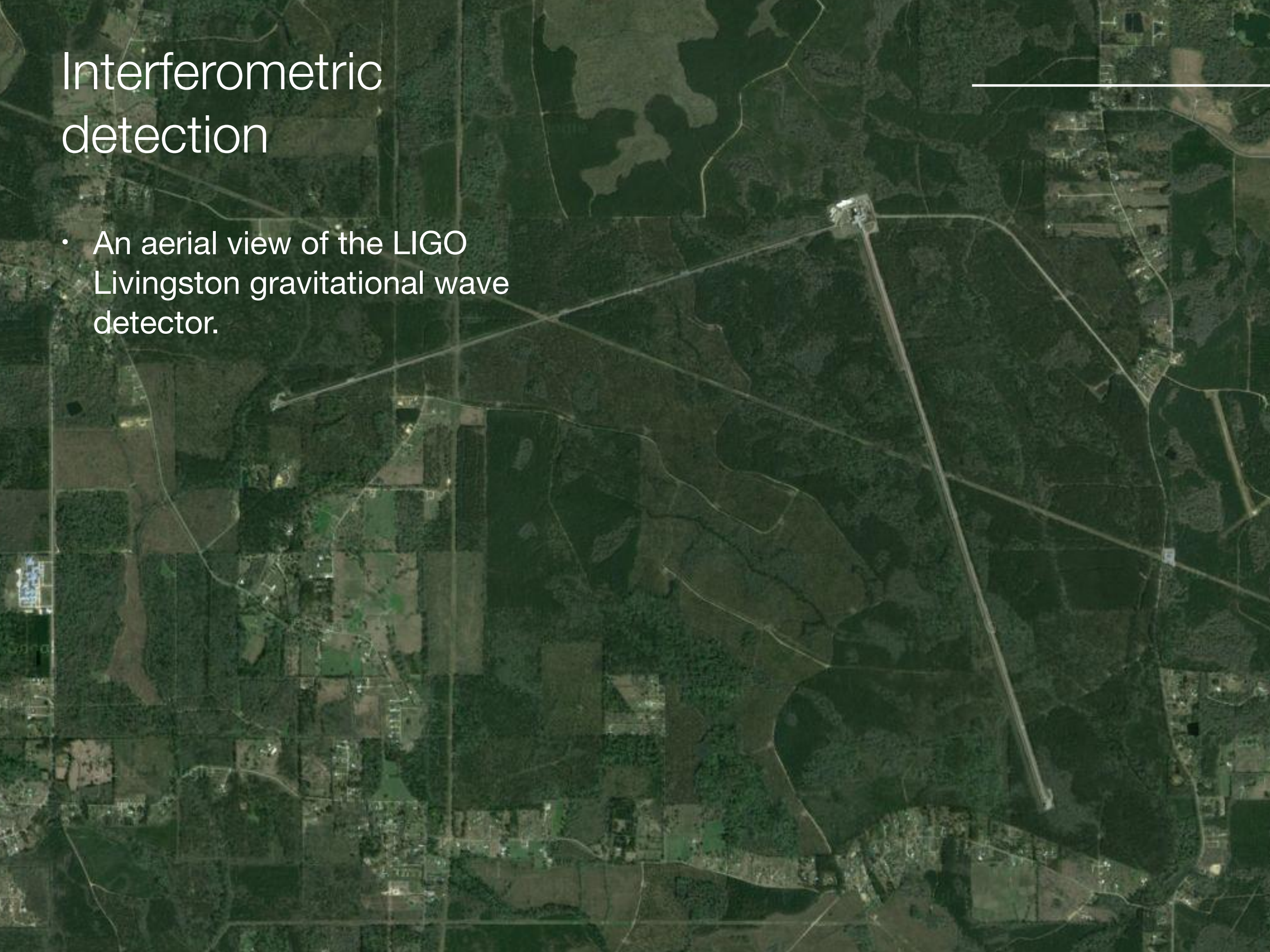


# Interferometric detection



# Interferometric detection

- An aerial view of the LIGO Livingston gravitational wave detector.



# The global network

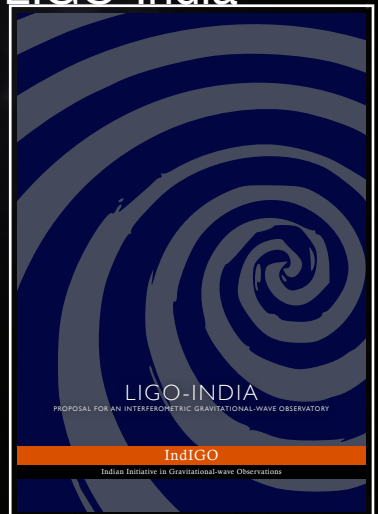


GEO600



Virgo

LIGO-India



LIGO Livingston



LIGO Hanford

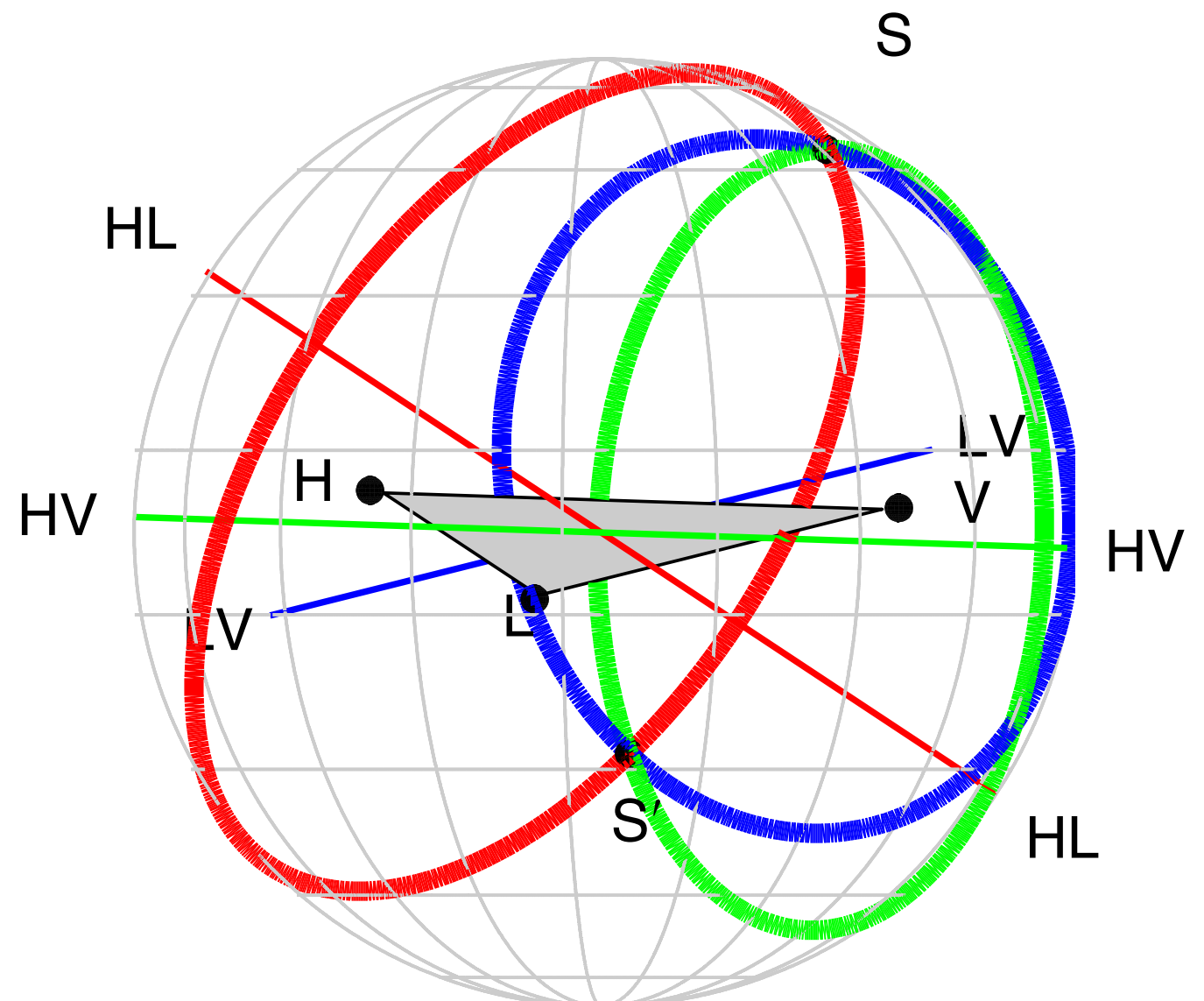
KAGRA



Data SIO, NOAA, U.S. Navy, NGA,  
Image Landsat  
Image IBCAO  
Image U.S. Geological Survey

# How can we locate it?

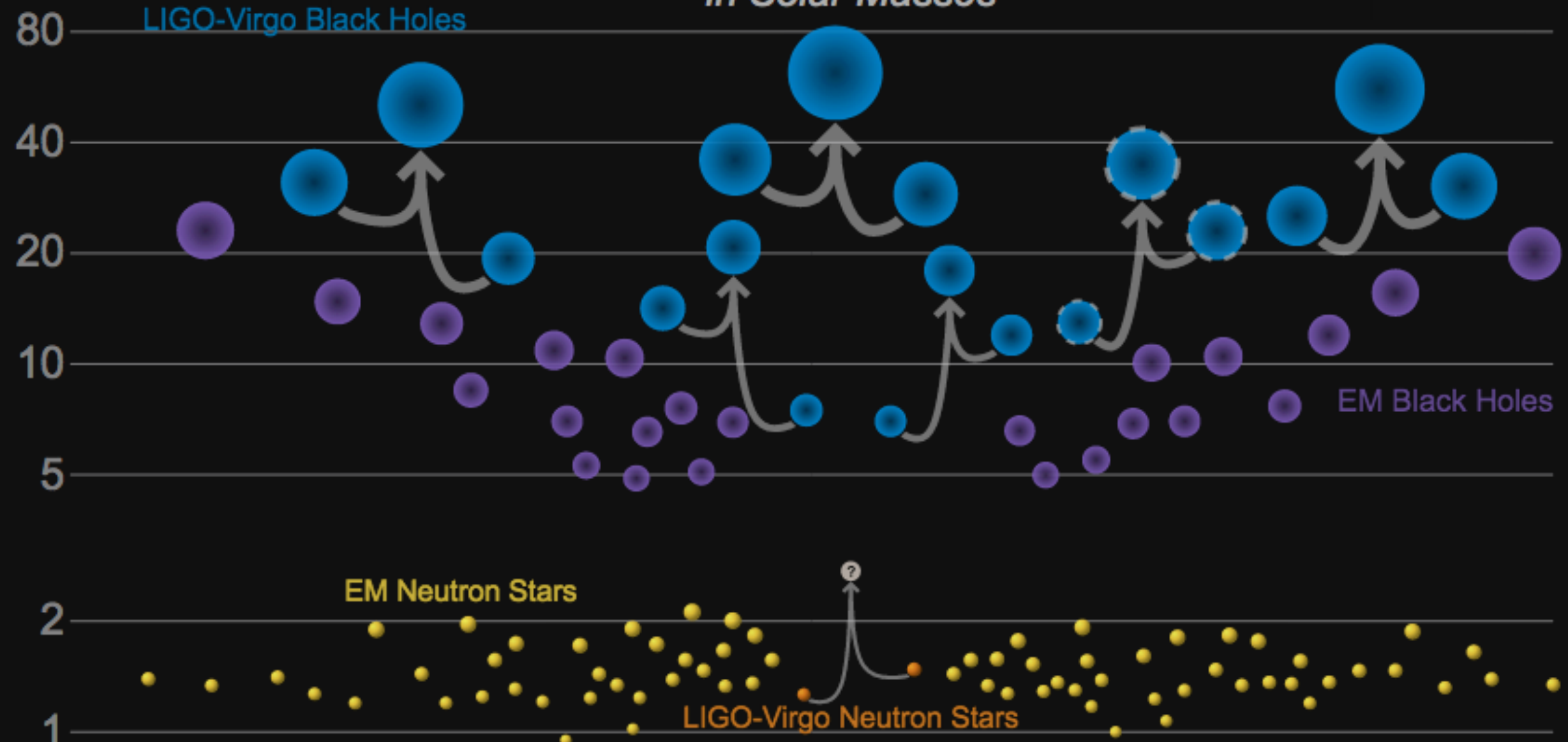
- Sky localisation information is key to GW multi-messenger astronomy.
- The time delay (with associated timing uncertainty) determines the bulk of the localisation ability.
- For four or more detectors there is a unique intersection region of all of the annuli.
- Additional antenna response modulation refine the estimate.



# BBH masses

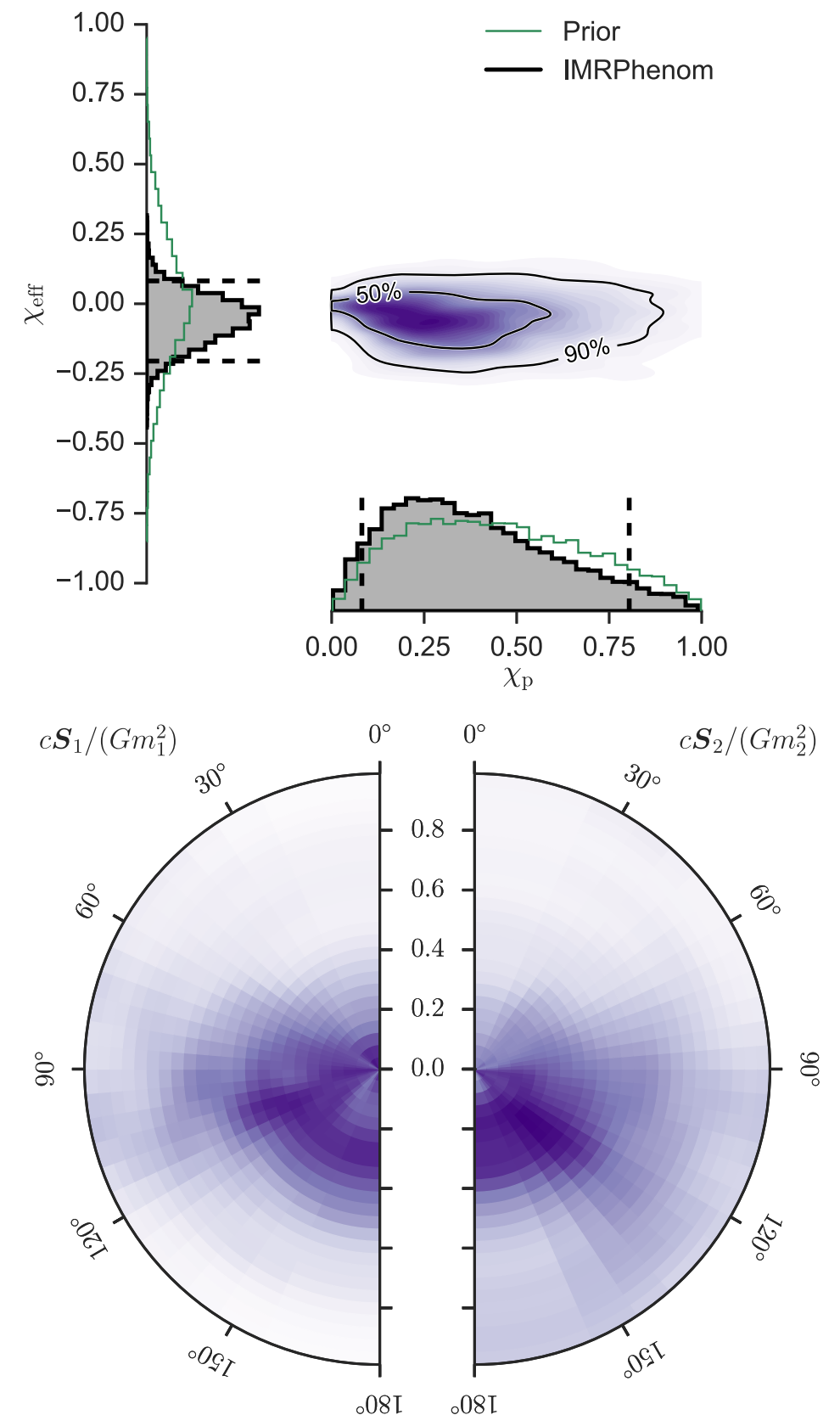
## Masses in the Stellar Graveyard

*in Solar Masses*



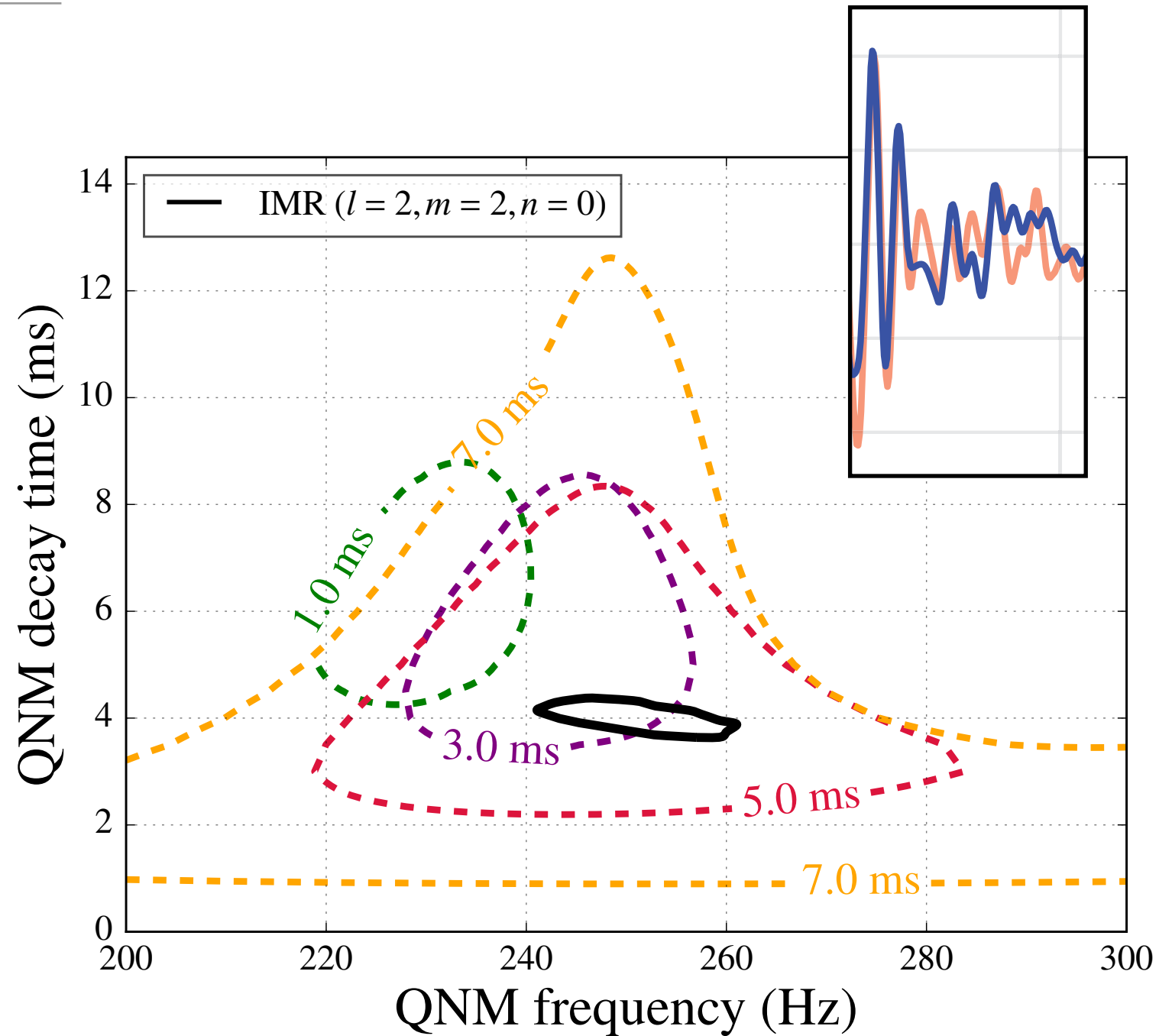
# GW150914 spin

- Spin affects the relativistic motion of the binary but has subtle influence on the waveform (extra/less cycles, modulation).
- The spin measurement for GW150914 suggests that the individual spins were either small, or they were pointed opposite from one another, cancelling each other's effect.
- Spin components in the orbital plane are poorly contained.



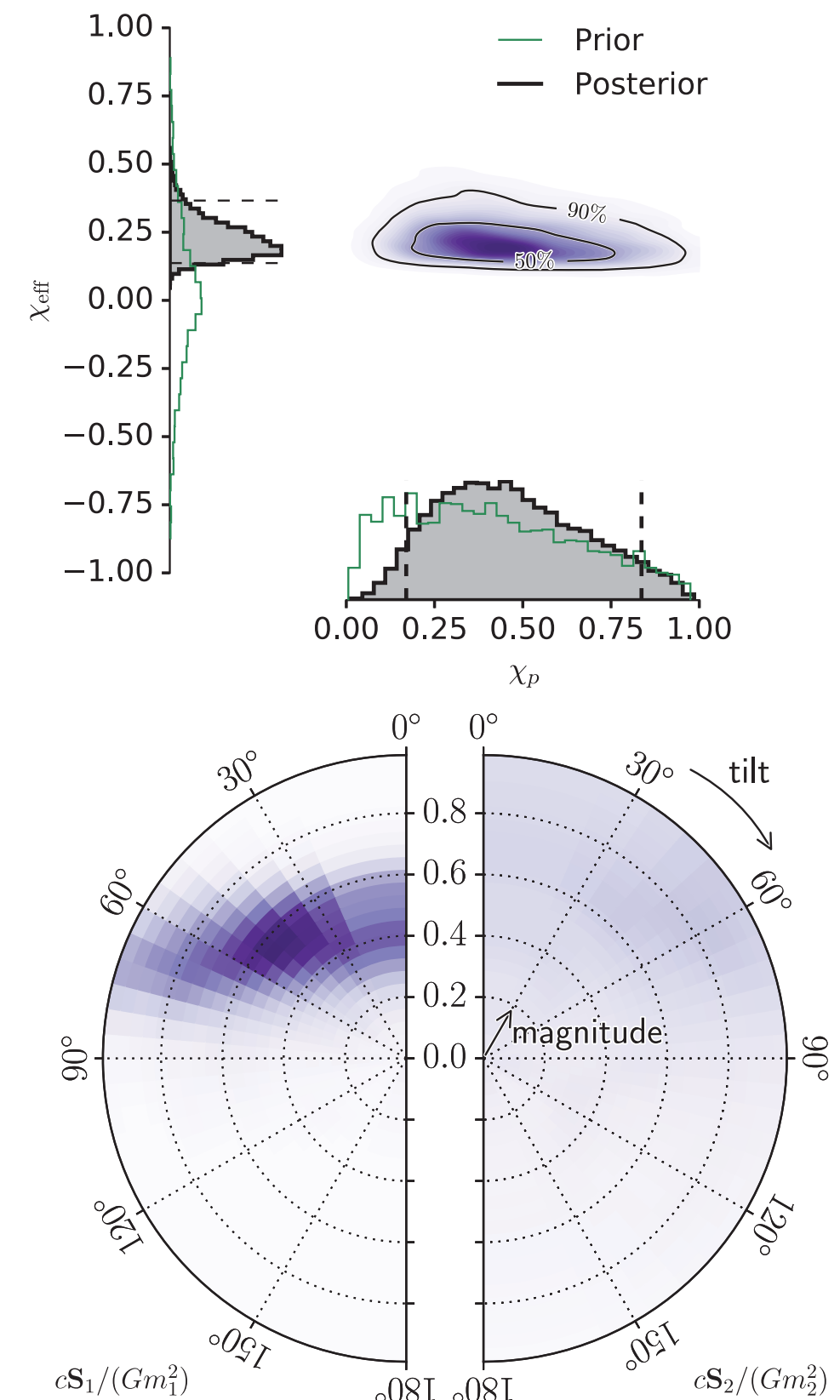
# Is general relativity right?

- We perform 3 main GR consistency tests.
- We test if the final mass and spin of the final black hole is consistent with predictions based on the inspiral.
- We test each post-newtonian expansion coefficient.
- We constrain the compton wavelength of the graviton to  $<10^{13}$  km.
- **GR passes all tests.**



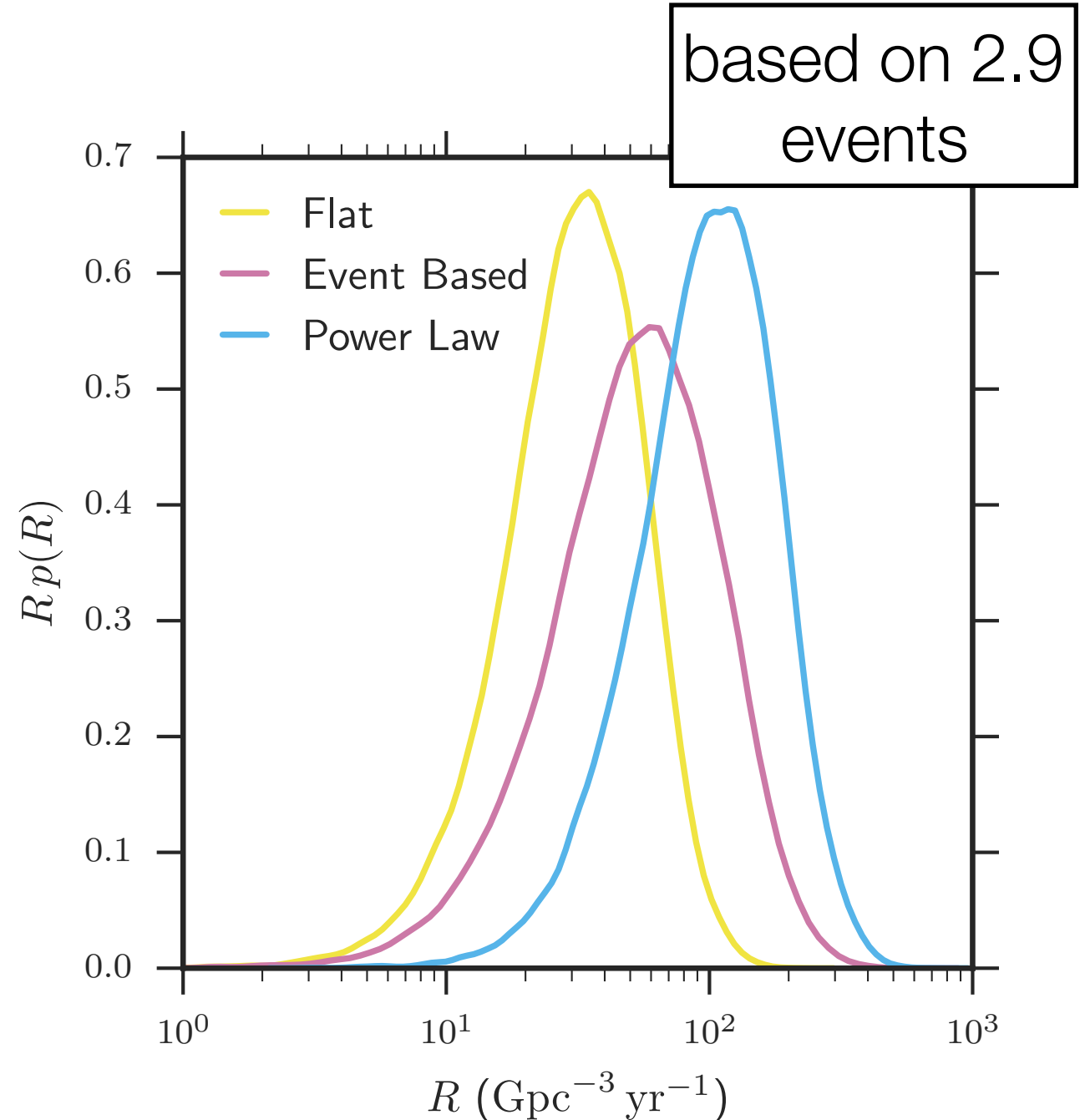
# GW151226 spin

- At 99% confidence at least one of the components had non-zero spin.
- With 99% confidence we can also say the spin of that component was  $>0.2$
- Again, the data are not informative regarding precession effects in the orbital plane.
- Spin can also give us an indication of the binary system formation mechanism.

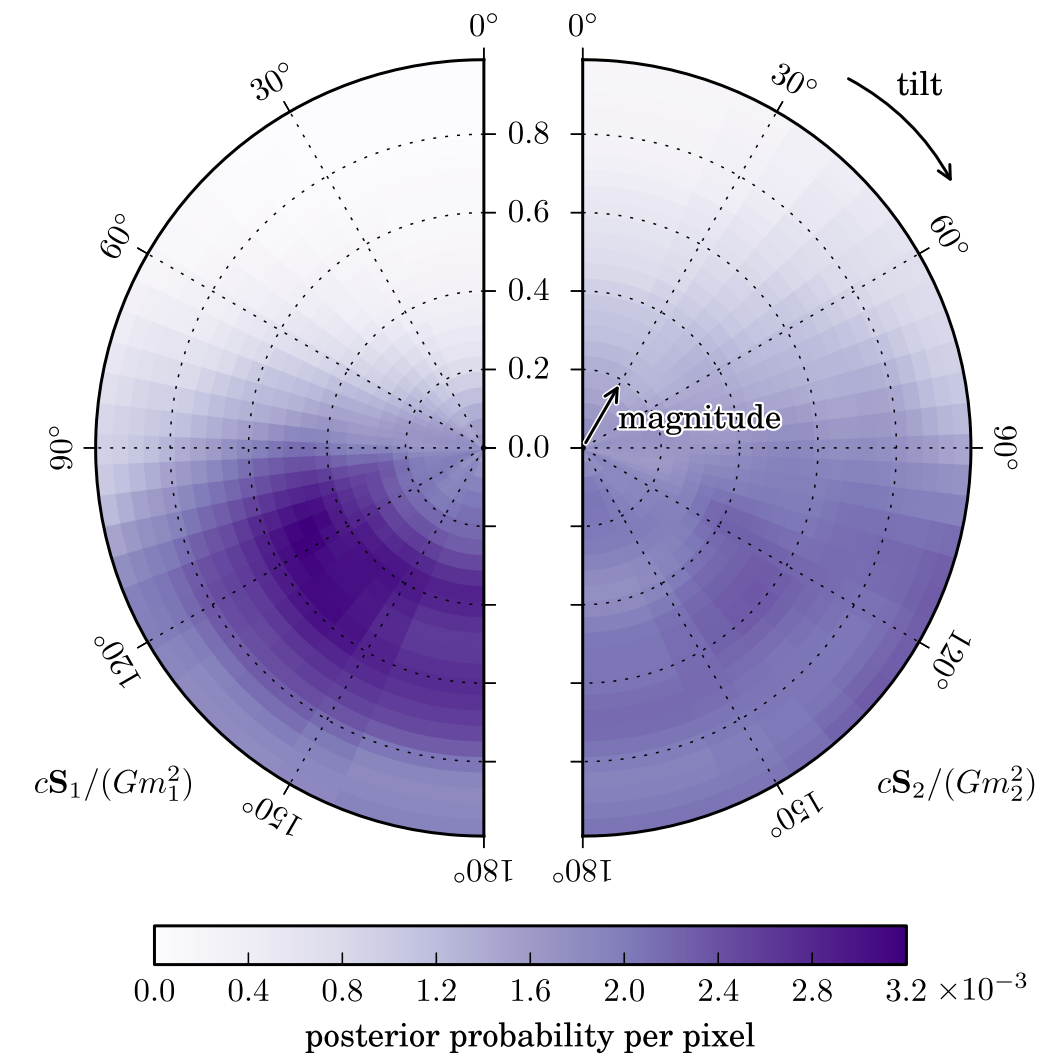
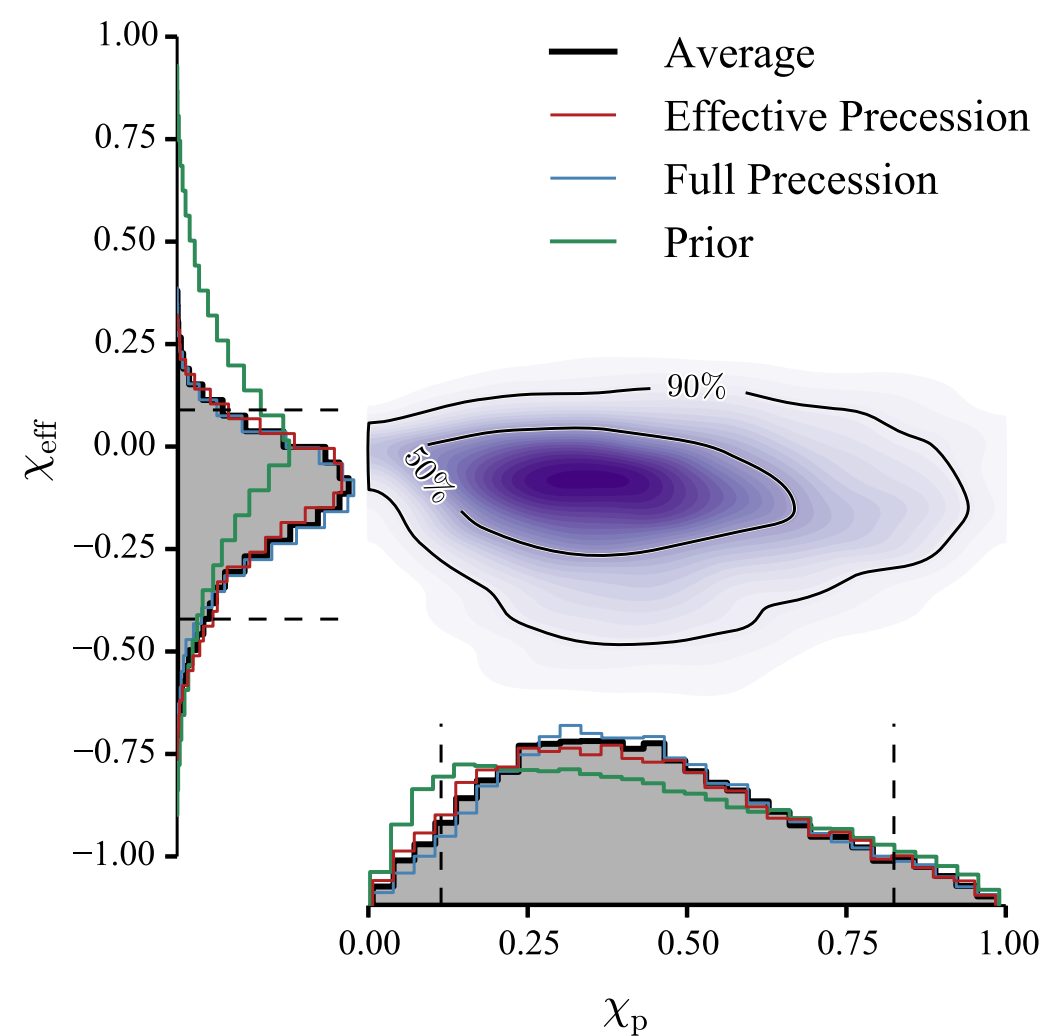


# How common is this?

- We need to know how many events there are how sensitive our detectors were.
- We've only detected 6 event(s) (at present) and hence extrapolating the astrophysical event rate is hard.
- Uncertainties stem from Poisson counting noise, distance errors, calibration, and prior mass distributions.

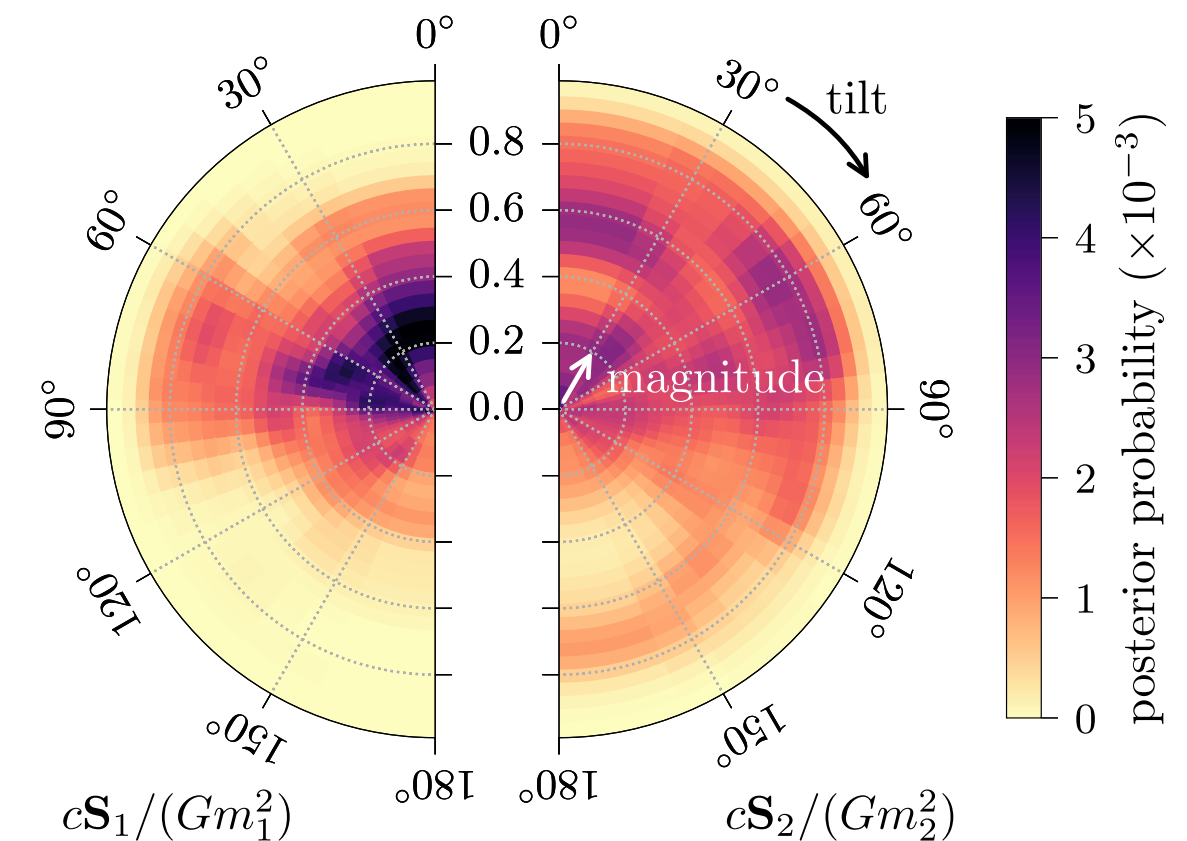
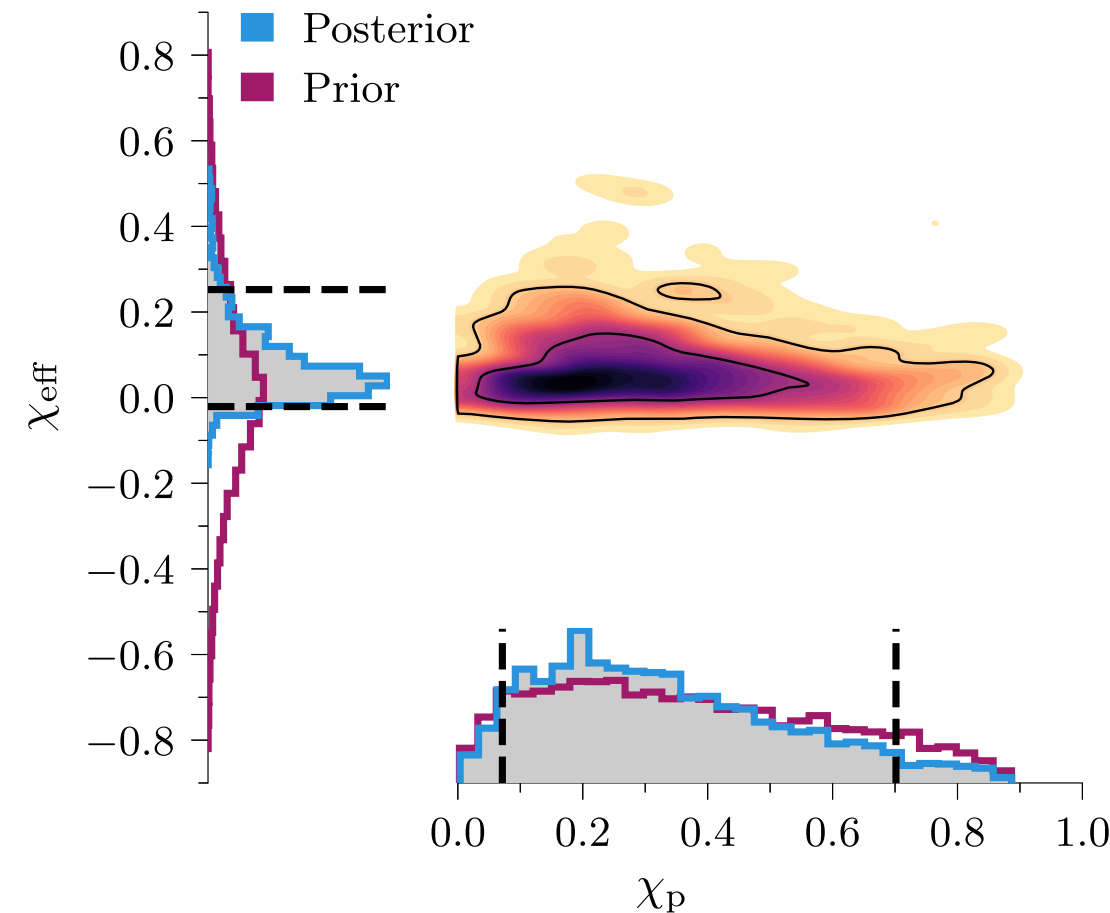


# GW170104 spin



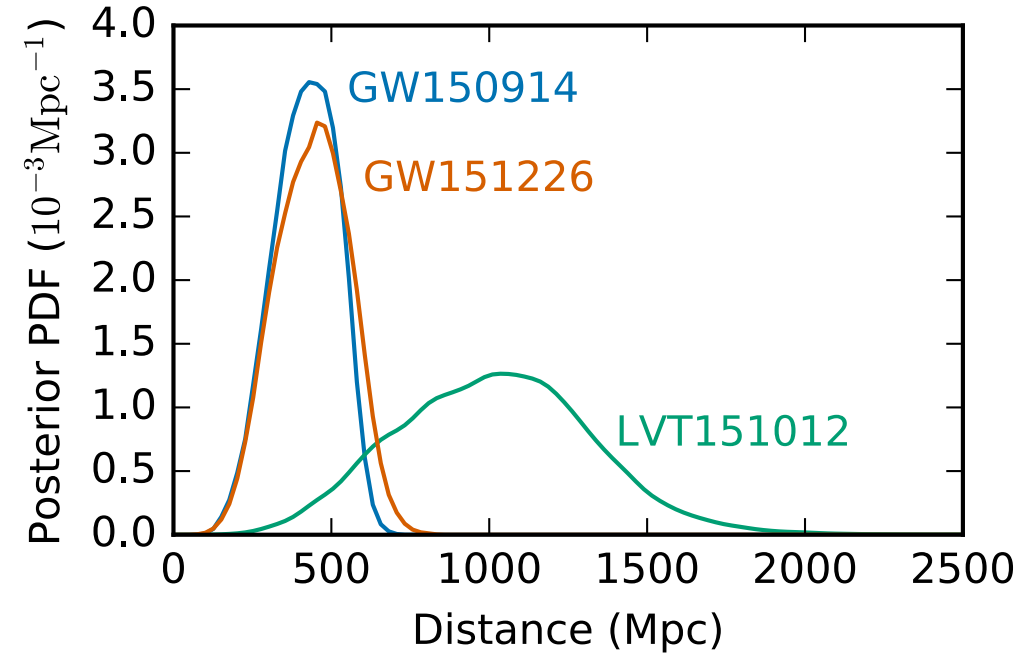
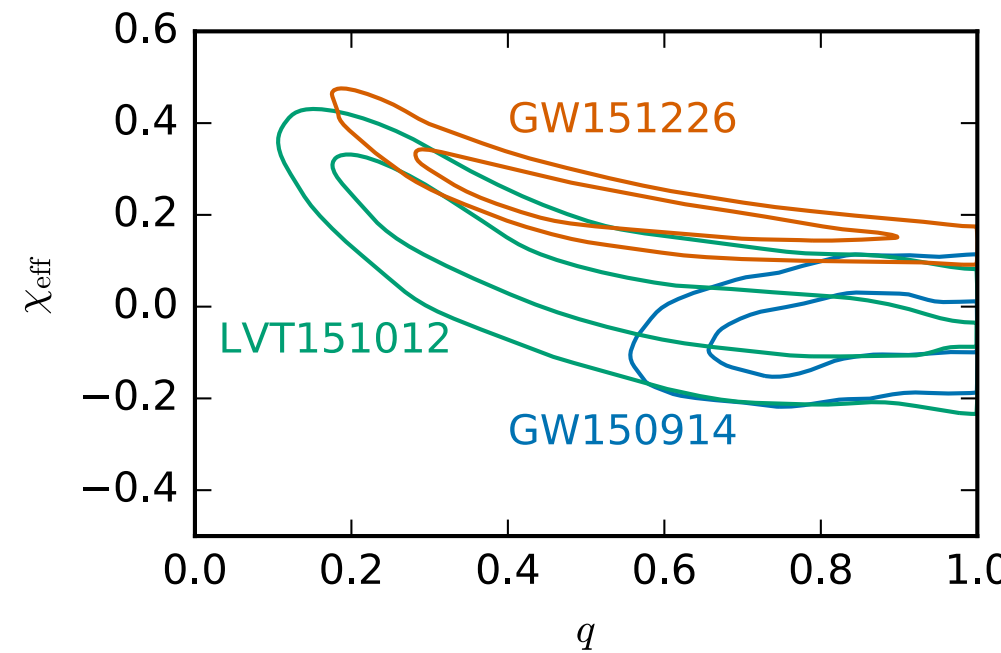
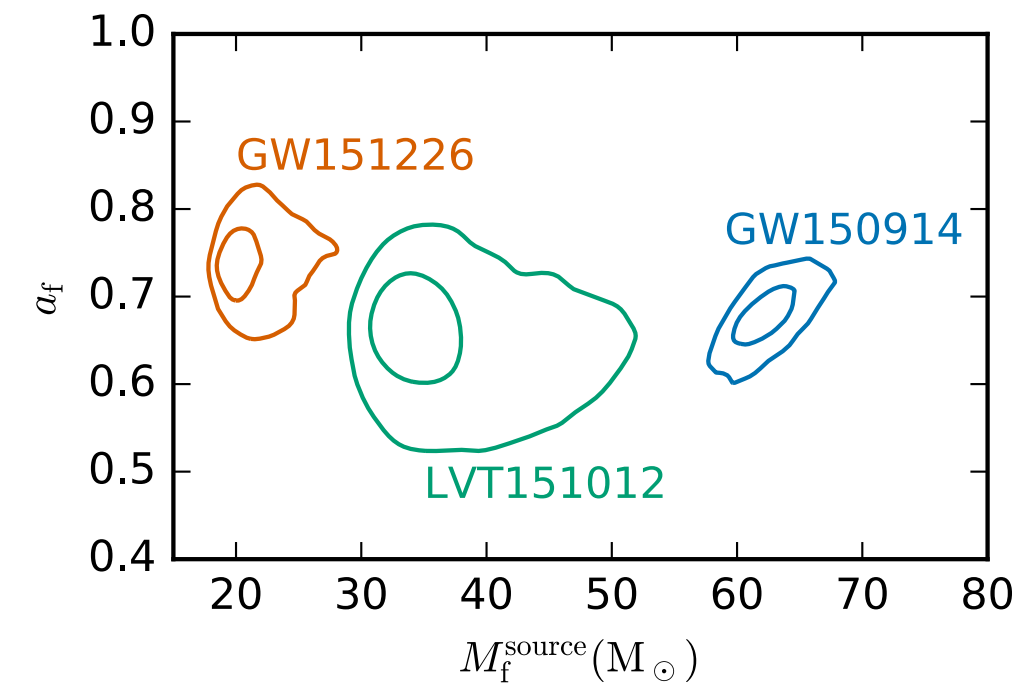
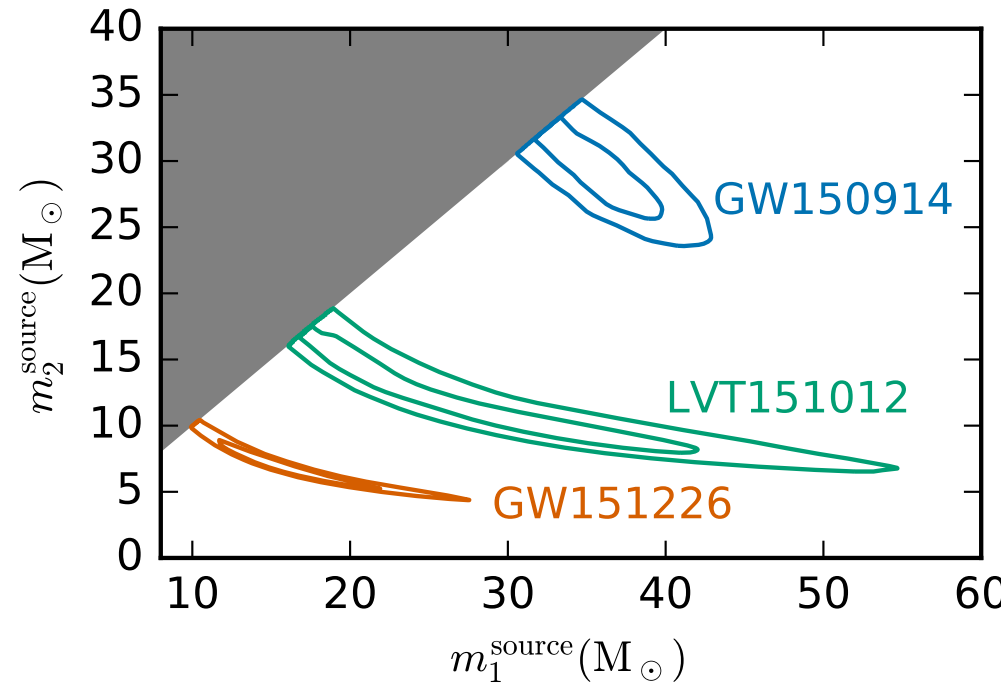
- The measurements disfavour a large total spin positively aligned with the orbital angular momentum, but do not exclude zero spins.

# GW170608 spin



- In this case the data constrains the total effective spin to be small and likely positive. As with the others sources, we are insensitive to in-plane spin.

# Source properties



# What about the final black hole?

- The final black hole has a mass of  $3 M_{\odot}$  less than the sum of its components.
- It has a well constrained final spin of  $\sim 0.7$ .
- This is due to the fact that the final spin is mostly a function of the orbital angular momentum at merger.

